

ornl

OAK RIDGE NATIONAL LABORATORY

LOCKHEED MARTIN

Application of Electrolytic In-Process Dressing for High-Efficiency Grinding of Ceramic Parts

Research Activities: 1995-96

B. P. Bandyopadhyay

RECEIVED
APRO41997
OSTI

Ceramic Technology Project



DISTRIBUTION OF THIS DOCUMENT IS UNLIMITED

MANAGED AND OPERATED BY LOCKHEED MARTIN ENERGY RESEARCH CORPORATION FOR THE UNITED STATES DEPARTMENT OF ENERGY This report has been reproduced directly from the best available copy.

Available to DOE and DOE contractors from the Office of Scientific and Technical Information, P. O. Box 62, Oak Ridge, TN 37831; prices available from (423) 576-8401, FTS 626-8401.

Available to the public from the National Technical Information Service, U.S. Department of Commerce, 5285 Port Royal Road, Springfield, VA 22161.

This report was prepared as an account of work sponsored by an agency of the United States Government. Neither the United States Government nor any agency thereof, nor any of their employees, makes any warranty, express or implied, or assumes any legal liability or responsibility for the accuracy, completeness, or usefulness of any information, apparatus, product, or process disclosed, or represents that its use would not infringe privately owned rights. Reference herein to any specific commercial product, process, or service by trade name, trademark, manufacturer, or otherwise, does not necessarily constitute or imply its endorsement, recommendation, or favoring by the United States Government or any agency thereof. The views and opinions of authors expressed herein do not necessarily state or reflect those of the United States Government of any agency thereof.

DISCLAIMER

Portions of this document may be illegible electronic image products. Images are produced from the best available original document.

Application of Electrolytic In-Process Dressing for High-Efficiency Grinding of Ceramic Parts

Research Activities: 1995-96

B. P. Bandyopadhyay

University of North Dakota Department of Mechanical Engineering Grand Forks, ND

Date Published: February 1997

Funded by
Office of Heavy Vehicle Technologies
Office of Transportation Technologies
Energy Efficiency and Renewable Energy
U.S. Department of Energy

Prepared by the
OAK RIDGE NATIONAL LABORATORY
Managed by
Lockheed Martin Energy Research Corporation
for the
U.S. Department of Energy
under Contract No. DE-AC05-96OR22464

PREFACE

This two-part, combined report describes the subcontracted research work conducted by Biswanath Prasad Bandyopadhyay of the Department of Mechanical Engineering, University of North Dakota, during two subsequent summers in the laboratory of Dr. H. Ohmori, RIKEN, Tokyo, Japan. The main focus of the work is Electrolytic In-Process Dressing (ELID), a method which promises improvements in the efficiency of grinding ceramics and the quality of the parts produced. Part I of this report addresses the basic aspects of ELID grinding as they affect the rate of material removal, the normal forces developed during grinding, and the production of conditions which improve the ratio of the volume of material removed to that of the abrasives consumed (Gratio). Part II of the report addresses the effects of ELID grinding on the bending strength of silicon nitride.

The work described herein contributes to the Cost-Effective Ceramic Machining effort, a series of research and development projects in industry, universities, and national laboratories, which began in 1991. The objectives are to develop novel and improved methods for reducing the relatively high costs associated with machining and finishing structural ceramic components for energy-efficient engines. The work is supported by the Department of Energy, Office of Transportation Technologies, Propulsion System Materials Program, Robert B. Schulz, Program Manager. D. Ray Johnson is the Oak Ridge National Laboratory Project Manager.

Peter J. Blau, Task Leader Metals and Ceramics Division Oak Ridge National Laboratory October 1996

APPLICATION OF ELECTROLYTIC IN-PROCESS DRESSING (ELID) FOR HIGH EFFICIENCY GRINDING OF CERAMIC PARTS

Part 1: 1995

TABLE OF CONTENTS

	PAGE
1.0	SUMMARY
2.0	INTRODUCTION
3.0	EXPERIMENTAL SET UP
	3.1 Grinding Wheels 2 3.2 Grinding Fluid 3 3.3 Power Supply 3 3.4 Materials 3 3.5 Measuring Instruments Used 4
4.0	RESULTS and DISCUSSION
	4.1 Results with Cast Iron Fiber Bonded (CIFB) Wheels44.2 Modified ELID Dressing54.3 Results with Wheels with other Metallic Bonds64.4 Results with Wheels with Different Abrasive Friability6
5.0	CONCLUSIONS
6.0	ACKNOWLEDGMENTS
7.0	REFERENCES

LIST OF FIGURES

1.	Experimental Set Up	
2.	Grinding Wheels	. 9
3.	Power Supply	10
4.	Workpiece Material	10
5.	Relationship Between the Volume of Material Removed and the Normal Grinding Force, Conventional Grinding with a CIFB-D wheel	. 11
6.	Relationship Between the Volume of Material Removed and the Normal Grinding Force, ELID grinding with a CIFB-D wheel	12
7.	Relationship Between the Volume of Material Removed and the Normal Grinding Force, ELID grinding with a CIFB-D wheel	13
8(a).	Grinding Wheel Surface after Truing and Mechanical Dressing	14
8(b).	Grinding Wheel Surface after Conventional Grinding	14
9(a).	Grinding Wheel Surface after ELID Dressing	15
9(b).	Grinding Wheel Surface after ELID Grinding	15
10.	Relationship Between the Volume of Material Removed and the Normal Grinding Force, Conventional Grinding with a CIFB-D Wheel	16
11.	Relationship Between the Volume of Material Removed and the Normal Grinding Force, ELID Grinding with a CIFB-D Wheel	17
12.	Relationship Between the Volume of Material Removed and the Normal Grinding Force, ELID Grinding with modified ELID Dressing with a CIFB-D Wheel	18
13.	The Electrical Behavior during the Modified ELID Dressing	19
14.	Relationship Between the Volume of Material Removed and the Normal Grinding Force, Conventional Grinding with a CB Wheel	20

15.	Relationship Between the Volume of Material Removed and the Normal Grinding Force, ELID Grinding with a CB Wheel	1
	the Normal Grinding Police, Edib Grinding with a CB wheel	_
16.	Relationship Between the Volume of Material Removed and	
	the Normal Grinding Force, Conventional Grinding with a BB Wheel 2:	2
17.	Relationship Between the Volume of Material Removed and	
	the Normal Grinding Force, ELID Grinding with a BB Wheel	3
18.	Relationship Between the Volume of Material Removed and	
	the Normal Grinding Force, Conventional Grinding with	_
	a C.I. Powder Bonded Wheel	4
19.	Relationship Between the Volume of Material Removed and	
	the Normal Grinding Force, ELID Grinding with a C.I. Powder Bonded Wheel 2:	5
20.	Relationship Between the Volume of Material Removed and	
	the Normal Grinding Force, Conventional Grinding with a MBG-660 Wheel 26	6
21.	Relationship Between the Volume of Material Removed and	
	the Normal Grinding Force, ELID Grinding with a MBG-660 Wheel	7
22.	Relationship Between the Volume of Material Removed and	
	the Normal Grinding Force, Conventional Grinding with a RVG Wheel 28	8
23.	Relationship Between the Volume of Material Removed and	
25.	the Normal Grinding Force, ELID Grinding with a RVG Wheel	9
24.	Relationship Between the Volume of Material Removed and	_
	the Normal Grinding Force, Conventional Grinding with a MBG-600 Wheel 30	J
25.	Relationship Between the Volume of Material Removed and	
	the Normal Grinding Force, ELID Grinding with a MBG-600 Wheel	1

LIST OF TABLES

TABLE		PAGE		
I.	Technical Specifications of various ELID Power Supplies		3	
II.	Comparison of G-Ratios		7	

1.0 SUMMARY

The application of Electrolytic In-Process Dressing (ELID) for highly efficient and stable grinding of ceramic parts is discussed. This research was performed at the Institute of Physical and Chemical Research (RIKEN), Tokyo, Japan, June 1995 through August 1995. Experiments were conducted using a vertical machining center. The silicon nitride work material, of Japanese manufacture and supplied in the form of a rectangular block, was clamped to a vice which was firmly fixed on the base of a strain gage dynamometer. The dynamometer was clamped on the machining center table. Reciprocating grinding was performed with a flat-faced diamond grinding wheel. The output from the dynamometer was recorded with a data acquisition system and the normal component of the force was monitored.

Experiments were carried out under various cutting conditions, different ELID conditions, and various grinding wheel bond types. Rough grinding wheels of grit sizes #170 and #140 were used in the experiments. Compared to conventional grinding, there was a significant reduction in grinding force with ELID grinding. Therefore, ELID grinding can be recommended for high material removal rate grinding, low rigidity machines, and low rigidity workpieces. Compared to normal grinding, a reduction in grinding ratio was observed when ELID grinding was performed. A negative aspect of the process, this reduced G-ratio derives from bond erosion and can be improved somewhat by adjustments in the ELID current. The results of this investigation are discussed in detail in this report.

2.0 INTRODUCTION

The author participated in the Electrolytic In-Process Dressing (ELID) research program at RIKEN during the summer of 1994 (June through August). The focus of that research effort was to investigate the application of ELID grinding for ceramic components requiring a "mirror" surface finish. The mirror surface finish was obtained with a fine, #4000 mesh size grinding wheel. A detailed report explaining the ELID principle and the results of the mirror finish grinding with ELID has been published [1]. Mirror finish grinding with ELID is expected to find widespread application in the electronic and optical industries. However, for general engineering applications, both high material removal rates and stable grinding of structural ceramics are required. During the summer of 1995, the author rejoined the ELID research team at RIKEN, Tokyo, Japan to further investigate high efficiency and stable grinding of ceramics. The results of ELID grinding on silicon nitride specimens are discussed in detail in this report.

3.0 EXPERIMENTAL SET UP

The current experiments were conducted on a vertical machining center. A flat-faced, metal bonded diamond grinding wheel was installed on the machine spindle. The positive terminal of a power supply was connected to the grinding wheel using a smooth brush sliding contact, and the fixed electrode is connected to the negative terminal. The negative copper electrode was 1/6 of the wheel periphery in length and had a width of 2 mm more than the wheel rim thickness. The gap between the wheel and the electrode could be adjusted mechanically. A clearance of approximately 0.1 mm was kept between the positive and negative poles. Electrolysis occurs in the presence of a supply of suitable grinding fluid and when an electric current is applied. The silicon nitride work material, in the form of a rectangular block, was clamped to a vice which was firmly fixed on the base of a strain gage dynamometer. The dynamometer was clamped on the machining center table and the reciprocating grinding operation was performed. The output from the dynamometer was recorded by a data acquisition system and the normal component of the grinding force was monitored. The experimental set up is shown in Fig.1.

3.1 Grinding Wheels

Straight metal-bonded diamond grinding wheels were used in the experiment. The specification of the wheels is as follows:

- 1) Various types of metal bonded wheels
- 2) Straight wheel (flat-faced)
- 3) Wheel Diameter = 150 mm
- 4) Wheel Width = 10 mm
- 5) Grit Size = #140 and #170
- 6) Concentration = 100

The grinding wheels used in these experiments are shown in Fig. 2.

3.2 Grinding Fluid

Noritake AFG-M grinding fluid, diluted to 50:1, was used in these experiments.

3.3 Power Supply

A direct pulse generator was used as a power supply. This is a modified power source from a conventional electro-discharge machine. The power source is shown in fig. 3. This power supply is capable of supplying different output voltages, current setting, and pulse on-off time settings. In the experiments, open voltage of 60 V and 90 V (square wave) with a peak current of 16 A and 24 A respectively were used. The pulse width in the experiment was 4 μ s on-time and 4 μ s off-time.

Currently more sophisticated power supplies are available in the market under the trade name FUJI ELIDER POWER SUPPLY. The technical specifications of these power units are given in Table I.

Table I: TECHNICAL SPECIFICATIONS OF VARIOUS ELID POWER SUPPLIES

MODEL	Peak Voltage Eo(V)	Peak Current Ip(A)	Pulse Timing τ on\off (μs)	Source (V/Phase/Kw)	Size(mm), Weight (Kg) (width/height/depth/Wt)
ED 903	90	3	1 ~ 10	200/1/0.3	460/317/420/abt.30
ED 905	90	5	1 ~ 10	200/1/0.5	460/317/420/abt.30
ED 910	90	10	1 ~ 10	200/1/0.9	460/317/420/abt.30
ED 920	90	20	1 ~ 10	200/3/1.8	460/850/570/abt.120
ED 620	60	20	1 ~ 10	200/3/1.2	460/850/570/abt.120
ED 630	60	30	1 ~ 10	200/3/1.8	460/850/570/abt.120
ED 1503C	150	3	5/5 fixed	200/1/0.9	420/200/350.abt.25
ED 1510	150	10	200/3/1.8	200/3/1.8	460/850/570/abt.120
ED 1520	150	20	200/3/3.6	200/3/3.6	460/1150/720/abt.160

3.4 Materials

Silicon nitride materials in the form of a rectangular block were used in these experiments. The dimensions of the workpiece material was 50x50x20. Some representative work materials are

shown in Fig. 4. This type of silicon nitride was supplied by RIKEN and was of Japanese manufacture. Its exact composition and processing route are not known.

3.5 Measuring Instruments Used

The surface finish was measured by a Mitutoyo 501 surface roughness measuring instrument using a 5 micron diamond stylus. The grinding wheel surface was characterized by the olympus microscope model OVM 100 NM. The multi-component strain gage dynamometer from Advanced Mechanical Technology, Inc. MC-12 Series was used for measurement of grinding force.

4.0 RESULTS and DISCUSSION

ELID grinding consists of the following four steps:

- I) Truing: Truing is required so that the initial eccentricity of the wheel is reduced. Truing was performed with a SiC wheel of grit size of #100. The operation was performed at 300 rpm.
- ii) Mechanical Dressing: This was performed with an aluminum oxide stick of grit size # 400 also at 300 rpm.
- iii) Pre-Dressing of the Wheel by Electrolysis: Pre-Dressing, also known as ELID dressing, was also performed at 300 rpm for 30 minutes for all the wheels. The electrical behavior, ELID grinding mechanism are discussed in details elsewhere [1-3].
- iv) Grinding Process with Electrolytic In-Process Dressing: ELID grinding was carried out at the recommended cutting speed. The conditions of electrolysis of processes iii and iv differ due to the changing wheel surface condition which occurs during electrolysis.

4.1 Results with Cast Iron Fiber Bonded (CIFB) Wheels

Conventional and ELID grinding were performed with a CIFB-diamond grinding wheel. All the grinding wheels were trued and dressed as described above before conventional grinding. This ensured that the same wheel condition was present for conventional and ELID grinding. This series of experiments was conducted under the following conditions: cutting speed = 1200 m/min, table feed rate = 5000 mm/min, depth of cut = 0.01 mm., width of cut = 5 mm, CIFB-D wheel with grit size # 170 (average grain size = 80 µm). The relationship between the volume of material removed and the normal grinding force in conventional grinding is shown in Fig. 5. During this process there is a continuous increase in the grinding force due to wheel loading and wear. The grinding force reached around 38 Kgf when the total volume of material removed was 6000 mm³. The relationship between the volume of material removed and the normal grinding force during ELID grinding is shown in the Fig. 6.

Both ELID dressing and ELID grinding were performed at 60 V, Ip = 16 amp, with "on"-time

and "off"-time both equal to 4 µs. The outer surface of the wheel became yellow after the ELID dressing due the formation of iron oxides [3]. Compared to the data in Fig. 5, grinding force is less during ELID grinding. This effect is more visible after 4500 mm³ of material has been removed. The effects of changing the ELID conditions were studied by performing ELID grinding with increased voltage, such as 90 V, Ip = 24 amp. The results are presented in the Fig. 7. The grinding force is less compared to both conventional (Fig. 5) and ELID grinding with 60 V (Fig. 6). A significant reduction in the grinding force takes place after 4500 mm³ of material removal. The grinding force stabilized at only 5 Kgf after 6000 mm³ of material removal and remained almost constant.. Therefore, the full potential of the ELID grinding could be utilized only after 6000 mm³ of material had been removed. In practice, this could be achieved by using a "dummy" workpiece in the beginning for a certain period of time followed by the grinding the actual ceramic component. The other alternative is to use modified ELID dressing, a process which will be discussed later.

Three surface roughness parameters, center line average R_a , ten point height of the roughness profile R_a , and maximum peak to valley height of the profile R_a , were measured after certain intervals. These results are presented in the Figures 5, 6, and 7.

A section of the grinding wheel after truing and mechanical dressing is shown in Fig. 8 (a), and the wheel surface condition after 6000 mm³ of material removal by conventional grinding is shown in 8 (b). The worn grains are visible in the Fig. 8 (b). The sections of the wheel after ELID dressing with 60 V and ELID grinding with 60 V and 5675 mm³ of material removal are shown in Figures 9 (a) and (b), respectively. There is no significant difference in grain sharpness in these two cases. This is because the characteristics of the abrasive protrusions are controlled before and during the grinding by the ELID process.

4.2 Modified ELID Dressing

Conventional grinding and ELID grinding were performed with CIFB-D grinding wheels of grit size #170 under different grinding conditions: cutting speed = 1200 m/min, feed rate = 5000 mm/min, depth of cut = 0.05 mm, width of cut = 2 mm. ELID dressing was performed with 90 V for 30 minutes and the ELID grinding was done using 60 V. The results are presented in Figures 10 and 11. Compared to conventional grinding, lower grinding force was obtained in the case of ELID grinding. As pointed out earlier, stable ELID grinding was established after approximately 6000 mm³ of material had been removed. Comparing Figures 5 and 10, we find that the grinding force is less under the conditions used to create Fig. 10. However, the material removal rate in the case of grinding, as shown in Fig. 10, is 500 mm³/min which is double that of the grinding as shown in Fig. 5. In the conditions for Fig. 10, the material was predominantly removed by brittle fracture. Therefore, less energy was required for the material removal. Since the above grinding conditions were found the most favorable, the rest of the experiments were conducted under these conditions.

The relationship between the volume of material removed and the grinding force with modified ELID dressing is shown in the Fig. 12. The ELID grinding was performed with 60 V. Modified ELID dressing was performed in two stages. In the first stage, the ELID dressing was performed with 90 V for 30 minutes. The oxide layer formed during ELID dressing was mechanically

removed by an aluminum oxide stick of grit size # 400 at 300 rpm. Then the second stage of ELID dressing was performed with 90 V, also for 30 minutes. The electrical behavior during this modified form of ELID dressing is shown in Fig. 13. ELID grinding was then performed using a 60 V supply. The grinding force remained low and almost constant from the beginning (Fig. 12). Therefore, by applying modified ELID dressing, as explained above, stable ELID grinding with the attendant low grinding force can be achieved almost from the beginning.

4.3 Results with Wheels with other Metallic Bonds

Results of conventional grinding and ELID grinding with cobalt bonded (CB) wheel and bronze bonded (BB) wheels are shown in Figures 14 through 17. The grinding conditions were as follows: cutting speed = 1200 m/min, feed = 5000 mm/min, depth of cut = 0.05 mm, width of cut = 2 mm, grit size of # 140 (average grain size 96 µm). ELID dressing was performed at 60 V for 30 minutes. A lower voltage was selected than that used for ELID dressing of a CIFB-D wheel. This is because the ionization of CB and BB wheels is easier. The color of the CB and BB bonded wheels after ELID dressing was dark pink and gray blue, respectively, because of the differences in their oxide layers [3]. ELID grinding provided significantly lower grinding force which remained constant for a long period of time. The grinding force was found to be lower with CB and BB wheels compared to the CIFB wheel. These wheels are therefore, recommended for grinding of materials such as tungsten carbides.

Results of conventional and ELID grinding with cast iron powder bonded wheel under the same cutting conditions are shown in Figures 18 and 19. ELID dressing was performed with 90 V for 30 minutes. ELID produced significantly lower grinding force compared to conventional grinding. In conventional grinding, self-dressing was observed after 7000 mm³ of material removal. Such self-dressing was not observed when grinding was performed with the CIFB-D wheel (see Fig. 5). This is because that the cast iron fiber bond is stronger than cast iron powder bonded wheels.

4.4 Results with Wheels with Different Abrasive Friability

The next series of experiments was performed with grinding wheels with different abrasive friability. Diamond grinding wheels with MBG 660, RVG, and MBG 600 diamond were used in those experiments. RVG diamond is the most friable one and MBG-660 is the least friable. The bond material for all the wheels was steel. The cutting force and the G-ratio were monitored in this series of experiments.

There is a reduction in G-ratio when grinding was performed with ELID. These results are presented in Table II. It should be noted that for high material removal rates with conventional grinding frequent wheel dressing is required. This is a non-productive part of the time, and for metal bonded wheels it may be quite high. Dressing will also remove some amount of diamond layer from the wheel. In ELID grinding however, the force remains lower and almost constant grinding can be performed for a very long time. The relationship between the volume of material removed and the normal grinding force with the above-mentioned wheels for conventional and ELID grinding are presented in Figures 20 through 25. Compared to conventional grinding a significant reduction in grinding force was noticed when ELID grinding was performed.

TABLE II. COMPARISON OF G-RATIOS FOR SILICON NITRIDE

	G-RATIO			
WHEEL TYPE	CONVENTIONAL GRINDING	ELID GRINDING		
MBG-600	131	87		
RVG	175	105		
MBG-660	134	66		
C.I. POWDERBONDED	174	58		

[RVG: MOST FRIABLE, MBG-660: LEAST FRIABLE, STEEL BONDED WHEELS]
CUTTING CONDITIONS:V=1200 m/min; f=5000 mm/min; DOC=0.05 mm; WOC= 2 mm; GRIT= # 140

5.0 CONCLUSIONS

- a) Compared to conventional grinding, there is a significant reduction of normal grinding force with ELID grinding. Therefore, ELID grinding is recommended for heavy material removal grinding, low rigidity machines, and low rigidity workpieces.
- b) The full potential of ELID grinding i.e., reduced grinding force can be utilized only after it has been stabilized. However, the newly proposed modified ELID dressing can provide reduced and almost constant grinding force immediately at the start of grinding.
- c) Compared to conventional grinding, a reduction in G-ratio was found when ELID grinding was performed. G-Ratio can be improved by optimizing the ELID current.

6.0 ACKNOWLEDGEMENTS

This research was sponsored by the U. S. Department of Energy, Assistant Secretary for Energy Efficiency and Renewable Energy, Office of Transportation Technologies, as part of the Propulsion System Materials Program, under contract No. 80X-ST621V with Lockheed Marietta Energy Systems, Inc.

7.0 REFERENCES

1 .B. P. Bandyopadhyay, "Electrolytic-In-Process Dressing (ELID) for High Efficiency, Precision Grinding of Ceramic Parts: An Experimental Study," ORNL Report # ORNL/SUB/94-SR707/1.

- 2. Ohmori, H., Takahashi, I, and Bandyopadhyay, B. P., "Ultraprecision Grinding of Structural Ceramics by Electrolytic In-Process Dressing," Accepted for publication in the *Journal of Materials Processing Technology*, Elsevier Science, Switzerland.
- 3. Ohmori, H., Takahashi, I, and Bandyopadhyay, B. P., "Highly Efficient Grinding of Ceramic Parts by Electrolytic In-Process Dressing (ELID) Grinding," Accepted for publication in the *Journal of Materials and Manufacturing Processes*, Marcel Dekker, N.Y.

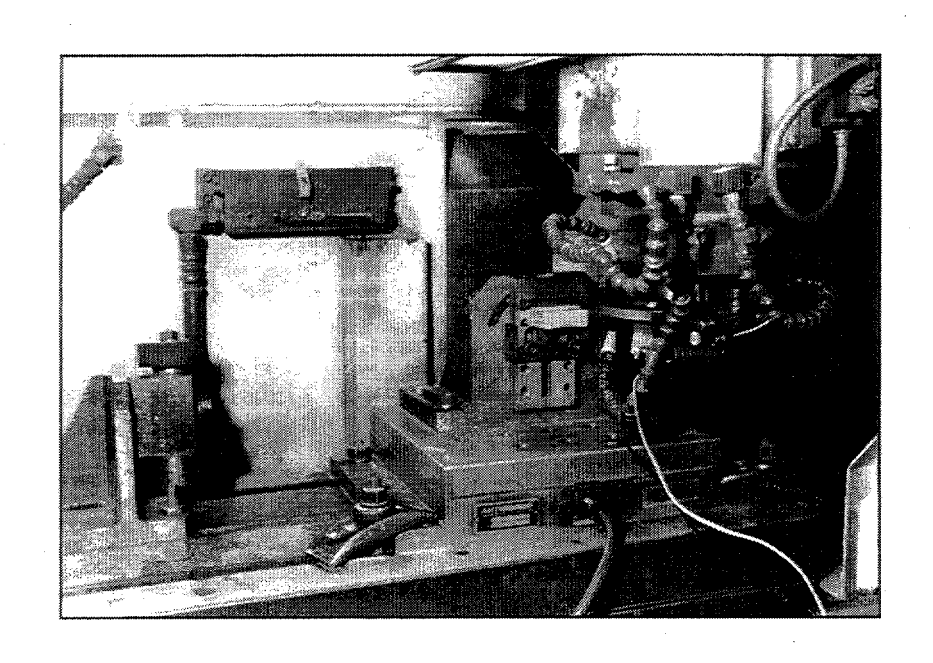


FIGURE 1: EXPERIMENTAL SET UP



FIGURE 2: GRINDING WHEELS



FIGURE 3: POWER SUPPLY

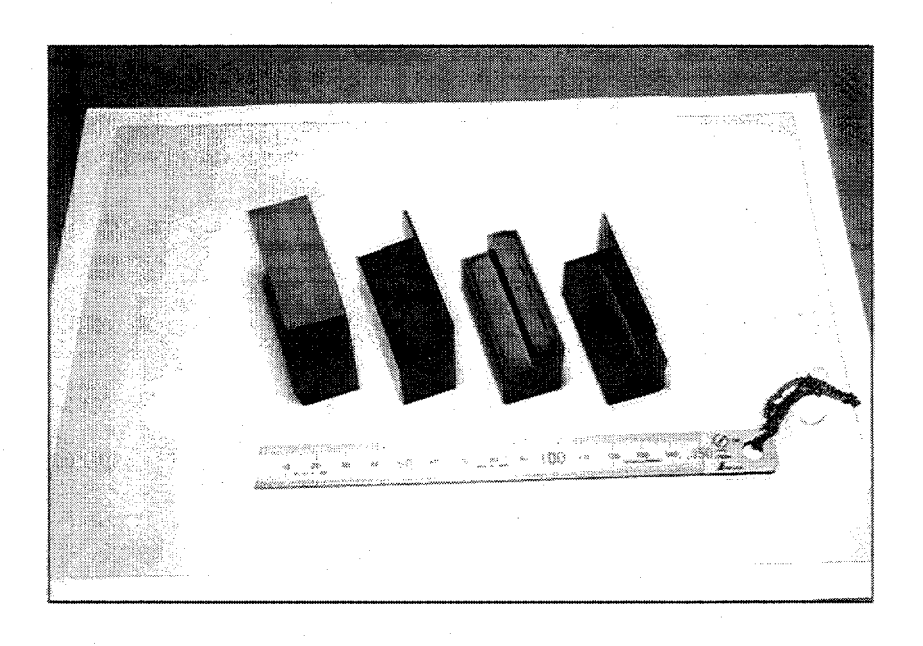


FIGURE 4: WORKPIECE MATERIAL

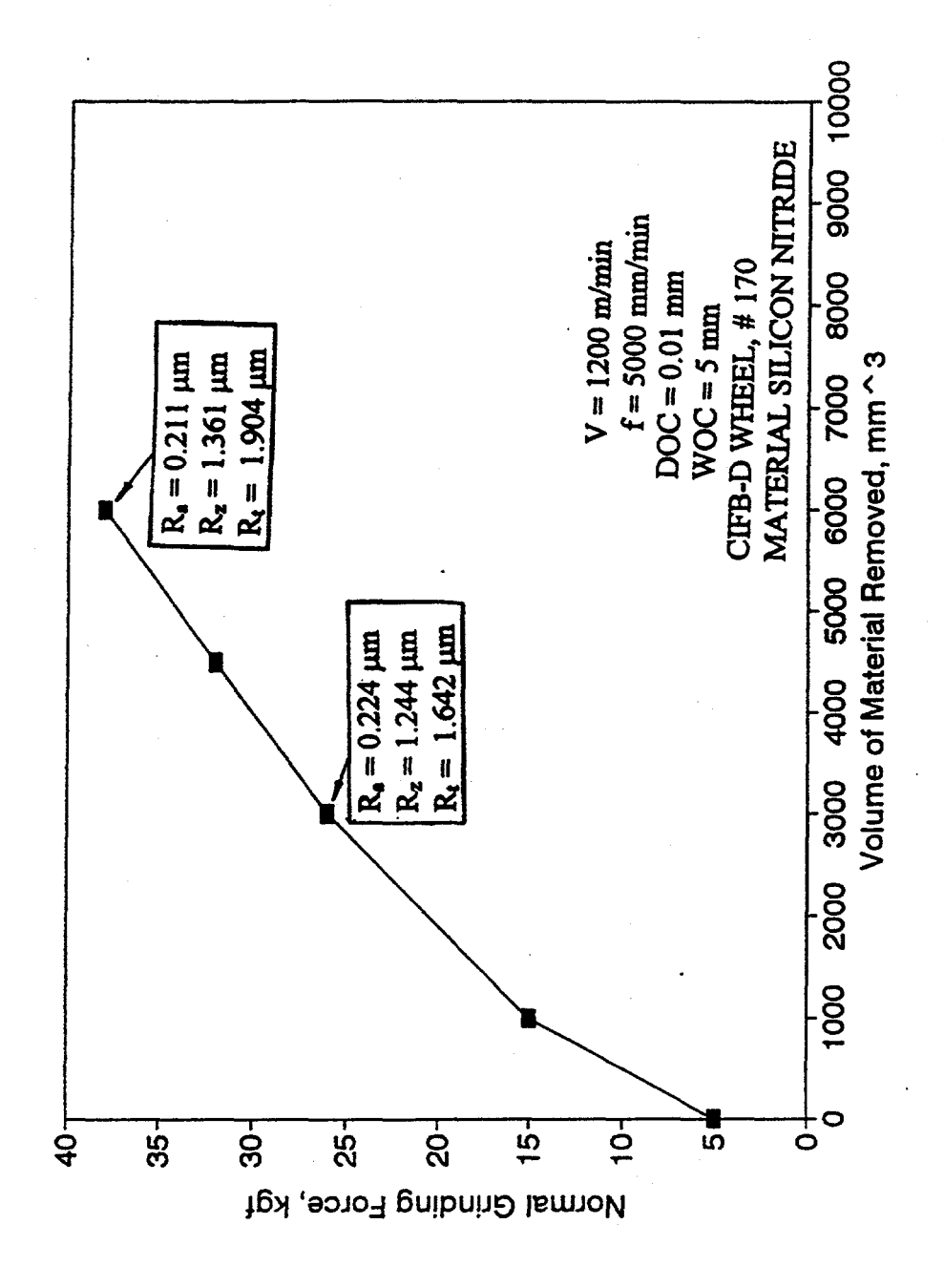
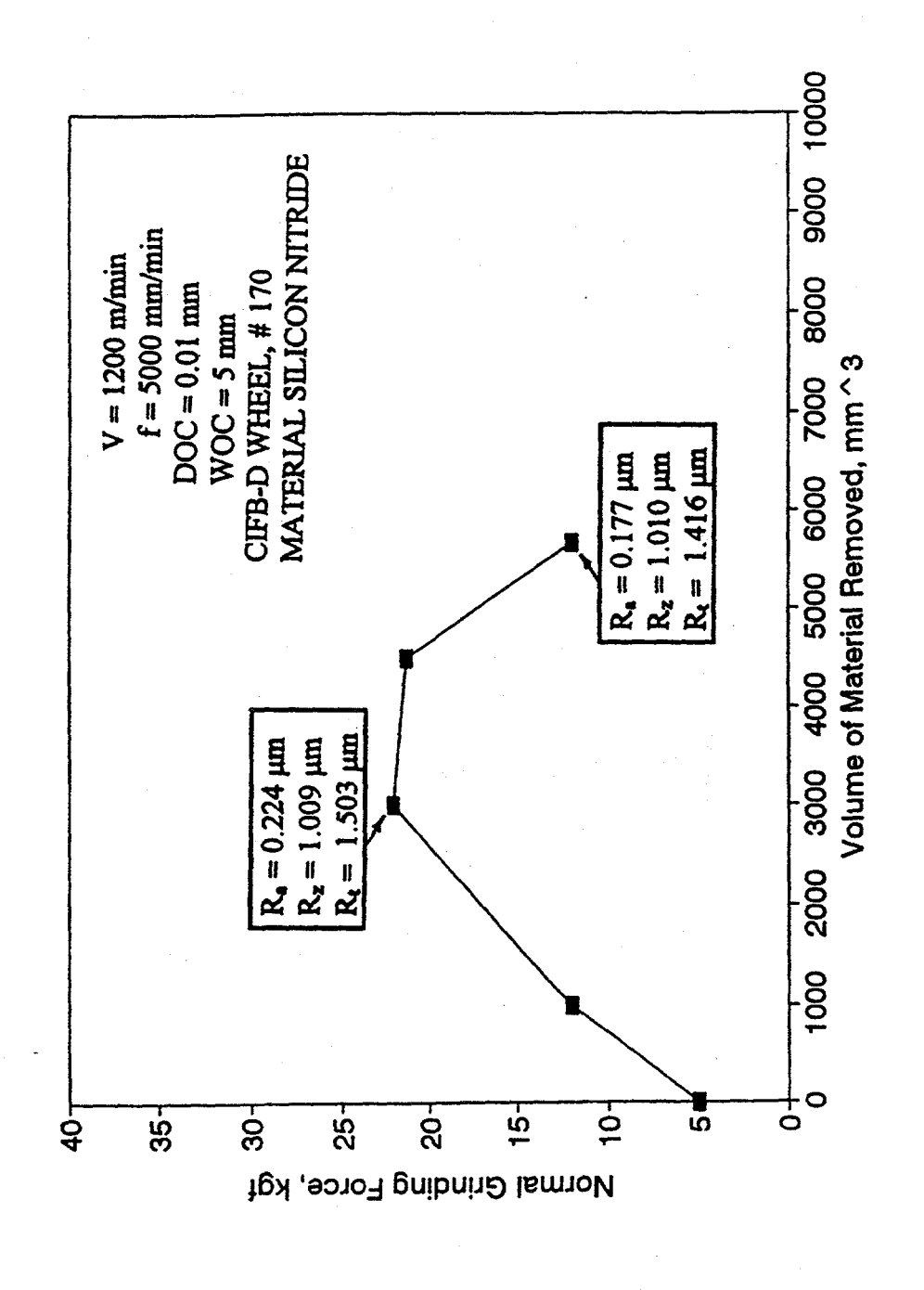


FIGURE 5: RELATIONSHIP BETWEEN THE VOLUME OF MATERIAL REMOVED AND THE NORMAL GRINDING FORCE (CONVENTIONAL GRINDING)



RELATIONSHIP BETWEEN THE VOLUME OF MATERIAL REMOVED (ELID GRINDING, V = 60 Volt, $I_p = 16$ amp, $\tau_{on} = \tau_{off} = 4 \mu s$) AND THE NORMAL GRINDING FORCE FIGURE 6:

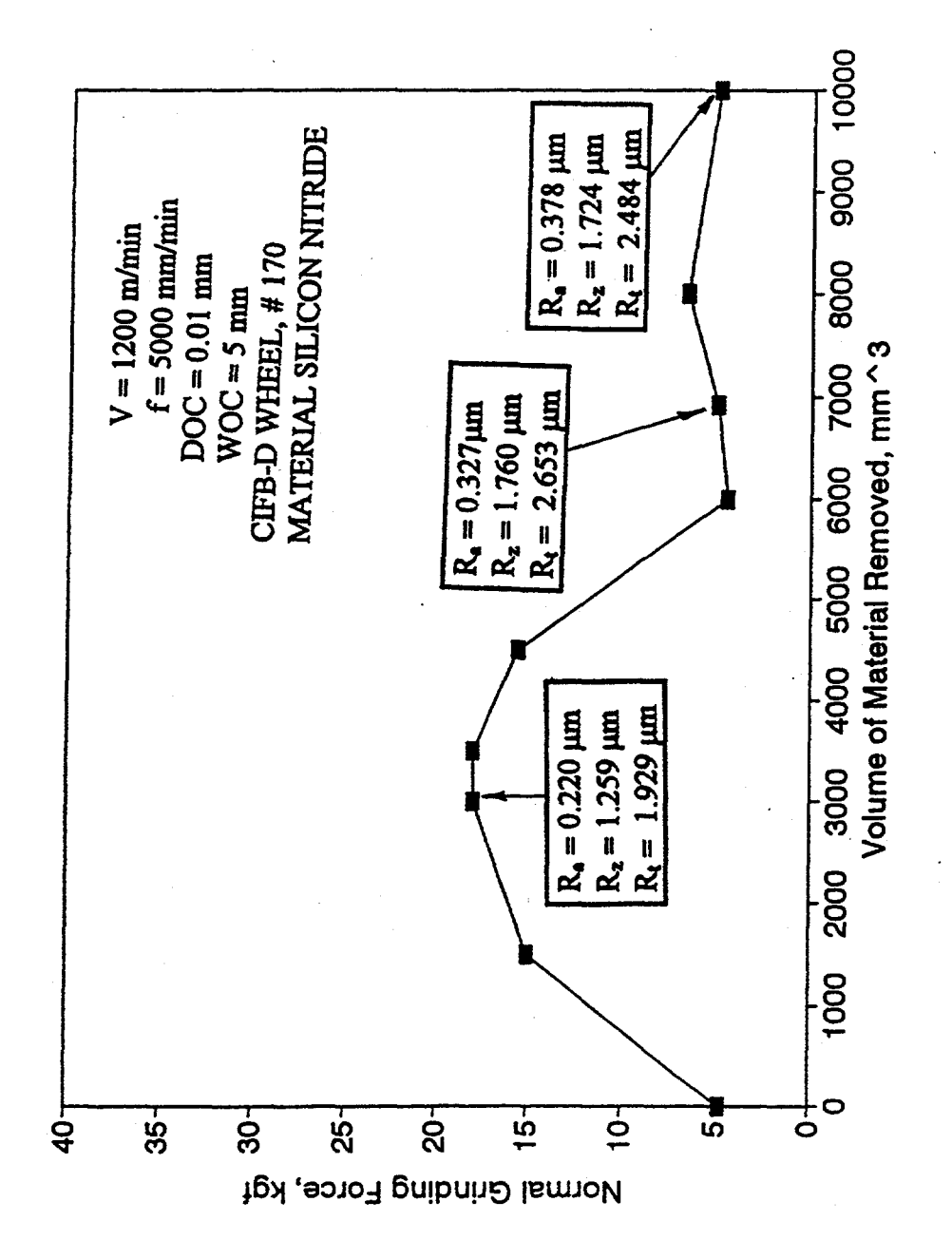
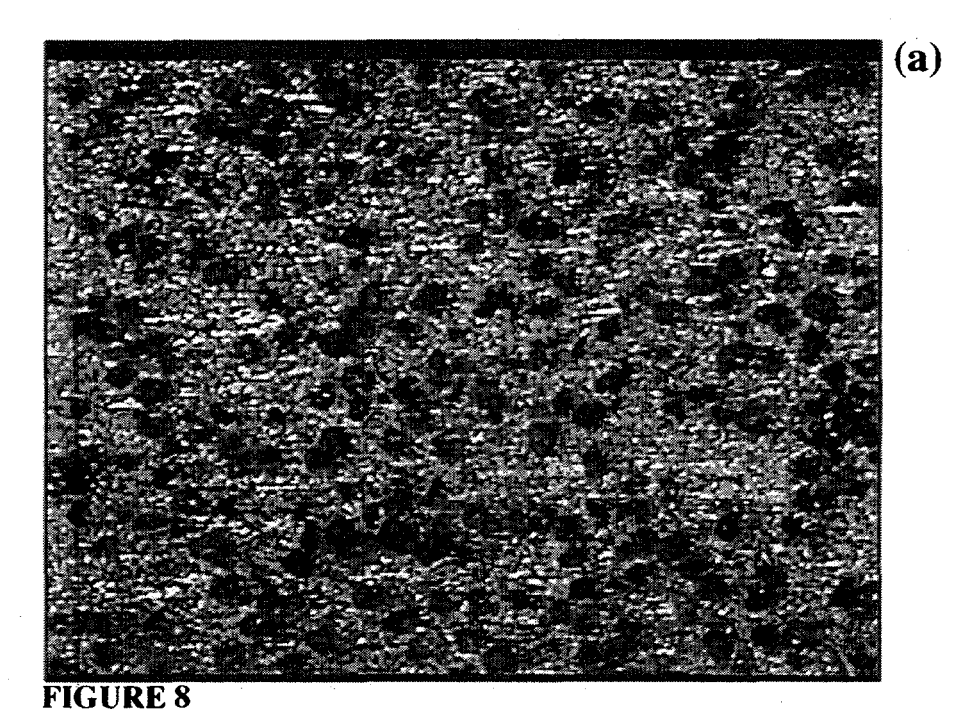


FIGURE 7: RELATIONSHIP BETWEEN THE VOLUME OF MATERIAL REMOVED (ELID GRINDING, V = 90 Volt, $I_p = 24$ amp, $\tau_{on} = \tau_{off} = 4 \mu s$) AND THE NORMAL GRINDING FORCE

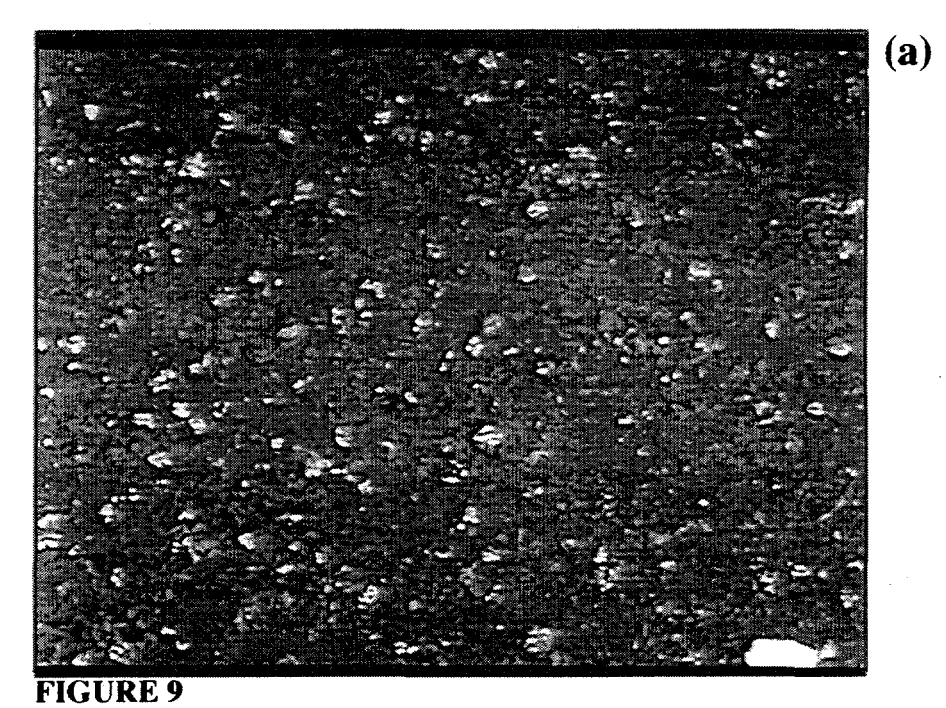


GRINDING WHEEL SURFACE AFTER TRUING AND MECHANICAL DRESSING

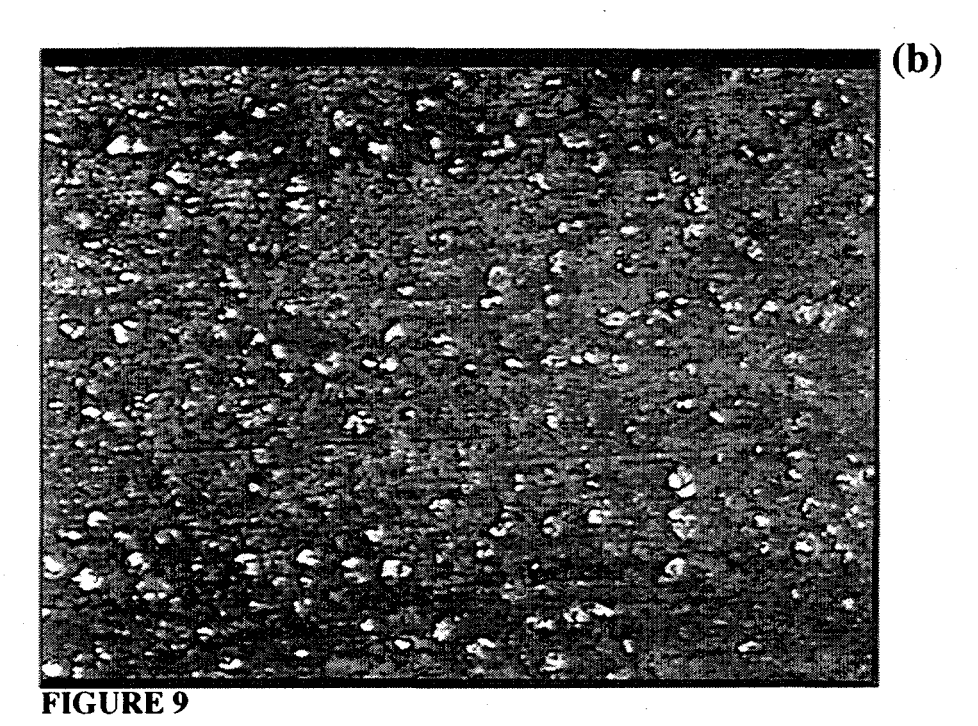


FIGURE 8

GRINDING WHEEL SURFACE AFTER CONVENTIONAL GRINDING



GRINDING WHEEL SURFACE AFTER ELID DRESSING



GRINDING WHEEL SURFACE AFTER ELID GRINDING

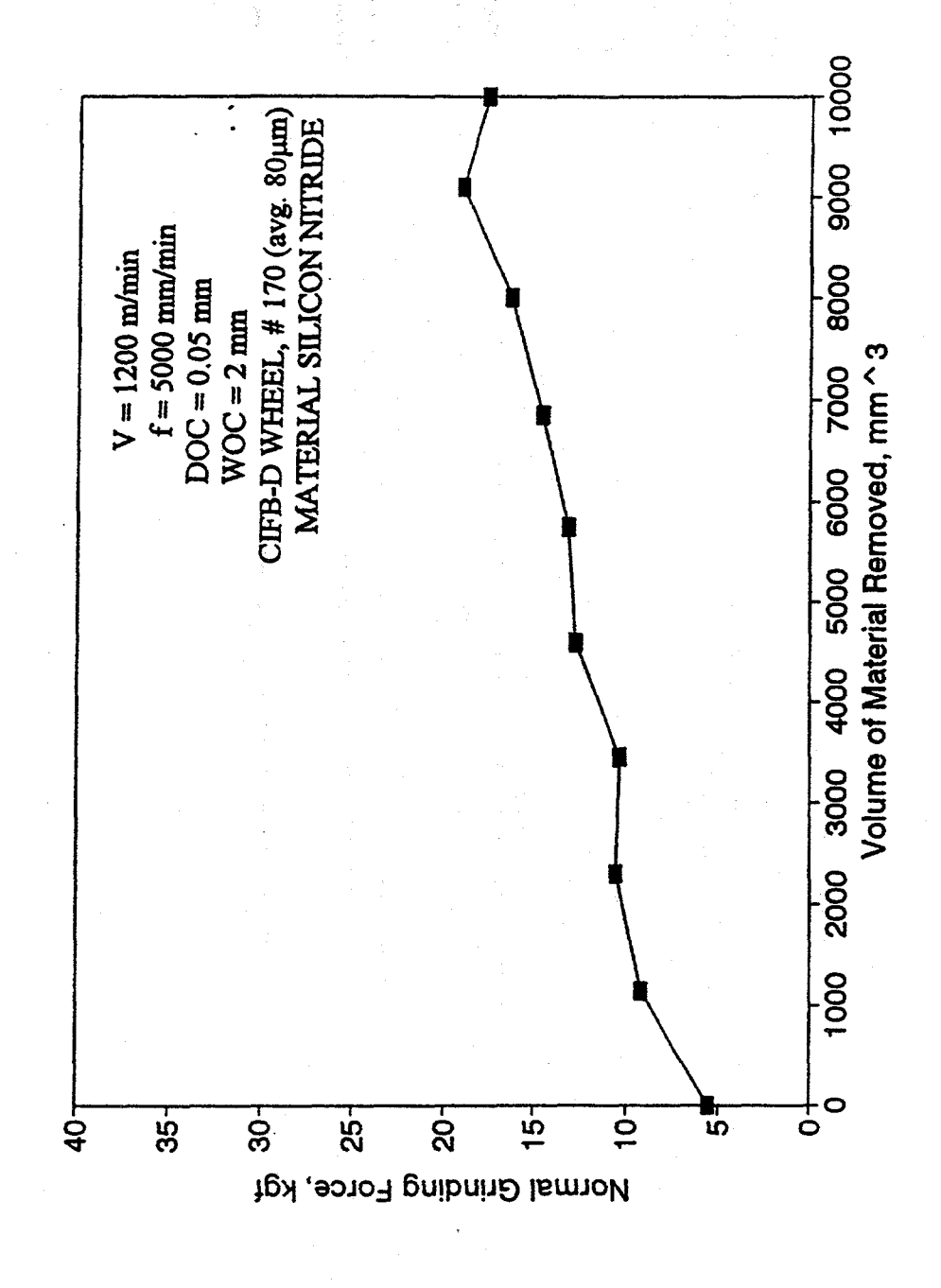


FIGURE 10: RELATIONSHIP BETWEEN THE VOLUME OF MATERIAL REMOVED AND THE NORMAL GRINDING FORCE (CONVENTIONAL GRINDING)

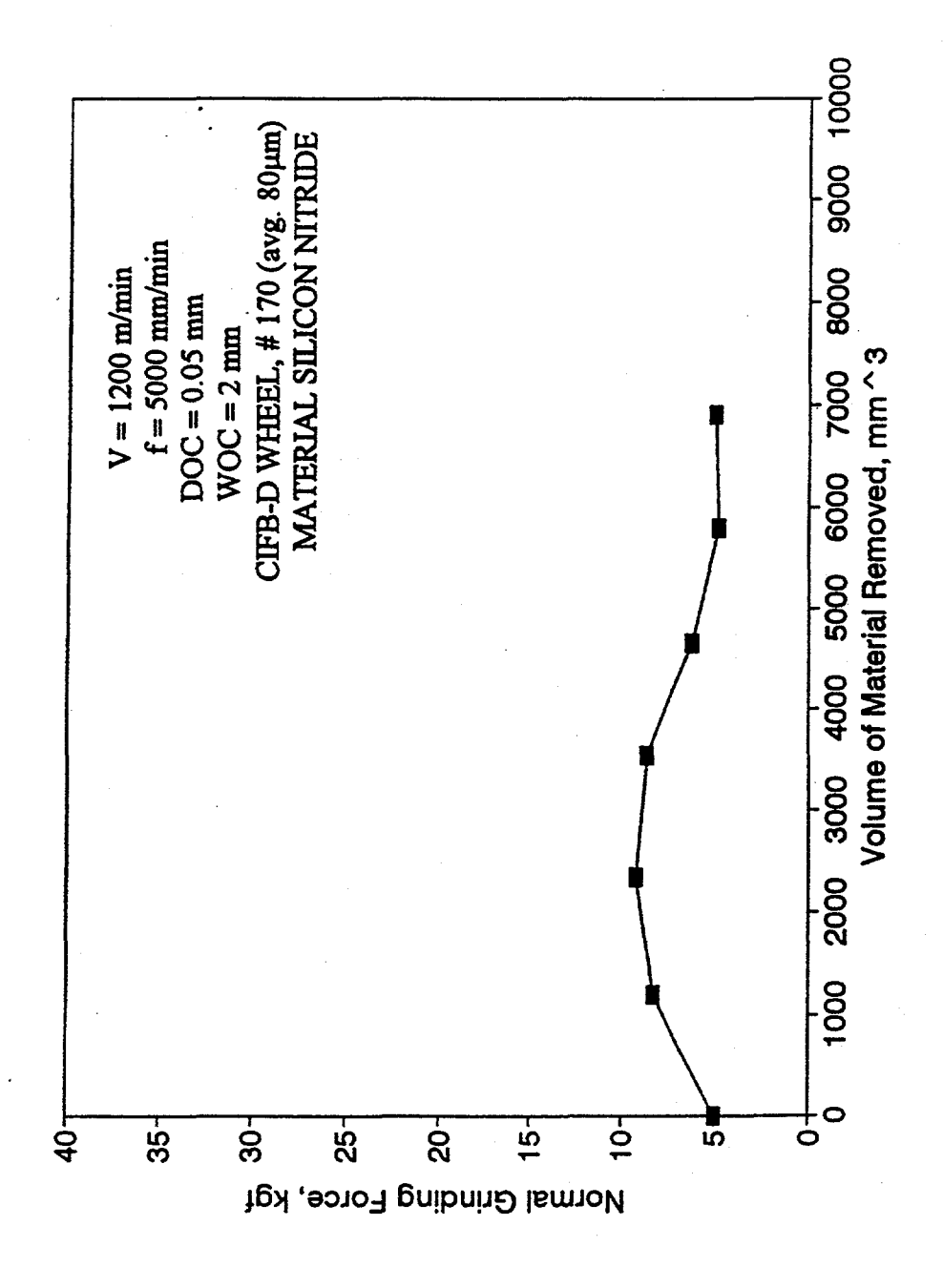
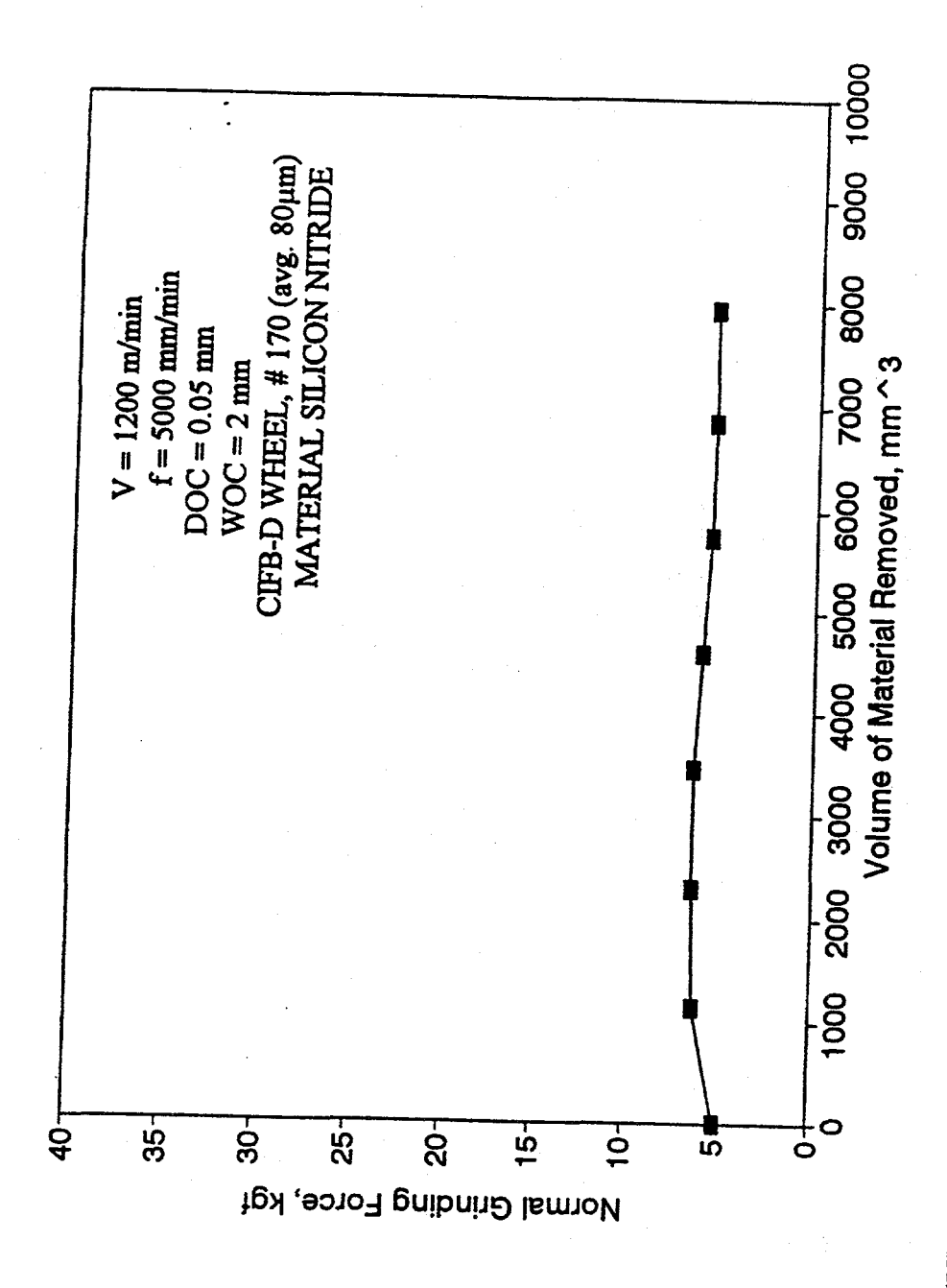


FIGURE 11: RELATIONSHIP BETWEEN THE VOLUME OF MATERIAL REMOVED (ELID GRINDING, V = 60 Volt, $I_p = 16$ amp, $\tau_{on} = \tau_{off} = 4 \mu s$) (ELID DRESSED FOR 30 min WITH 90 Volt) AND THE NORMAL GRINDING FORCE



RELATIONSHIP BETWEEN THE VOLUME OF MATERIAL REMOVED (ELID GRINDING, V = 60 Volt, $I_p = 16 \text{ amp}$, $\tau_{on} = \tau_{off} = 4 \mu s$) AND THE NORMAL GRINDING FORCE FIGURE 12:

(ELID DRESSED IN TWO STAGES: 1. AT 90 Volt FOR 30 min

2. REMOVE THE OXIDE LAYER THEN ELID DRESSED AT 90 Volt FOR 30 min)

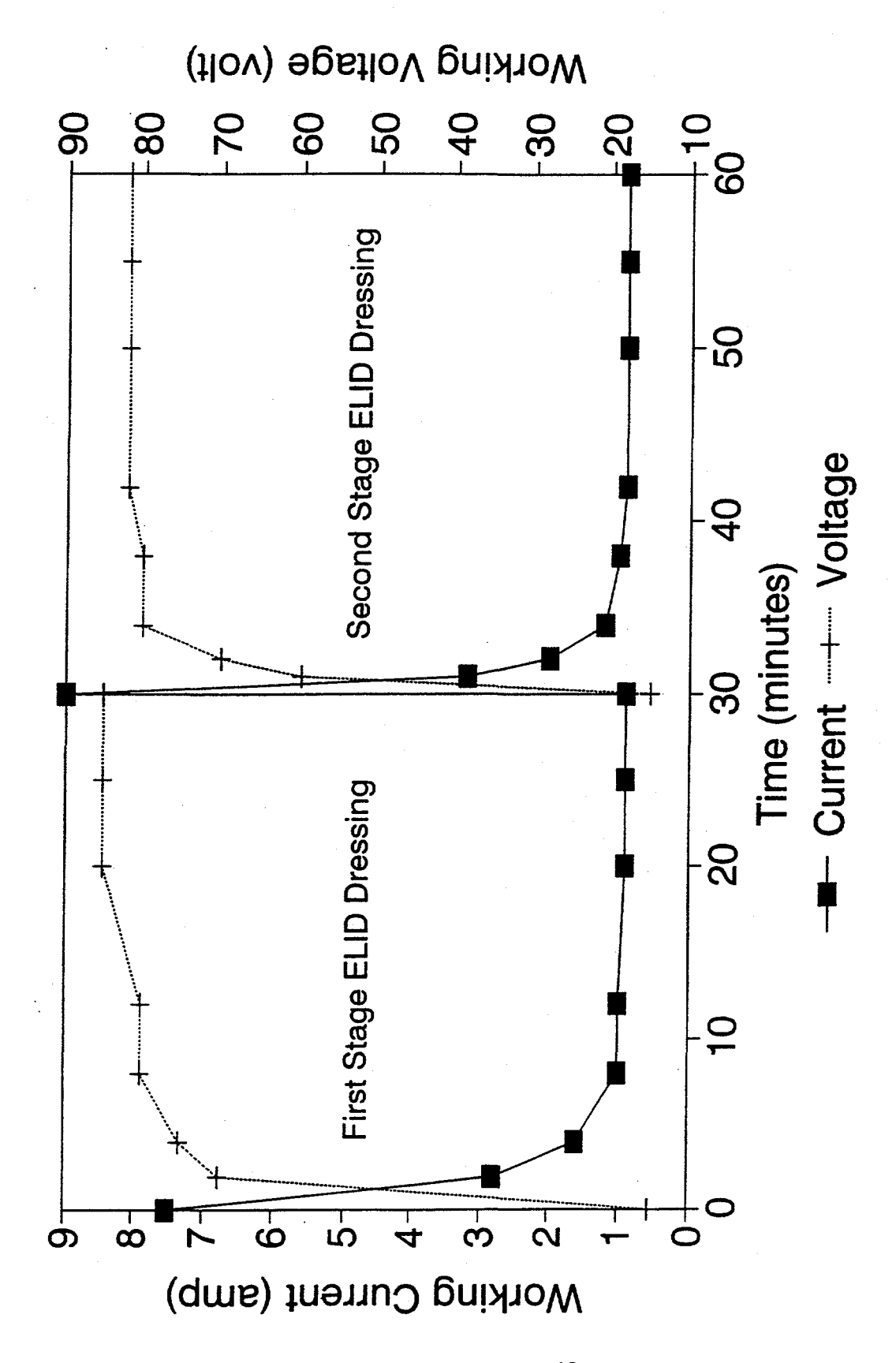
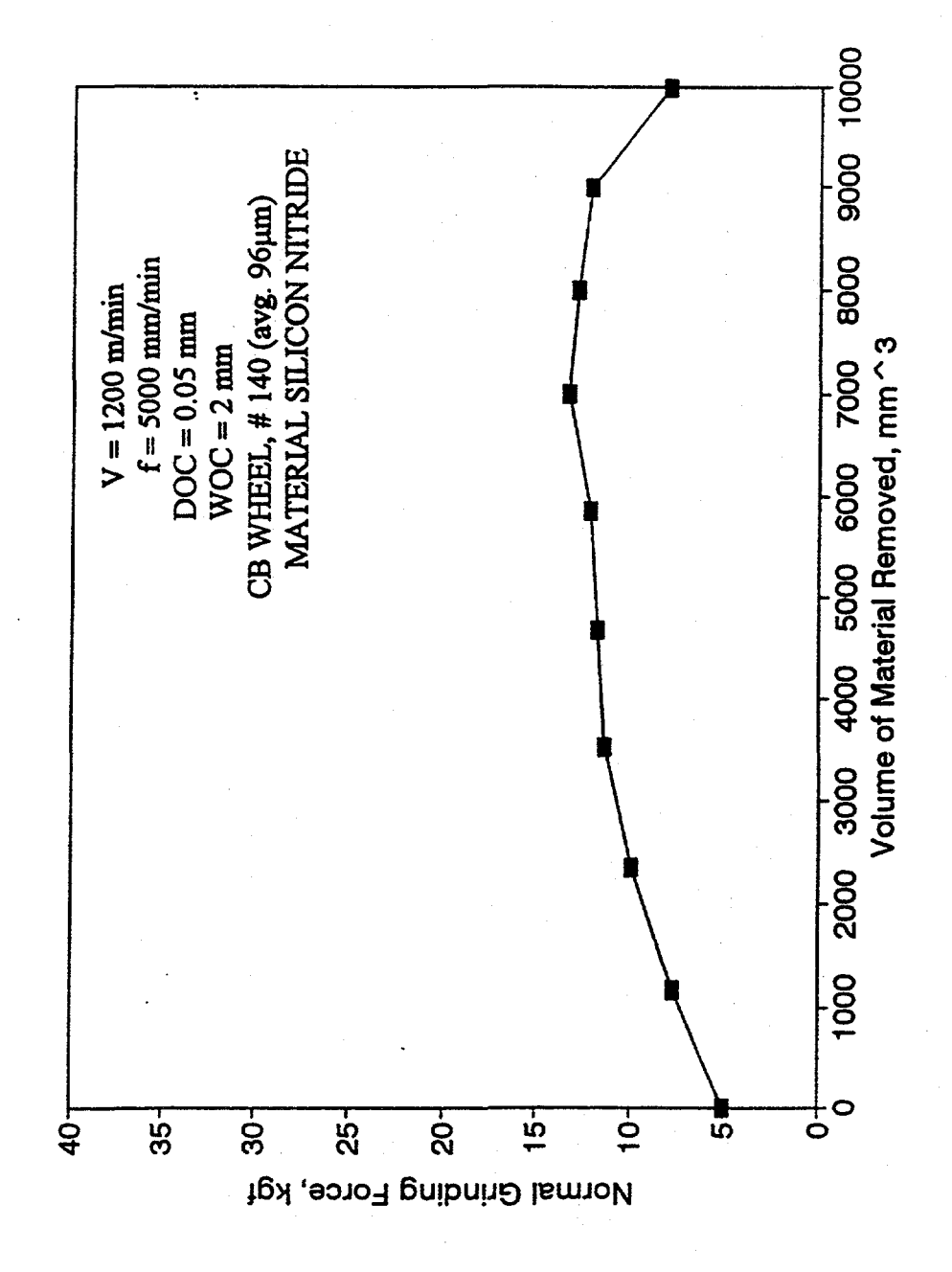
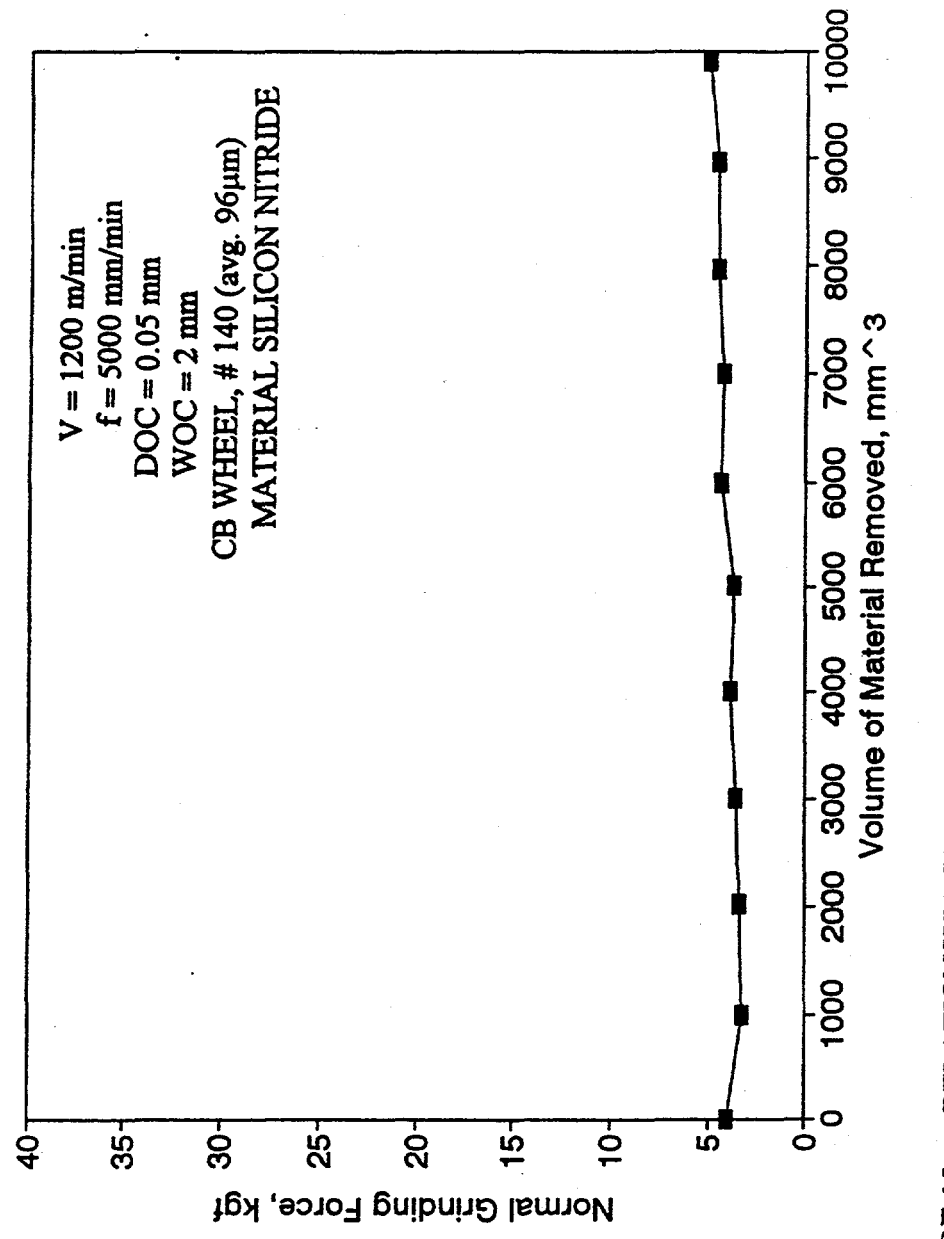


FIGURE 13: ELECTRICAL BEHAVIOR OF MODIFIED ELID DRESSING



RELATIONSHIP BETWEEN THE VOLUME OF MATERIAL REMOVED AND THE NORMAL GRINDING FORCE (CONVENTIONAL GRINDING) FIGURE 14:



RELATIONSHIP BETWEEN THE VOLUME OF MATERIAL REMOVED (ELID GRINDING, V = 60 Volt, $I_p = 16$ amp, $\tau_{on} = \tau_{off} = 4 \mu s$) (ELID DRESSED FOR 30 min WITH 60 Volt) AND THE NORMAL GRINDING FORCE FIGURE 15:

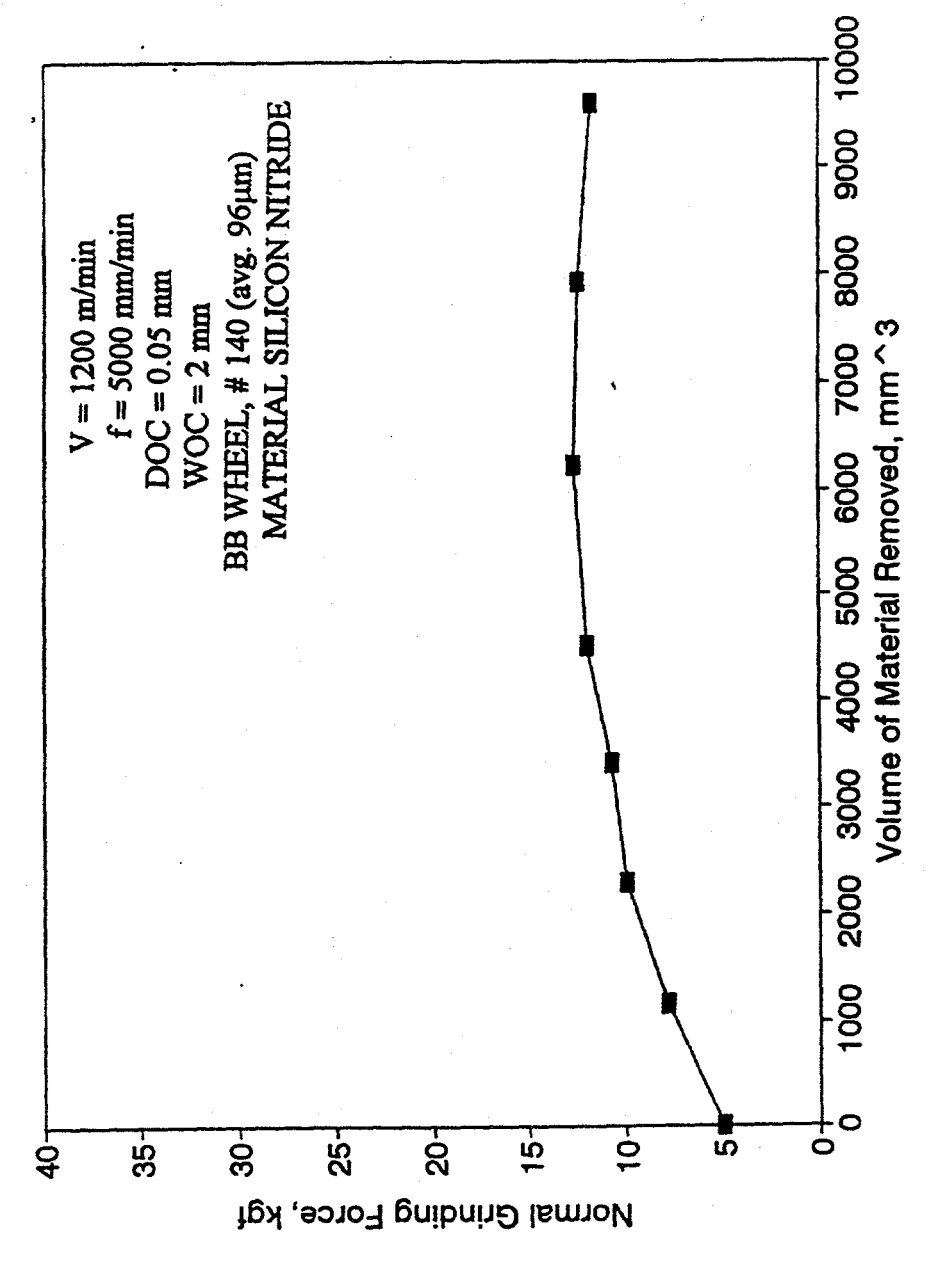


FIGURE 16: RELATIONSHIP BETWEEN THE VOLUME OF MATERIAL REMOVED AND THE NORMAL GRINDING FORCE (CONVENTIONAL GRINDING)

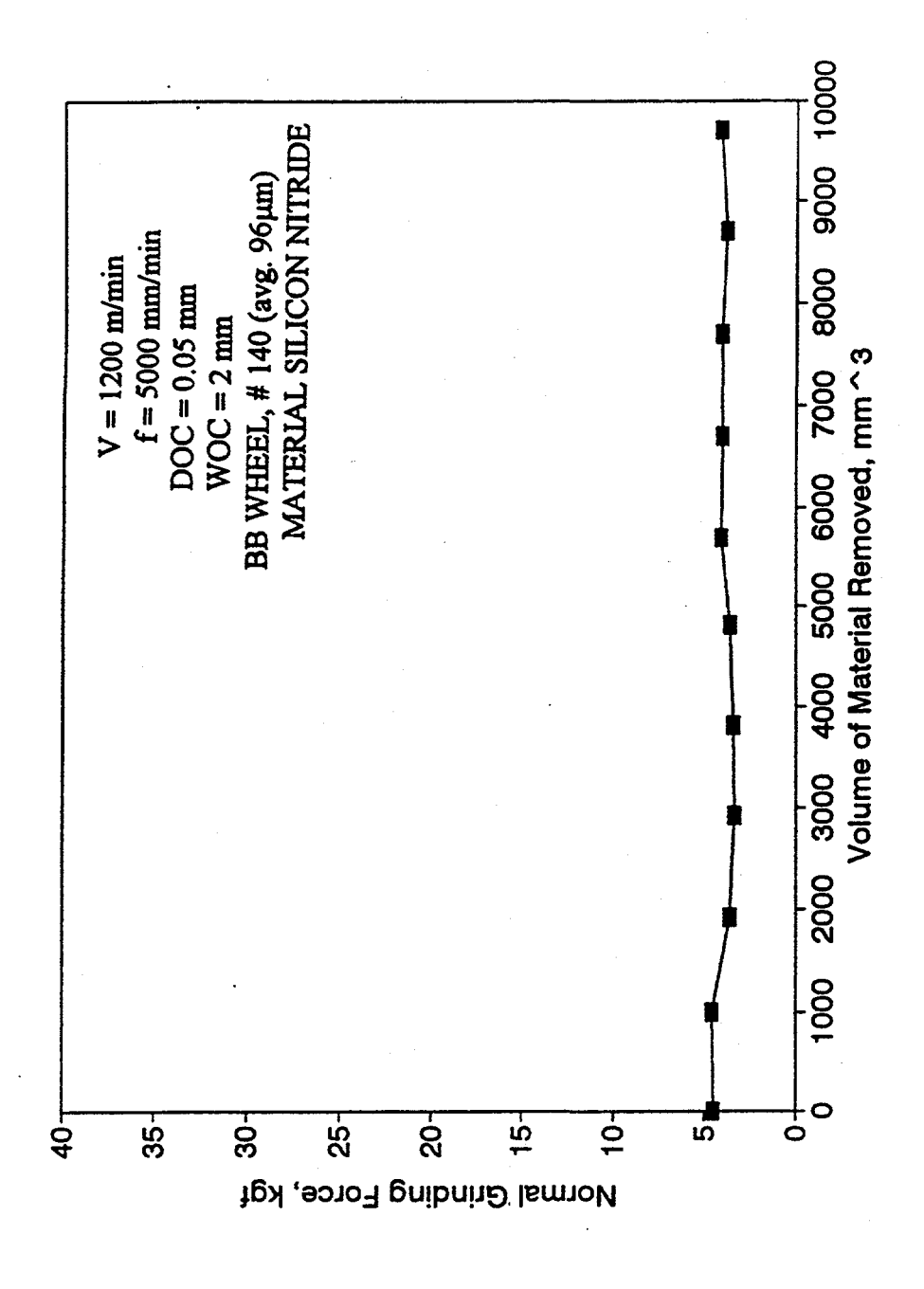


FIGURE 17: RELATIONSHIP BETWEEN THE VOLUME OF MATERIAL REMOVED (ELID GRINDING, V = 60 Volt, I_p = 16 amp, $\tau_{on} = \tau_{off} = 4 \mu s$) (ELID DRESSED FOR 30 min WITH 60 Volt) AND THE NORMAL GRINDING FORCE

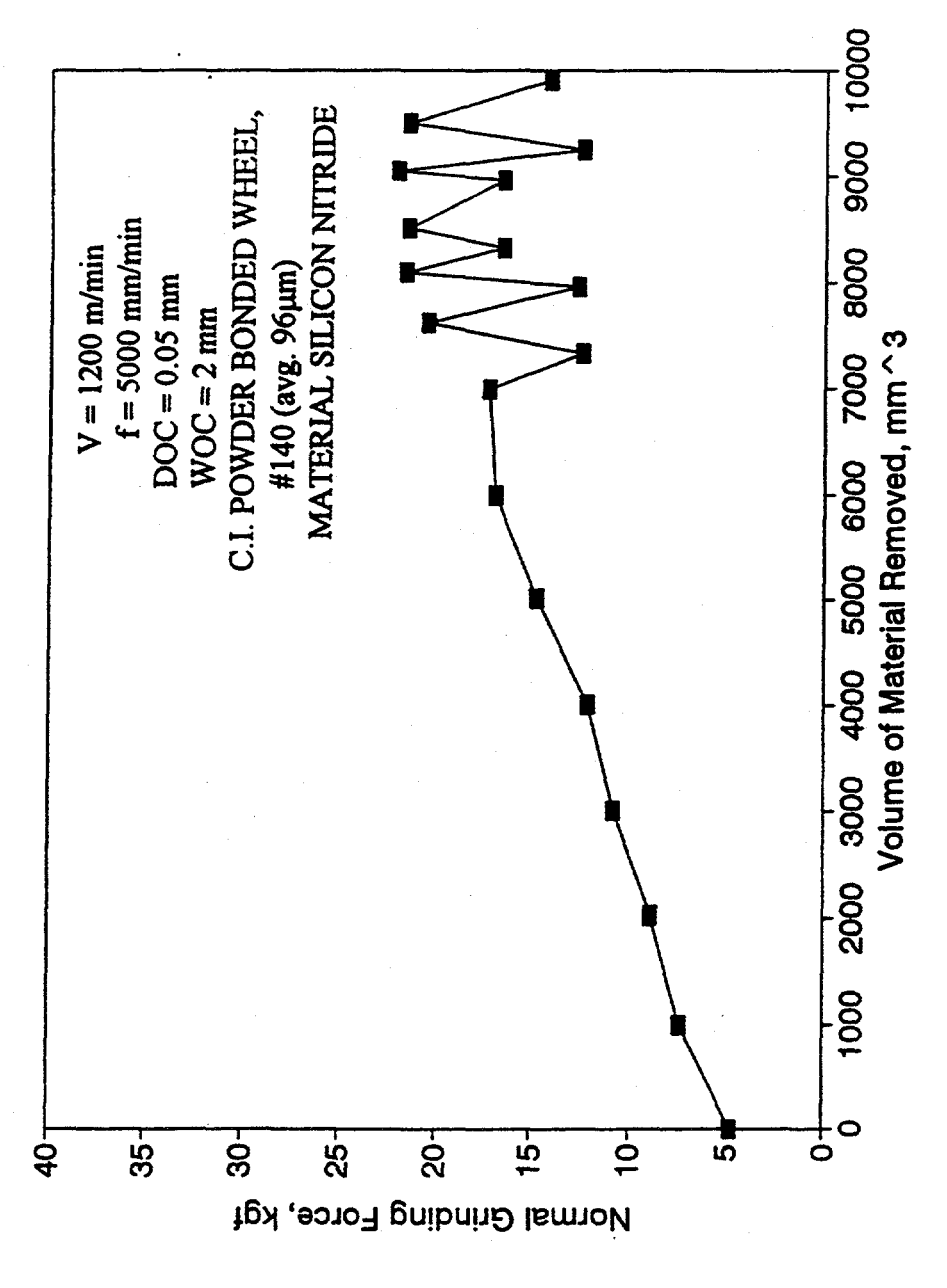
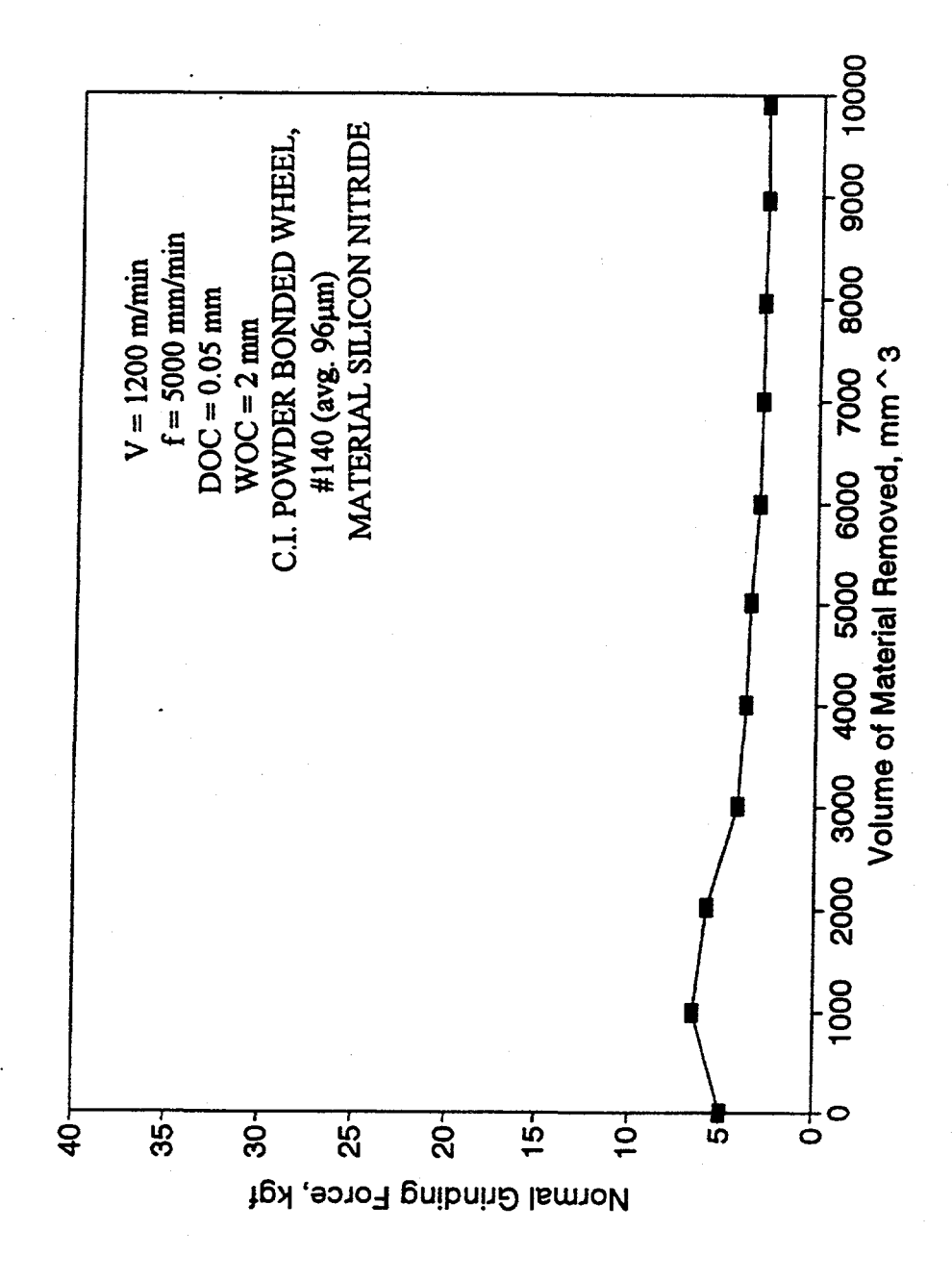
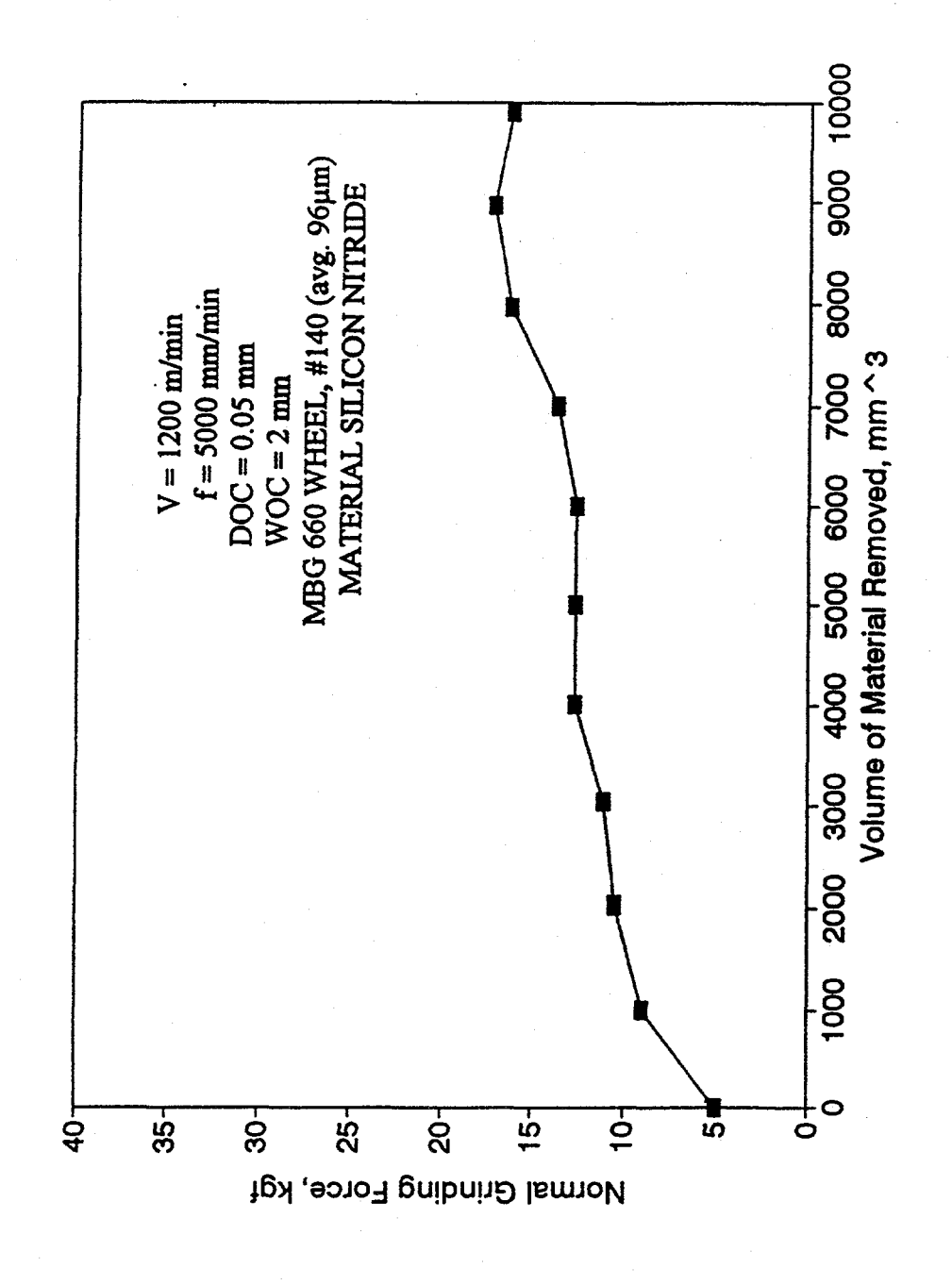


FIGURE 18: RELATIONSHIP BETWEEN THE VOLUME OF MATERIAL REMOVED AND THE NORMAL GRINDING FORCE (CONVENTIONAL GRINDING)



RELATIONSHIP BETWEEN THE VOLUME OF MATERIAL REMOVED (ELID GRINDING, V = 60 Volt, $I_p = 16 \text{ amp}$, $\tau_{on} = \tau_{off} = 4 \mu s$) (ELID DRESSED FOR 30 min WITH 90 Volt) AND THE NORMAL GRINDING FORCE FIGURE 19:



RELATIONSHIP BETWEEN THE VOLUME OF MATERIAL REMOVED AND THE NORMAL GRINDING FORCE (CONVENTIONAL GRINDING) FIGURE 20:

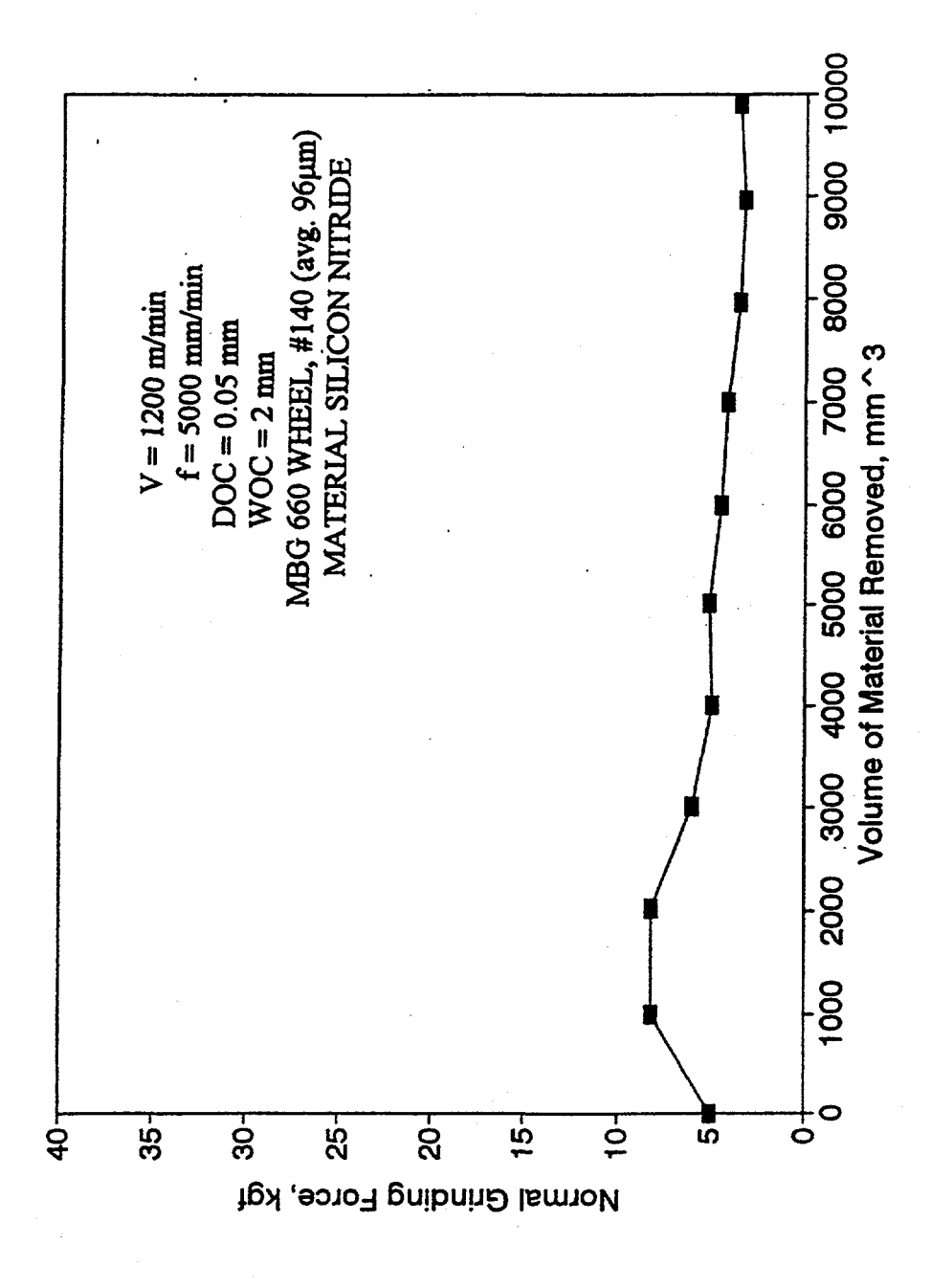
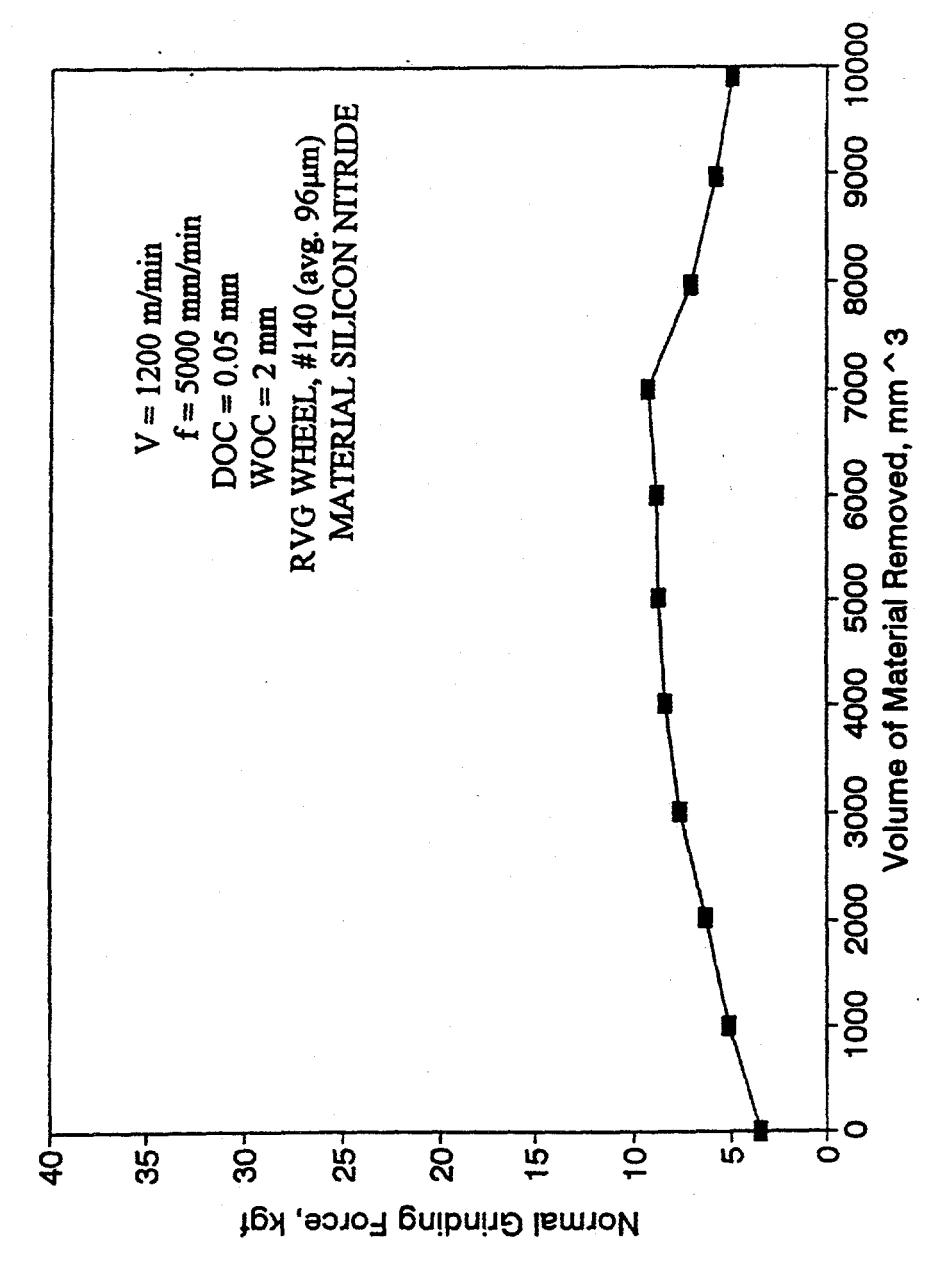
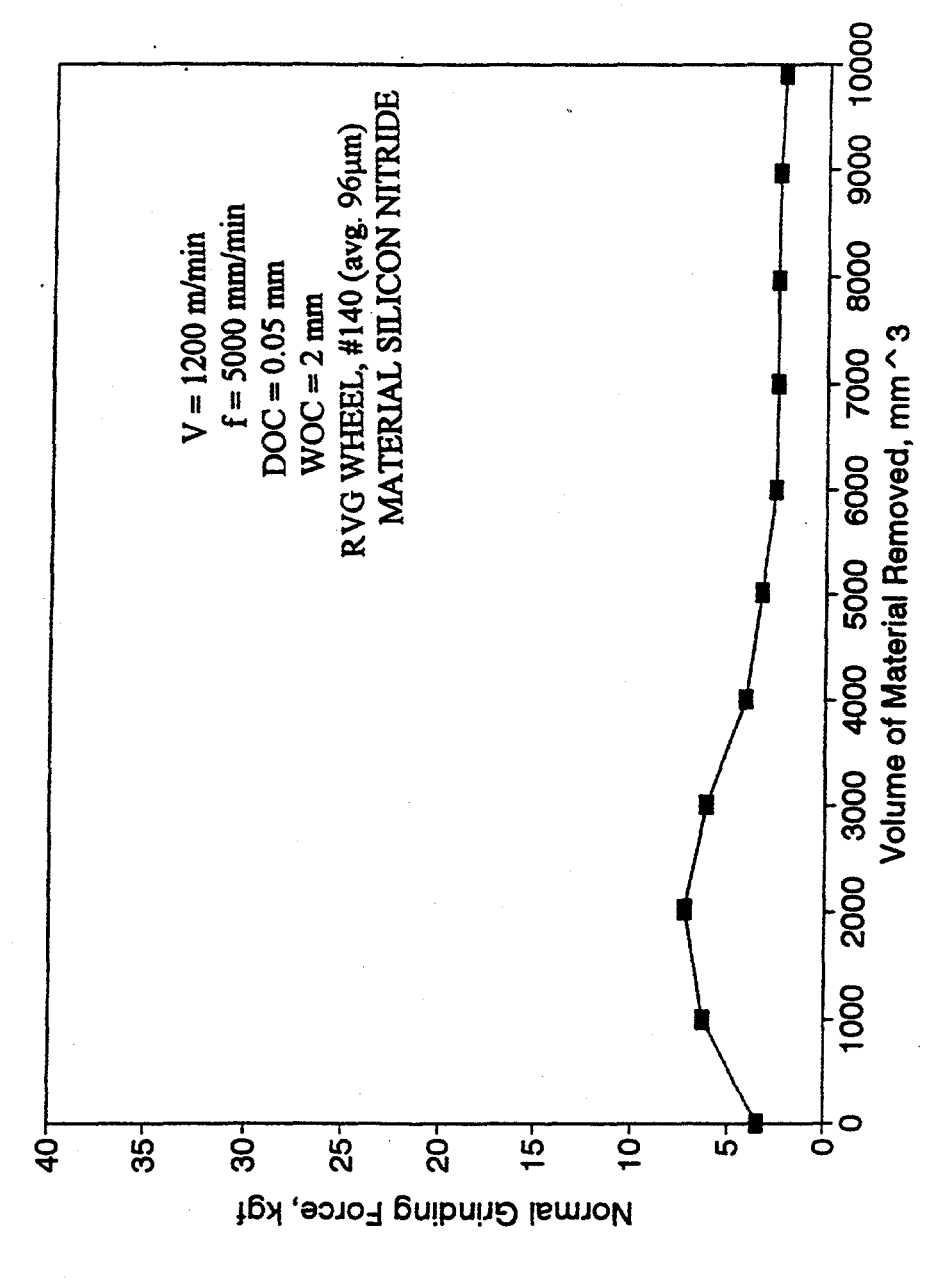


FIGURE 21: RELATIONSHIP BETWEEN THE VOLUME OF MATERIAL REMOVED (ELID GRINDING, V = 60 Volt, $I_p = 16$ amp, $\tau_{on} = \tau_{off} = 4 \mu s$) (ELID DRESSED FOR 30 min WITH 90 Volt) AND THE NORMAL GRINDING FORCE



RELATIONSHIP BETWEEN THE VOLUME OF MATERIAL REMOVED AND THE NORMAL GRINDING FORCE (CONVENTIONAL GRINDING) FIGURE 22:



RELATIONSHIP BETWEEN THE VOLUME OF MATERIAL REMOVED (ELID GRINDING, V = 60 Volt, $I_p = 16$ amp, $\tau_{on} = \tau_{off} = 4 \mu s$) (ELID DRESSED FOR 30 min WITH 90 Volt) AND THE NORMAL GRINDING FORCE FIGURE 23:

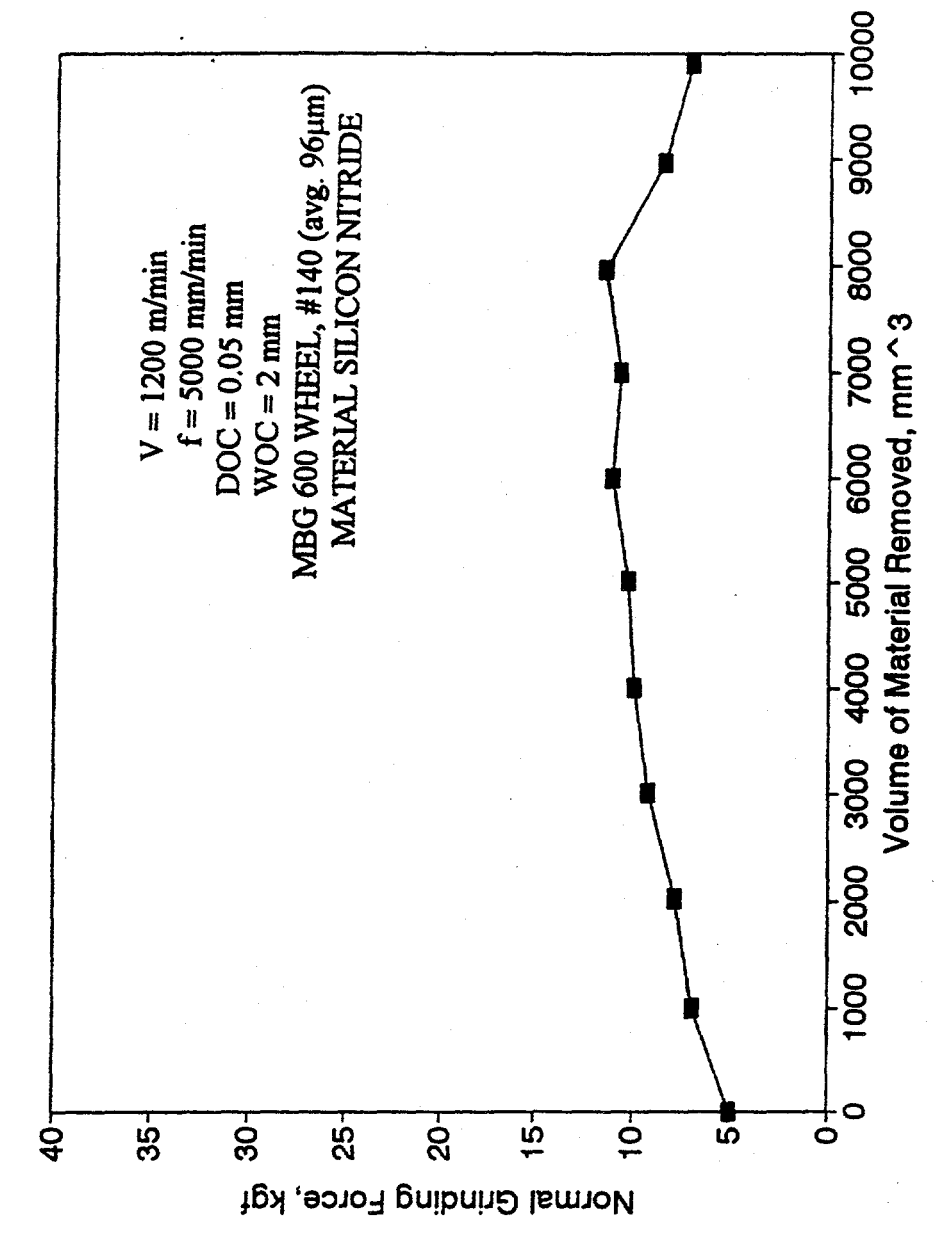


FIGURE 24: RELATIONSHIP BETWEEN THE VOLUME OF MATERIAL REMOVED AND THE NORMAL GRINDING FORCE (CONVENTIONAL GRINDING)

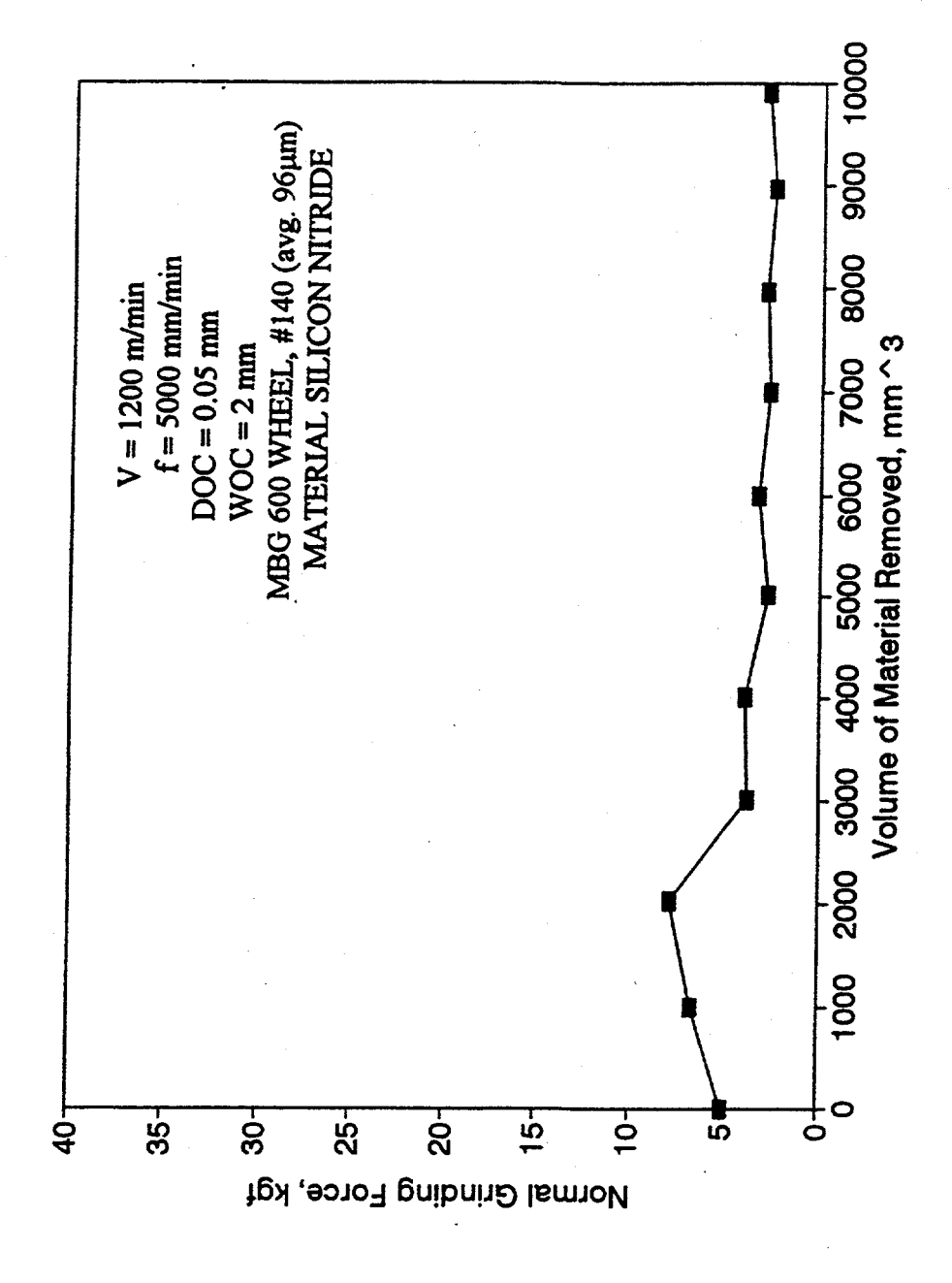


FIGURE 25: RELATIONSHIP BETWEEN THE VOLUME OF MATERIAL REMOVED (ELID GRINDING, V = 60 Volt, $I_p = 16 \text{ amp}$, $\tau_{on} = \tau_{off} = 4 \mu s$) (ELID DRESSED FOR 30 min WITH 90 Volt) AND THE NORMAL GRINDING FORCE

APPLICATION OF ELECTROLYTIC IN-PROCESS DRESSING (ELID) FOR HIGH EFFICIENCY GRINDING OF CERAMIC PARTS

Part 2: 1996

TABLE OF CONTENTS

		PAG	E
A.		ECT OF ELID GRINDING ON THE STRENGTH OF THE SILICON	
	NITRID:	E SPECIMENS 3	5
	1.0	INTRODUCTION	5
			-
	2.0	RESULTS 3	5
	3.0	DISCUSSION OF THE RESULTS	6
		3.1 SEM Topography of ELID Ground Ceramics	
		3.2 AFM Topography of ELID Ground Ceramics	7
	4.0	CONCLUSIONS	7
В.	PREC	ISION SURFACE GRINDING CHARACTERISTICS OF CERAMIC MATRIX	
٠.		POSITE AND STRUCTURAL CERAMICS WITH ELID	
	1.0	INTRODUCTION	8
	2.0	EXPERIMENTAL METHODS AND MACHINING CONDITIONS 3	ያ
	2.0	2.1 Materials	
		2.2 Grinding Wheels	
		2.3 Machining Conditions	
		2.4 Power Supply	
		2.5 Measuring Instruments Used	
	3.0	RESULTS AND DISCUSSION 4	1
		3.1 Surface Roughness by each Wheel	
		3.2 Grinding Resistance	
		3.3 SEM Observation Results	
		3.4 Dulled Area at Ground Edges	
	4.0	CONCLUSIONS	3
AC	KNOWLI	EDGMENTS	4
KEI	LKENC	SS	4

LIST OF TABLES

	PAG	GE
1.	Grain Size of Diamond Grinding Wheels Used	36
2.	Surface Roughness of Si_3N_4 by AFM	37
3.	Characteristics of Composite Ceramics and Silicon Carbide	39
4.	Grinding Wheels Used	39
5.	Machining Conditions	40
6.	ELID Conditions	40

LIST OF FIGURES

	PAGE
1.	Effects of the Grinding Direction on the Bending Strength of SiC Specimens 46
2.	Transverse Rupture Strength as a Function of Wheel Grit Size in Longitudinal and Transverse Grinding
3.	Effects of Annealing on Four-Point Bending Strength
4.	Principle of ELID Grinding
5.	The Plate with the MOR Specimens 50
6.	The Effect of ELID Grinding on the Strength of Si ₃ N ₄ Specimens
7.	The Effect of ELID Grinding on the Strength of Si ₃ N ₄ (at elevated temperature) 52
8.	SEM Micrographs
9.	AFM Micrographs
10.	Surface Roughness After Finish Grinding by Different Wheels
11.	Results of 3-Dimensional Surface Profile Measurement
12.	Influence of Wheel Velocity on the Grinding Force Due to Wheel Type 61
13.	Relationship between the Grinding Force and the Volume of Material Removed for Composite Ceramics
14.	Relationship between the Grinding Force and the Volume of Material Removed for Silicon Carbide
15.	SEM Micrographs of CMC after Finish Grinding
16.	Depth and Width of Dulled Area at Edges in Ground Direction 65

A. THE EFFECT OF ELID GRINDING ON THE STRENGTH OF THE SILICON NITRIDE SPECIMENS

1.0 INTRODUCTION

A significant amount of research has been carried out on the effect of grinding parameters on the strength of ground ceramic specimens. Various investigators have also studied the effect of grinding direction. The results of these investigations are shown in Figs. 1-3 [1-4]. Figure 3 also shows the relationship between annealing temperature and bending strength of alumina ceramics at room temperature. It was determined that, before annealing, specimens ground in the transverse direction have a bending strength 60% lower than that of specimens ground longitudinally. The bending strength of the specimens ground in the transverse direction increased with the annealing temperature. At about 1200°C, the strength was approximately equal to that of the specimen ground in the longitudinal direction [4]. However, there is no significant effect of annealing temperature on the bending strength for the specimens ground in the longitudinal direction. No such data is available for silicon nitride specimens. Therefore, experiments were conducted to study the effect of finish ELID grinding on the bending strength of silicon nitride specimens.

2.0 RESULTS

Surface grinding operations were performed on sintered silicon nitride specimens (Kyocera's Si₃N₄ Type SN235). The form of the workpiece is modulus of rupture (MOR) specimens. Specimens were ground in longitudinal (PG) and in transverse (TG) direction using a size #140 grit bronze bonded wheel. The grinding operation was performed using a Kuroda Precision Industries surface grinder model #GS-CHF, with a 2.2 kW spindle. The principle of ELID surface grinding is shown in Fig. 4. A large number of MOR specimens were fixed on a plate with wax and mounted on the table of the grinding machine, as shown in Fig. 5. The following conditions were used: grinding wheel: ϕ 150 W 10 mm; wheel velocity: 1200 m/min; table speed: 20 m/min; traverse pitch 1 mm; depth of cut: 5 μ m; sparkout: 3 passes. The total depth of cut was around 70 μ m.

Four-point bending tests were performed at room temperature and at 1400°C. Room temperature bending test results are presented in the Fig. 6. A significant reduction in the bending strength was noticed when specimens were transversely ground (TG) compared with those ground longitudinally (PG). PG and TG ground specimens were annealed at 1200°C for two hours and the bending strength was determined. The strength of heat treated TG specimens increased significantly, as shown in Fig. 6. There was no significant change in the strength of the PG ground specimens after the annealing process. The TG specimens had the lowest strength. These specimens were ground with the application of ELID grinding using a #6000 grit size (average grain size = 3.15 μm) SD cast iron bonded wheel. The diameter of the wheel was 150 mm and the width was 10 mm. The following grinding conditions were used: wheel velocity: 2560 rpm; table speed: 20 m/min; traverse pitch: 0.6 mm; depth of cut: 0.5 μm; total depth of cut: 40 μm.

The power supply used in the experiment was EPD-10A, with a capacity of 90V, 10A. The following ELID conditions were used: Eo = 60V, Ip = 10A, τ on = τ off = 2 μ s, square wave. Noritake AFG-M grinding fluid, with 2% water dilution, was used in the experiment. The bending strength of the ELID ground specimens was determined (TGE). The ELID ground specimens were annealed and the bending strength of these specimens was also determined (TEH). The results are presented in Fig. 6. When applying ELID grinding, a significant improvement in the bending strength of Si₃N₄ specimens was achieved. The bending strength of the specimens was determined at 1400° C. The results are presented in Fig. 7. The maximum bending strength at the elevated temperature was found with the TGE specimens.

3.0 DISCUSSION

The mechanism for material removal in ceramic grinding is a combination of micro-brittle fracture and micro or quasi-plastic cutting [5, 6]. The quasi-plastic cutting mechanism, typically referred to as ductile mode grinding, results in grooves on the surface that are relatively smooth in appearance. On the other hand, the micro-brittle fracture mechanism results in surface fracture and fragmentation. Ductile regime grinding of ceramics is preferred since no grinding flaws are introduced in this mode. When observing the surfaces under a scanning electron microscope (SEM) and an atomic force microscope (AFM) one can easily differentiate these two modes.

3.1 SEM Topography of ELID Ground Ceramics

The surface grinding operation was carried out on the silicon nitride specimens with the application of ELID technology. Cast iron fiber bonded diamond grinding wheels of various grit sizes were used in the experiment. Grain size of the diamond grinding wheels is given in Table 1. Ground specimens were observed under a scanning electron microscope to detect the surface fracture damage from grinding. The specimens were sputter coated with Au-Pd to enable easier SEM imaging, as shown in the SEM micrographs in Fig. 8.

Table 1: GRAIN SIZE OF DIAMOND GRINDING WHEELS USED

Mesh Size No.	Grain Size (µm)	Average Grain Size (µm)
325	40-90	63.0
600	20-30	25.5
1200	8-16	11.6
2000	5-10	6.88
4000	2-6	4.06
6000	1.5-4	3.15
8000	0.5-3	1.76

The "white frosted" areas represent the surface fragmentation caused by brittle fracture of the workpiece. Specimens ground with a #325 grit wheel have a significant white frosted area confirming that brittle fracture predominantly removes the material. SEM micrographs show that with increasing grit size (finer grit size) the amount of surface fragmentation decreases. When ELID grinding was performed using a #4000 grit size wheel or finer, SEM micrographs did not show any surface fragmentation, suggesting that the material was removed in the ductile mode.

3.2 AFM Topography of ELID Ground Ceramics

Ground surfaces were observed by means of AFM. AFM topographies are shown in Fig. 9. The observed surface area was $18x18 \mu m^2$. The vertical scale for the first four specimens is 1000μ nm, whereas for the last three specimens, it is 100μ . The change in surface topography can be observed through AFM. The AFM surface topography also shows that the material was predominantly removed in the ductile mode when ELID grinding was performed using a #4000 mesh wheel or finer. The surface finish obtained from the AFM study is presented in Table 2.

Table 2: SURFACE ROUGHNESS OF Si₃ N₄ BY AFM

Wheel Mesh	R _a ,nm	R _{max} , nm	R _{rms} , nm	R _z ,nm
#325	112.7	1164.7	147.8	832.7
#600	126.5	1533.3	173.3	786.3
#1200	79.54	950.8	108.6	666.0
#2000	41.34	756.5	61.48	456.7
#4000	7.474	334.7	14.34	138.3
#6000	3.734	180.0	5.8	108.3
#8000	3.177	187.9	5.119	102.9

SEM and AFM studies reveal that the workpieces were predominantly ground in the ductile mode when ELID grinding was performed using a #4000 grit sized wheel or finer. When the TG workpieces were finish ELID ground using a #6000 grit sized wheel, the grinding mode was ductile. The TGE specimens therefore do not contain any significant micro cracks. This may be the reason for the improvement in the bending strength of the TGE specimens.

4.0 CONCLUSIONS

- a) The bending strength of the transversely ground Si₃N₄ specimens can be improved by annealing at 1200°C.
- b) A significant improvement in the bending strength of Si₃N₄ was achieved when finish ELID grinding was performed.

B. PRECISION SURFACE GRINDING CHARACTERISTICS OF CERAMIC MATRIX COMPOSITE AND STRUCTURAL CERAMICS WITH ELID

1.0 INTRODUCTION

Interest in applications for advanced ceramic materials has increased significantly in recent years. This increase is due to the unique physical and mechanical properties of these materials. Although ceramic materials generally lack toughness, they possess high hardness and strength at elevated temperatures, chemical stability, and superior high temperature wear resistance. Ceramic matrix composite (CMC) represents an emerging category of materials in the class of advanced ceramics. CMC retains the desirable properties of advanced ceramics with higher fracture toughness. The inherent brittleness is the major limitation preventing ceramic material from becoming widely accepted in modern designs [7-10]. CMC offers greater toughness thus increasing reliability by reducing fracture sensitivity. CMCs consist of a ceramic primary phase embedded with a secondary phase. Present applications for CMCs are in jet and automotive engines, dies for extrusion etc.

However, the cost of machining these materials is very high. Some studies suggest that the cost of grinding may account for up to 75% of the component costs for ceramics compared with 5% to 15% for metallic components [11]. The primary cost drivers in grinding structural ceramics are low efficiency due to low material removal rates, high superabrasive wheel wear rates, and wheel dressing times. Grinding costs can be reduced by maximizing the material removal rates (MRR). Metal bonded, diamond grinding wheels are suitable for high material removal. Cast Iron Fiber Bonded Diamond (CIFB-D) grinding wheels provide high grinding ratio and high MRR. However, these wheels are not suitable for long term continuous grinding for the reasons explained elsewhere [12-13].

A novel grinding technology that incorporates in-process dressing of metal bonded superabrasive wheels, known as Electrolytic In-Process Dressing (ELID) has been developed. The ELID provides dressing of the tough metal bonded wheels during the grinding process. In-process dressing controls the abrasive protrusions before and during the grinding process.

Surface grinding operations were performed on CMC and SiC material. The ELID grinding was performed with metal bonded CBN and diamond wheels using various grit sizes. Conventional surface grinding was performed with resinoid bonded diamond grinding wheels and various grit sizes. The results of this investigation are contained in this report.

2.0 EXPERIMENTAL METHODS AND MACHINING CONDITIONS

The experiments were conducted on a precision surface grinding machine (made by Karl Jung: JF 520). Traverse grinding operations were performed and surface roughness, grinding resistance, and surface topography were monitored.

2.1 Materials

Silicon carbide and composite ceramics from Cernax were used in the experiment. The composition of the composite ceramic is SiC:70%, Al₂O₃:20% Al:10% [14]. Table 3 shows their important properties.

Table 3: CHARACTERISTICS OF COMPOSITE CERAMICS AND SILICON CARBIDE

	SiC	СМС
Density (g/cm³)	3.9-4.0	3.28
Hardness (GPa)	176-186	(HRA 80)
Fracture toughness (MN/m ^{3/2})	3.5-4.5	6.0
Heat conductivity (W/mk)	87	147
Reinforced material particle diameter (µm)	-	500

Both the silicon carbide and composite ceramic samples were cut into $15 \times 15 \times 5$ mm, and four of each were glued to a fixture using wax.

2.2 Grinding Wheels

Table 4 shows the different types of grinding wheels used in the experiments.

Table 4: GRINDING WHEELS USED

·	ELID-Grinding	Conventional Grinding		
·	diamond wheels	diamond wheels	cBN wheels	
Rough Grinding	SD325N100M*	SD325N100B**	B325N100M	
Semi-finish Grinding	SD1000N100M	SD1000N100B	B1000N100M	
Finish Grinding	SD4000N100M	SD4000N100B	B4000N100M	

M: Cast iron bond

B: Resinoid bond

2.3 Machining Conditions

Table 5 shows the machining conditions used during the experiments.

Table 5: MACHINING CONDITIONS

	Rough Grinding	Semi-finish Grinding	Finish Grinding	
Wheel speed (m/min)	1200	1200	1200	
Cross feed pitch (mm/pass)	2.0	1.0	0.5	
Table speed (m/min)	20	20	20	
Depth of cut (µm)	5.0	3.0	1.0	
Total depth of cut (µm)	50	30	15	
Number of sparkouts	3 3 3			
Grinding fluid	Noritake Coolant: CEM (2% dilution of water)			

2.4 Power Supply:

A direct pulse generator was used as a power supply. Table 4 shows the ELID conditions used in the experiments. All the grinding wheels were trued with a WA #400 grit wheel. For ELID grinding, the initial electrolytic dressing was carried out for 30 minutes with the conditions shown in Table 6.

Table 6: ELID CONDITIONS

Open circuit voltage (V)	80		
Peak current (A)	14		
Pulse width τ on, off (μs)	2/2(on/off)		
Electrode gap (mm)	0.2		

2.5 Measuring Instruments Used

After finish grinding, the surface roughness was measured at the center of the specimen using a non-contact surface profile measuring instrument (made by Wyko: TOPO-3D). The grinding resistance (force) was monitored for rough grinding with the grinding dynamometer (made by Sato machinery: ST-ZGS1). The surface topography was observed using a scanning electron microscopy (SEM), (made by Nippon Denshi: JEL840). The dulled depth and width of the edge of the surface after finish grinding were measured in the ground direction using a contact type

surface roughness meter (made by Kosaka Laboratory: Type SE- 3) with a tip radius of 5 μm.

3.0 RESULTS AND DISCUSSION

3.1 Surface Roughness by each Wheel

SiC and composite ceramics were ground by using ELID technology. Cast iron bonded #4000 grit sized diamond and CBN wheels were used. These specimens were also ground by conventional means (non ELID) using a #4000 grit sized resin bonded wheel. Fig. 10 shows the surface roughness results (P-V value) of the finished surfaces using a non-contact surface profiling measuring instrument. Fig. 11 shows the 3-dimensional diagrams using the same measuring instrument.

The surface roughness of the composite ceramics is greater by a factor of 2 for each wheel (Fig. 10). This is because, as shown in Fig. 11, the silicon carbide showed very detailed grinding marks, while the matrix parts (Al₂O₃, Al) of the composite ceramics were ground with priority, resulting in level differences with the silicon carbide contained as reinforcement material. This has resulted in higher P-V value.

Comparing the surface roughness results obtained by the cast iron bond diamond wheel and cast iron bond CBN wheel, it is found that the CBN wheel produced rougher surfaces nearly 1.6 times that of the diamond wheel. The CBN abrasive has a hardness of 4700 (Knoop Hardness) and is soft compared to the diamond abrasive. Its compression strength is also low at 7.0 GPa compared to 9.8 GPa of the diamond abrasive. The diamond abrasive also has a higher heat conduction rate than the CBN abrasive, making it easier for the heat to be distributed during the grinding process. These are the reasons for the higher surface roughness with the CBN wheel because the crushing of abrasive, and the thermal and chemical wear were controlled for the diamond abrasive [15].

Comparing ELID grinding with the cast iron bond diamond wheel and resin bond diamond wheel (conventional grinding), the resin bond showed about 1.3 times greater P-V value. The P-V value by ELID grinding is smaller because of good grinding marks as compared to very deep grinding marks in the case of resin bond wheel, Fig. 11 (a) and 11 (b).

3.2 Grinding Resistance

Rough grinding was performed using three types of grinding wheels of grit size #325. Silicon carbide and composite ceramics were ground by 20 μ m (5 μ m x 4 times). The normal component of the grinding force was monitored. Fig. 12 shows the influence of wheel velocity on the normal component of the grinding force for various wheels. Fig. 13 shows the change in the grinding force with the volume of material removed for the composite ceramics. Fig. 14 shows the relationship between the grinding force and the volume of material removed for silicon carbides.

For all the three wheels, the grinding force showed no significant change and remained almost constant when the wheel speed was changed from 900 to 1800 m/min (Fig. 12). CBN wheels showed almost 5 times greater grinding resistance in all the wheel speeds.

Fig. 13 shows the change in the grinding force when composite ceramics were ground for a long period of time using three types of rough grinding wheels. In ELID grinding, using the cast iron bond CBN wheel, abnormal grinding noises were observed from the start of the grinding and the grinding resistance was also found to be high and equal to 50 N. Upon removal of 750 mm³, grinding force of 90 N was recorded. In a resin bond diamond wheel, the grinding resistance was 22 N at the start of the grinding, and increased linearly as the grinding continued, and became 40 N upon removal of 2500 mm³. For ELID grinding using the cast iron bond diamond wheel, the grinding resistance was 12 N at the start of grinding and increased to 30 N after removal of 1600 mm³, after which it remained almost constant.

Fig. 14 shows the grinding resistance when silicon carbide was ground in the same way using three types of rough grinding wheels. Cast iron bond CBN wheels also produced the same abnormal sound at the start of grinding as the composite ceramics, and grinding resistance was also observed to be high at 48 N at the start. As the grinding continued the grinding force increased significantly within a short time and thus the grinding was stopped.

Essentially, the same progress was observed for ELID grinding with cast iron bond diamond wheel and conventional grinding with the resin bond diamond grinding wheel from the start of grinding to removal of 1250 mm³. Afterwards, while ELID grinding showed no changes in the grinding resistance which was essentially stable at 28 N, the grinding force with the resin bond increased linearly to become 38 N upon removal of 2300 mm³. The resin bond is extremely soft and has a small vertical elastic coefficient (Young's modulus). Therefore when a resin bond was used for grinding of composite ceramics and silicon carbides, the area of contact between the work and wheel becomes greater due to wheel deformation, resulting in increased grinding resistance [16].

3.3 SEM observation Results

Fig. 15 shows the SEM micrographs of the ground surfaces of composite ceramics after finish grinding. When ground with the cast iron bond diamond wheel as shown in Fig. 15 (a), silicon carbides contained as reinforcement material shows very fine grinding marks as evident from the results of measuring the surface in Fig. 11 indicating that ductile mode grinding was carried out.

Compared with this, the surface ground using the resin bond diamond wheel shown in Fig. 15 (b) showed the presence of both grinding marks resulting from brittle fracture and ductile mode performed at both reinforcement material (silicon carbides) area and matrix area. The border between the silicon carbide contained as reinforcement material and matrix area is not clear.

When ground with the cast iron bond CBN wheel shown in 15 (c), grinding marks resulting from brittle fracture were seen over the whole surface. In particular, severely damaged fractures were seen at the border between the reinforced material and matrix.

3.4 Dulled Area at Ground Edges

Fig. 16 shows the results of dulled area measurement at the edges after ELID grinding using cast iron bond diamond grinding wheel and conventional grinding using resin bond diamond grinding wheel. A #4000 grit size wheel was used in the experiment.

ELID grinding of silicon carbide showed a dulled edge depth of about 0.5 μ m while grinding by resin bond showed 20 times greater dulled area depth of 10 μ m. On the other hand, ELID grinding of composite ceramics showed a dulled area depth of about 0.7 μ m while grinding by resin bond showed a 6-times greater dulled area depth of 4.5 μ m. Furthermore, the dulled area width was high and 6 times greater with the resin bond.

Because the resin bond has higher flexibility than the cast iron bond, therefore when the wheel contacts the work edge, elastic deformation occurs and insufficient removal of material occurs with respect to the set depth of cut, and as a result, the edges are ground with priority [17].

When silicon carbide and composite ceramics were ground using a resin bond diamond wheel, the dulled area depth of the silicon carbide was about two times greater. Scratch tests on the composite ceramics performed showed that the rate of wear is about half that of silicon carbide and this wear-tolerance is thought to be contributed to the difference in dulled area in grinding.

4.0 CONCLUSIONS

- 1) When silicon carbide and composite ceramics were finish ground by ELID using cast iron bond diamond wheels, the surface roughness (P-V value) was found to be 100 nm smaller than the resin bond diamond wheel.
- 2) SEM observation of the ground surfaces after finish grinding showed very fine grinding marks for ELID grinding using the cast iron bond diamond wheel and deep grinding marks at certain parts for grinding using the resin bond diamond wheel.
- 3) The grinding resistance for rough grinding was found to increase linearly with time with the resin bond diamond wheel. When ELID grinding was performed under the same conditions with the cast iron bond diamond wheel, the grinding force stabilized at about 30 N from around 1600 mm³ of material removal.
- 4) The dulled area at the edge in the ground direction for grinding of silicon carbide and composite ceramics was below 0.7 µm in the case of ELID grinding with the cast iron bond diamond wheel, which is about 1/6 of that of the resin bond diamond wheel.

The above conclusions confirm that ELID grinding can be successfully applied for high precision and high material removal grinding of structural ceramics and composite ceramics.

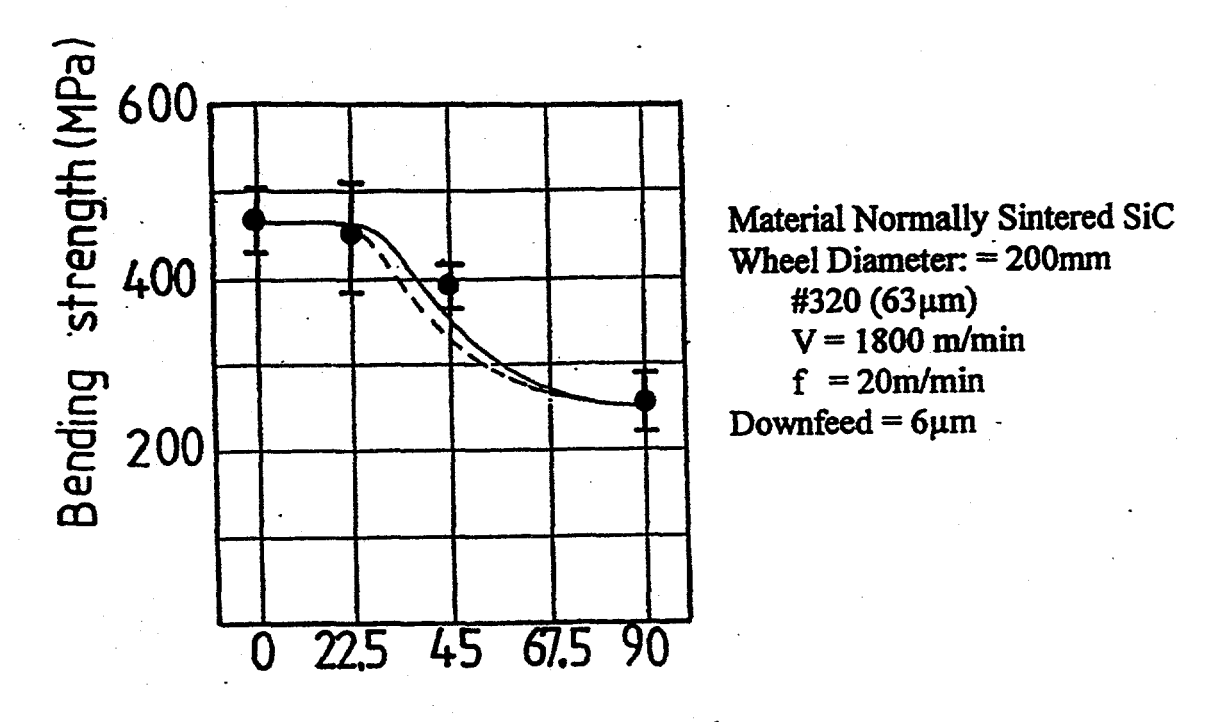
ACKNOWLEDGMENTS

Research was sponsored by the U.S. Department of Energy, Assistant Secretary of State for Energy Efficiency and Renewable Energy, Office of Transportation Technologies, as part of the Propulsion System Materials Program. In addition, the author acknowledges the efforts of the following personnel: The Institute of Physical and Chemical Research (RIKEN), Tokyo, Japan, Dr. H. Omori and Mr. I. Takahashi. The University of North Dakota, Ms. Joyce Medalen.

REFERENCES

- 1. Matsuo, Y., Ogasawara, T., Yasuda, E., and Kimura, S., "Experimental Study on the Bending Strength of SiC specimens with Ground Surfaces," Intersociety Symposium on Machining of Advanced Ceramic Materials and Components, American Ceramic Society, April 1987, pp 235-248.
- 2. Mayer, J. E. (Jr.), and Fang, J. P., "Diamond Grinding of Silicon Nitride Ceramic," Proceedings of the International Conference on Machining of Advanced Materials, NIST publication 847, Gaithersburg, Maryland, July, 1993, pp 205-222.
- 3. Ota, M., and Miyahara, K., "The Influence of Grinding on the Flexural Strength of Ceramics," 4th International Grinding Conference, SME, Dearborn, Michigan, July, 1990, paper #MR 90-538.
- 4. Matsuo, Y., Ogasawara, T., Kimura, S., Sato, S., and Yasuda, E., "The Effect of Annealing on Surface machining Damage of Alumina Ceramics," Journal of the Ceramic Society of Japan, (Intl. edition), Tokyo, Japan, Vol. 99, No. 5, pp 371-375.
- 5. Inasaki, I, "High Efficiency Grinding of Advanced Ceramics," Annals of CIRP, Vol. 35, No. 1, 1986, pp 211-214.
- 6. Inasaki, I., "Speed Stroke Grinding of Advanced Ceramics," Annals of CIRP, Vol. 37, No. 1, 1988, pp 299-302.
- 7. Jenkins, M. G., and Mello, M. D., "Fabrication, Processing, and characterization of Braided, Continuous SiC Fiber-Reinforced/CVI SiC Matrix Ceramic Composites", Materials and Manufacturing Processes, Marcel Dekker, NY, Vol. II, No.1, 1996, pp 99-118.
- 8. Holmes, T., "Wear Resistant Ceramic Matrix Composite (CMC) Materials Manufactured by Metal Oxidation Method", New Ceramics, No. 12, 1993, pp 1-6 (in Japanese).
- 9. Kogo, Y., "Reinforcement Mechanism of CMC", Journal of Japan Society for Precision Engineering, Vol. 60, No. 6, 1994, pp 780-783, (in Japanese)
- 10. Watanabe, A., "Manufacturing of Aluminum Matrix Composite Materials", Journal of Japan Society for Precision Engineering, Vol. 60, No. 6, pp 768-771, 1994 (in Japanese)
- 11. Jahanmir, S., Ives, L. K., Ruff, A. W., and Peterson, M. B., "Ceramic Machining: Assessment of Current Practice and Research Needed in the United States," NIST special publication 834, June 1992.
- 12. Ohmori, H., Takahashi, I., and Bandyopadhyay, B. P., "Highly Efficient Grinding of Ceramic Parts by Electrolytic In-Process Dressing (ELID) Grinding," Materials and Manufacturing Processes, Marcel Dekker, NY, Vol. 11, No. 1, pp 31-44, 1996.
- 13. Ohmori, H., Takahashi, I., and Bandyopadhyay, B. P., " Ultraprecision Grinding of

- Structural Ceramics by Electrolytic In-Process Dressing (ELID) Grinding," Journal of Materials Processing Technology, Elsevier Science, Switzerland, Vol. 57, pp 272-277, 1996.
- 14. Cernax Co., Ltd., Technical data Information of CMC, 1994, (in Japanese).
- 15. Ishikawa, T., "Characteristics of Superabrasive and its Application to Difficult-to-Grind Materials," Journal of Japan Society for Precision Engineering, Vol. 58, No. 12, 1992, pp 33-36, (in Japanese)
- 16. Unno, K., "Usage of CBN and Diamond Wheels," Industrial Review, Kogyo Chosakai, Tokyo, 1991, p 85 (in Japanese).
- 17. Suzuki, H., Hirano, M., Abe, M., Niino, Y., and Namba, Y., "Ductile Grinding of Chemical Vapor Deposited Silicon Carbide for X-Ray Mirrors," Journal of Japan Society for Precision Engineering, Vol. 61, No. 4, 1995, pp 571-575 (in Japanese).



 Φ , Grinding direction (deg.)

FIGURE 1. EFFECTS OF THE GRINDING DIRECTION OF THE BENDING STRENGTH OF SIC SPECIMENS

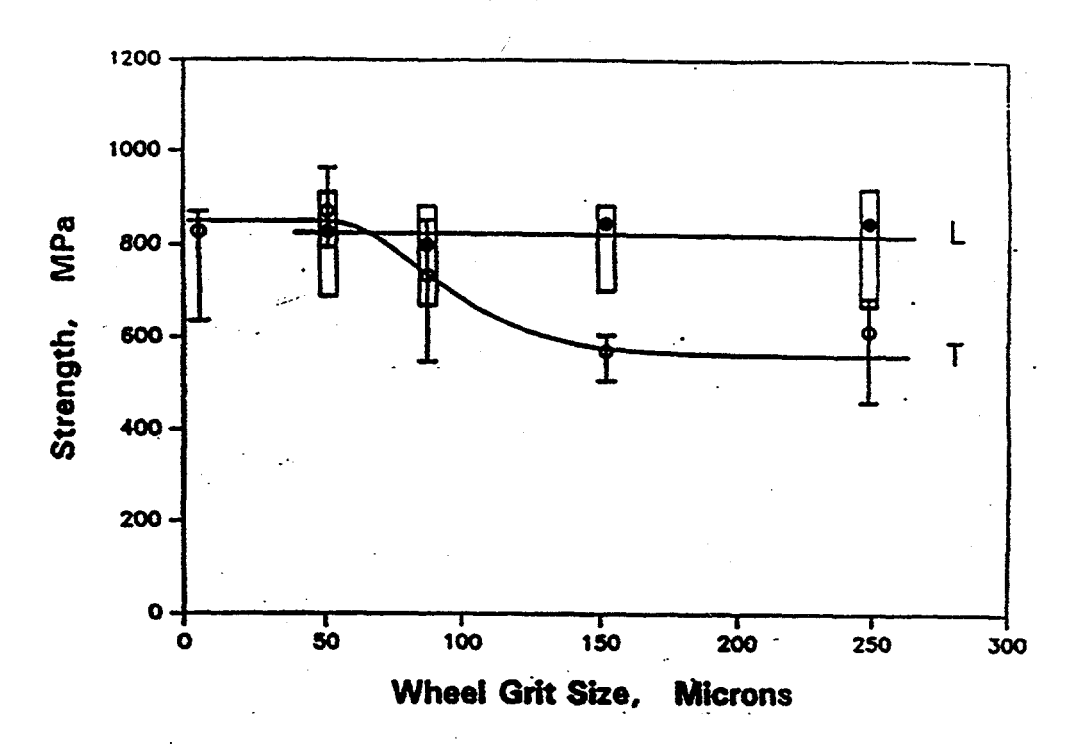


FIGURE 2. TRANSVERSE RUPTURE STRENGTH AS A FUNCTION OF WHEEL GRIT SIZE IN LONGITUDINAL (L) AND TRANSVERSE (T) GRINDING [2]

Material = HSPN Wheel: V = 1480 m/min d.o.c. = 0.0254 mm (rough) f = 670 mm/min (rough) = 0.00254 mm (finish) = 457 mm/min (finish)

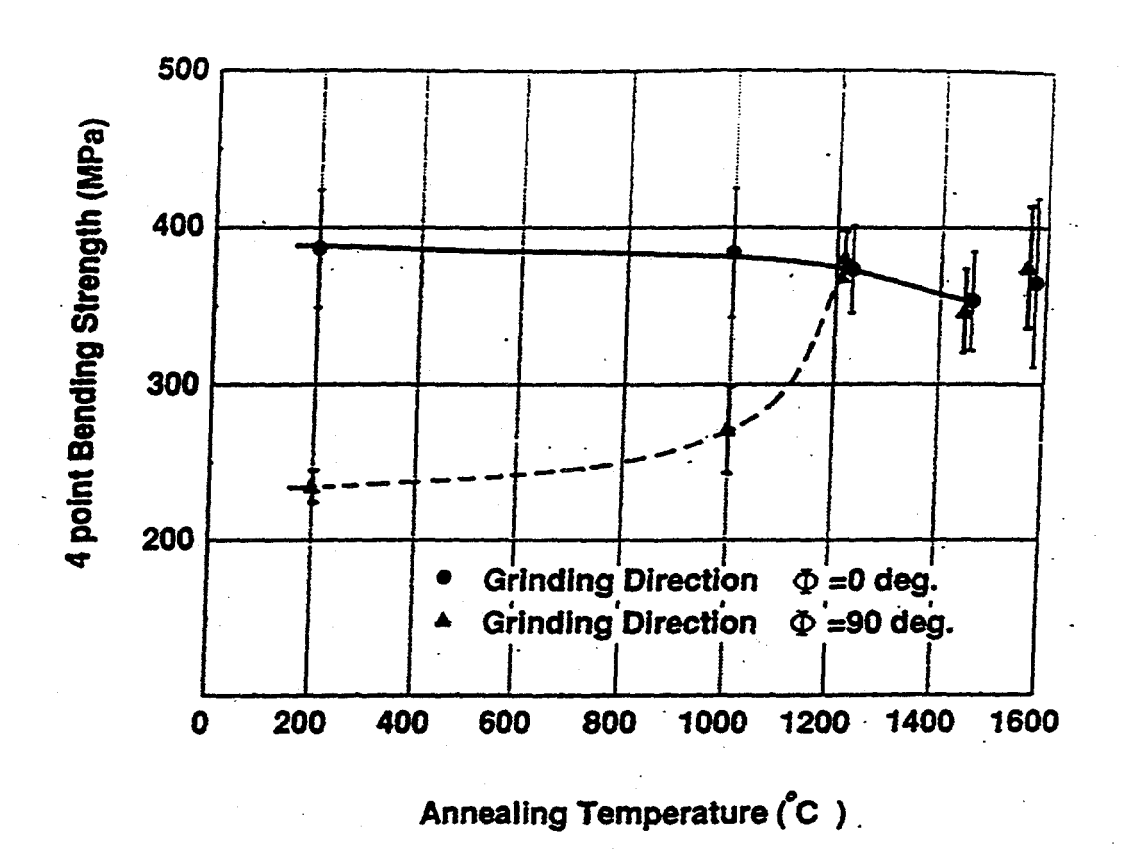


FIGURE 3. EFFECTS OF ANNEALING ON FOUR-POINT BENDING STRENGTH [4]

Material = Al_2O_3 Wheel: Diameter = 200 mm Downfeed = 8 μ m #170 (85-90 μ m) V = 1800 m/min f = 8-10 m/min

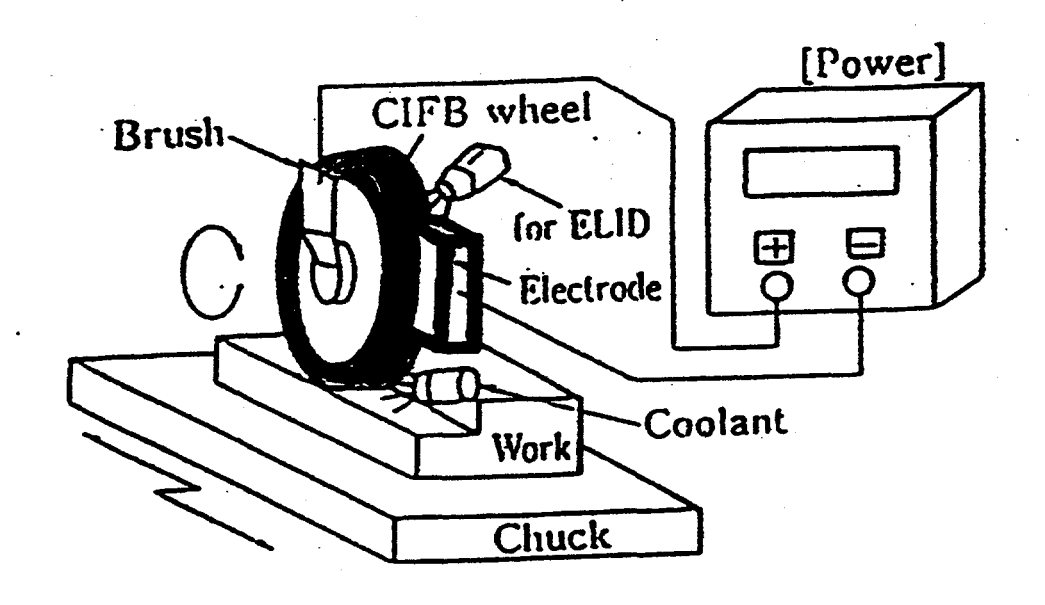


FIGURE 4. PRINCIPLE OF ELID GRINDING

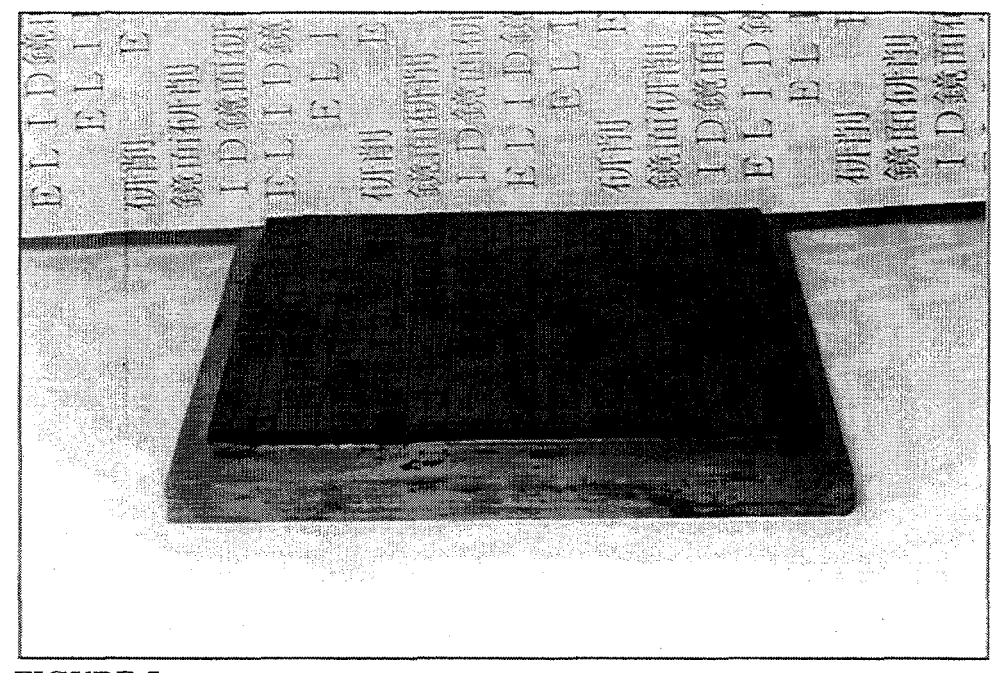
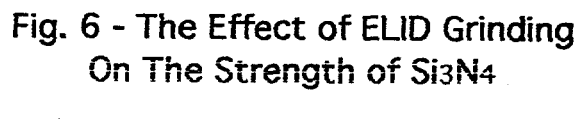
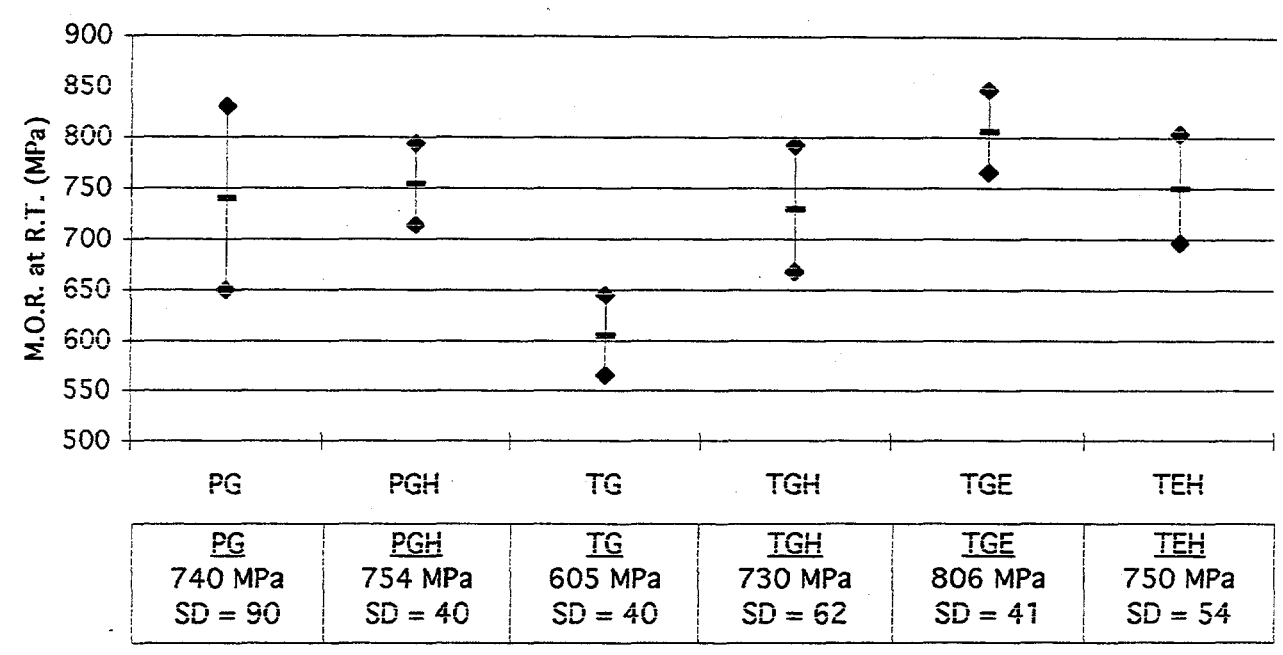


FIGURE 5.

THE PLATE WITH THE MOR SPECIMENS





PC	Darallal	Ground	with	#140	SD

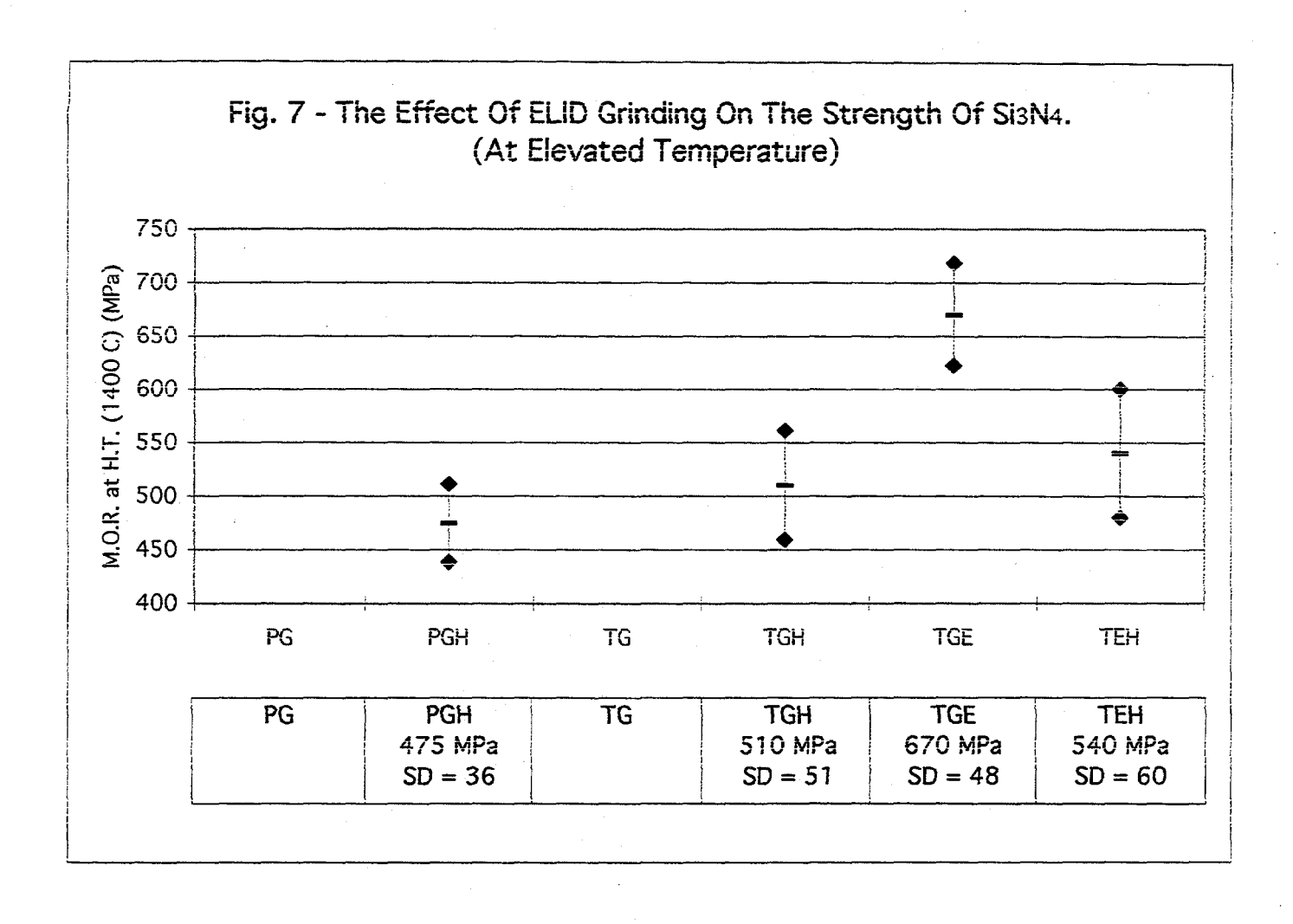
PGH Heat Treated after Parallel Grinding

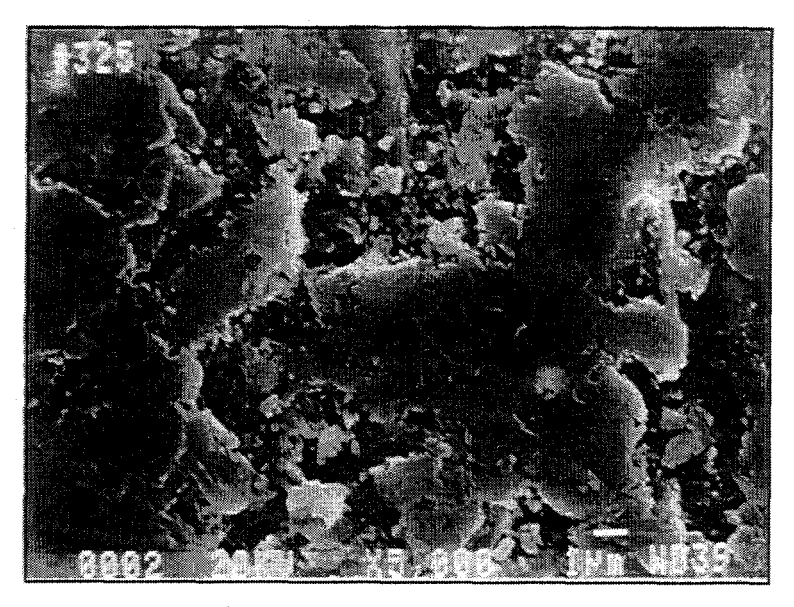
TG Transverse Ground

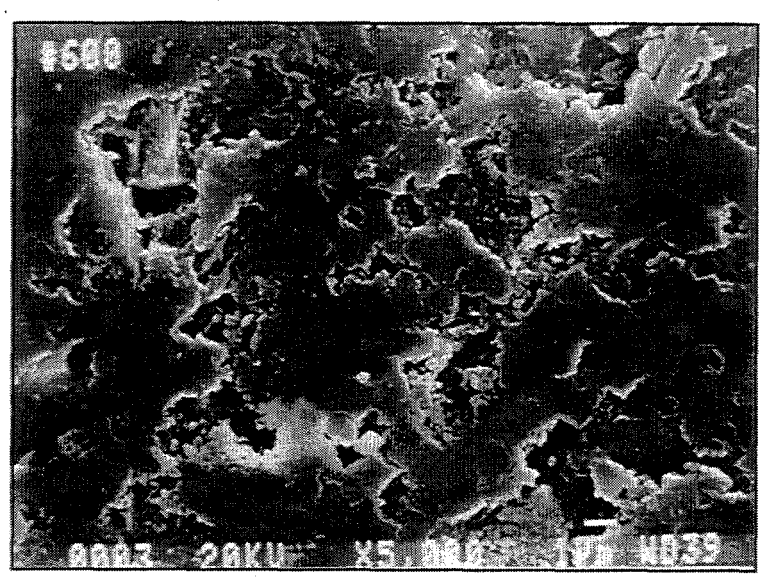
TGH Heat Treated after Transverse Grinding

TGE ELID Ground with #6000 SD-CIB Wheel after Transverse Grinding

TEH Heat Treated After ELID Grinding







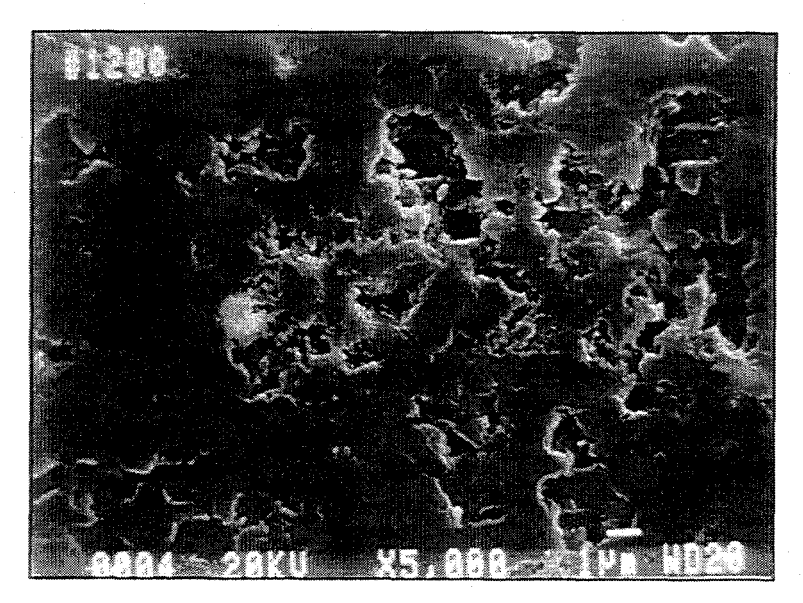
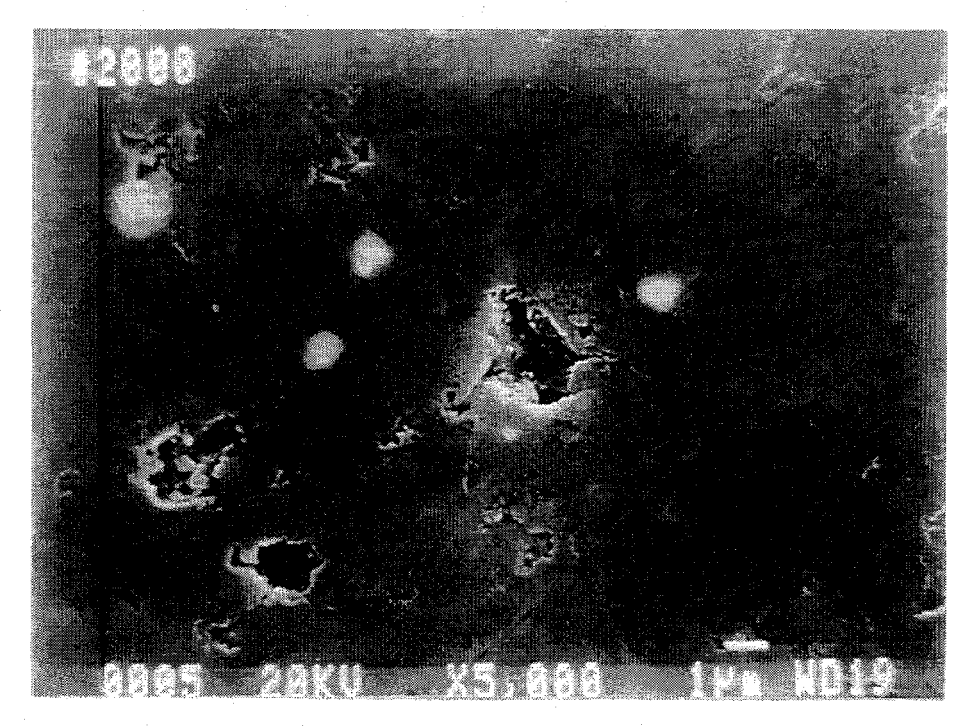


FIGURE 8: SEM MICROGRAPHS

53



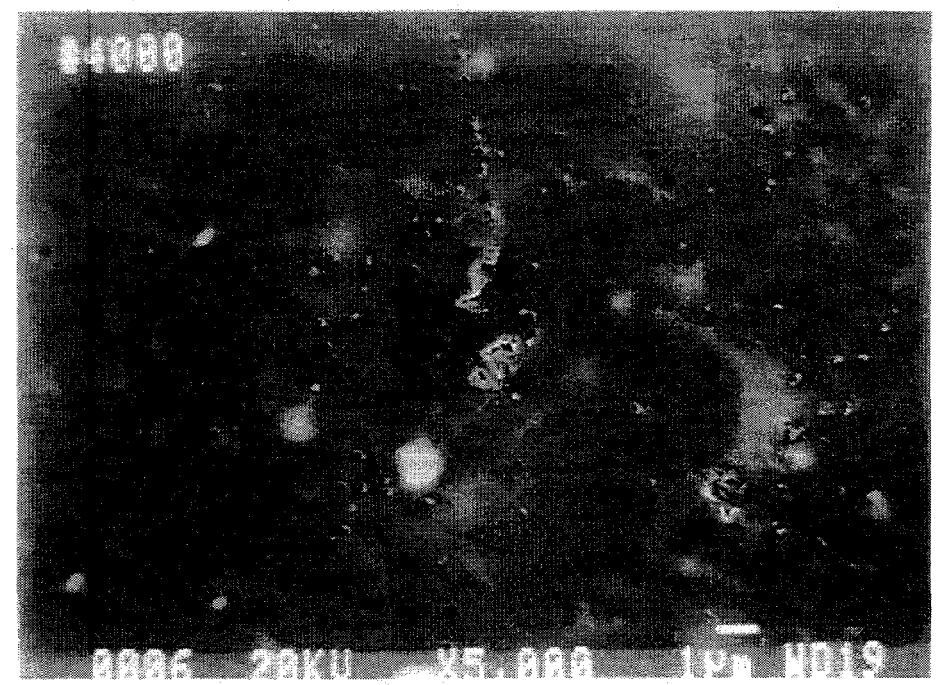
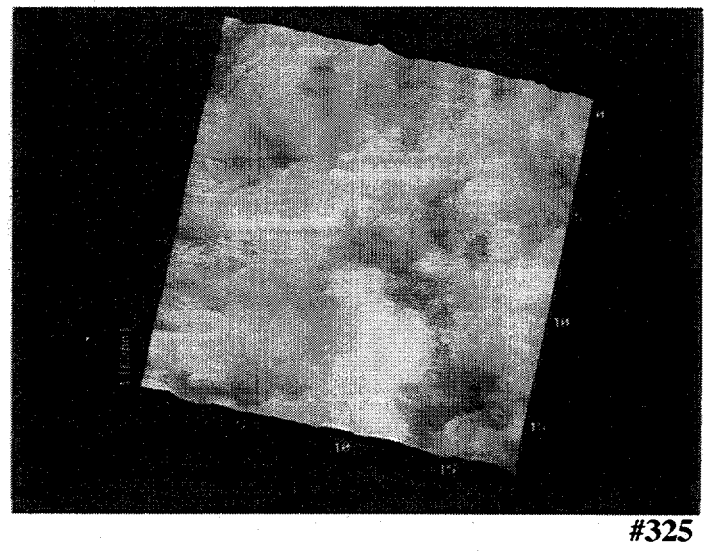
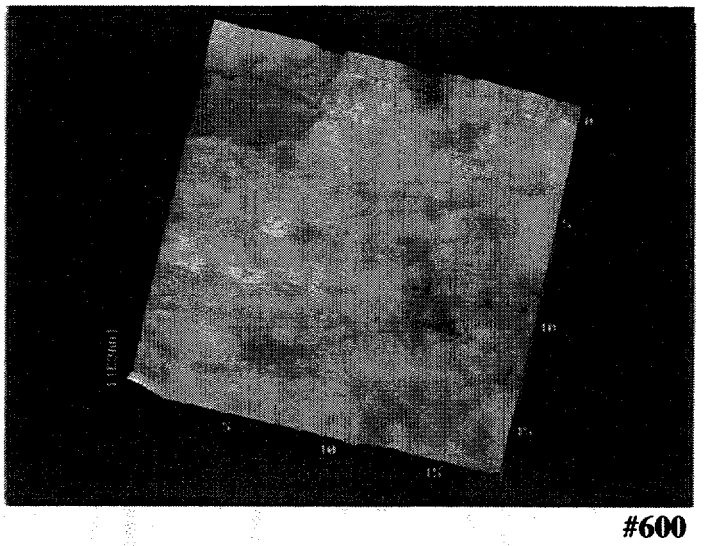


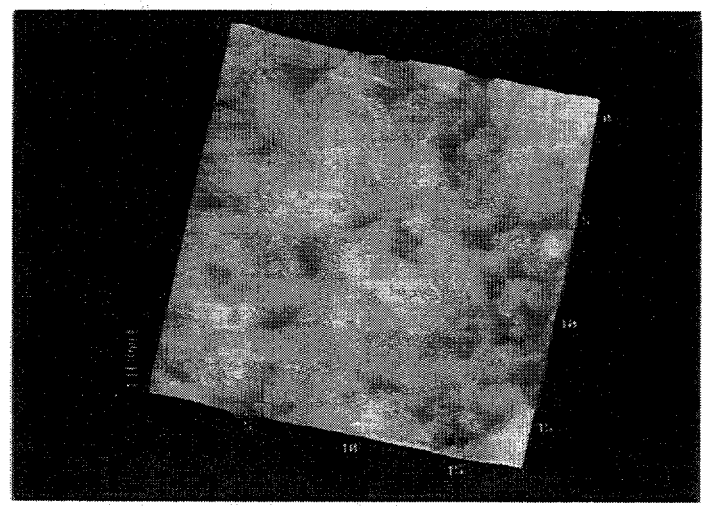
FIGURE 8: SEM MICROGRAPHS

54

Note: The original atomic force microscope images of surfaces ground with different grit sizes, as reproduced on pages 56-58, were prepared in color. Some of the details and topographic information have been lost in reproducing these images in black and white.

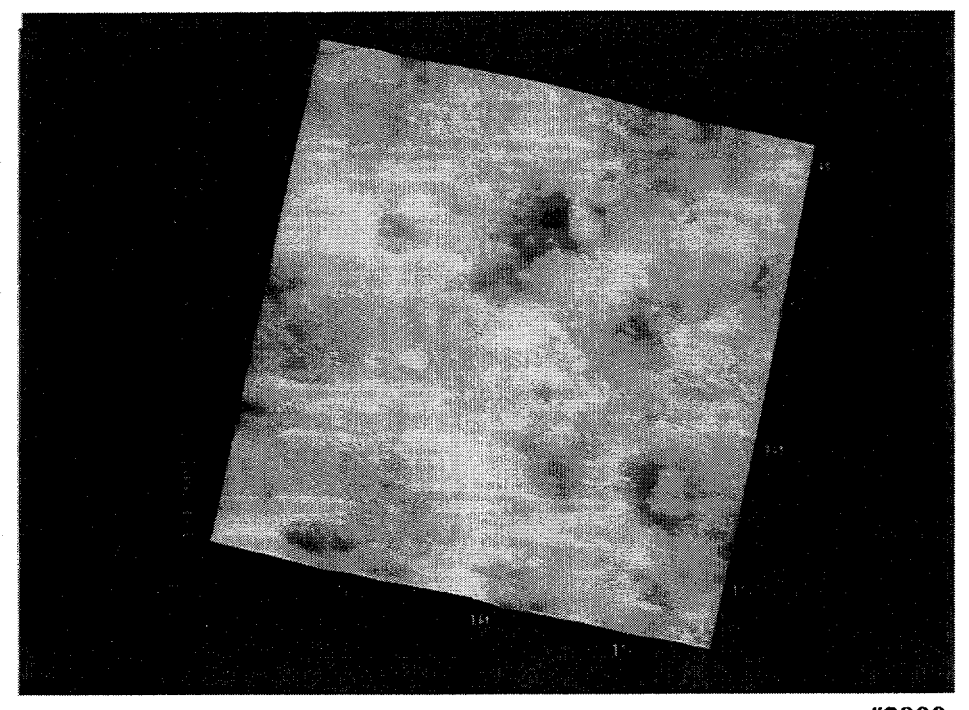




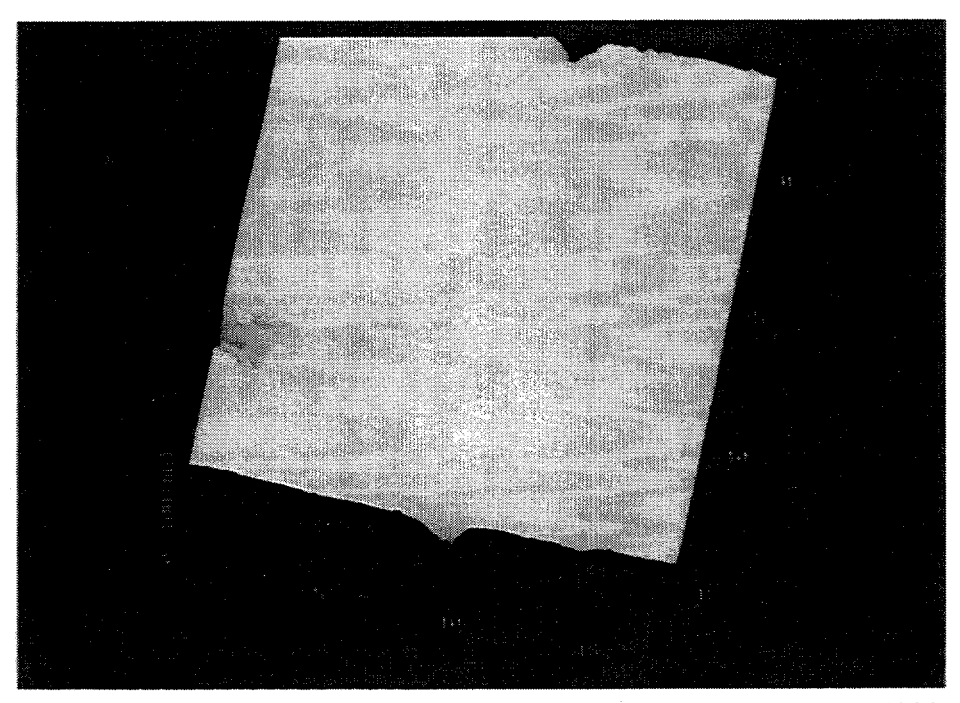


#1200

FIGURE 9: AFM MICROGRAPHS



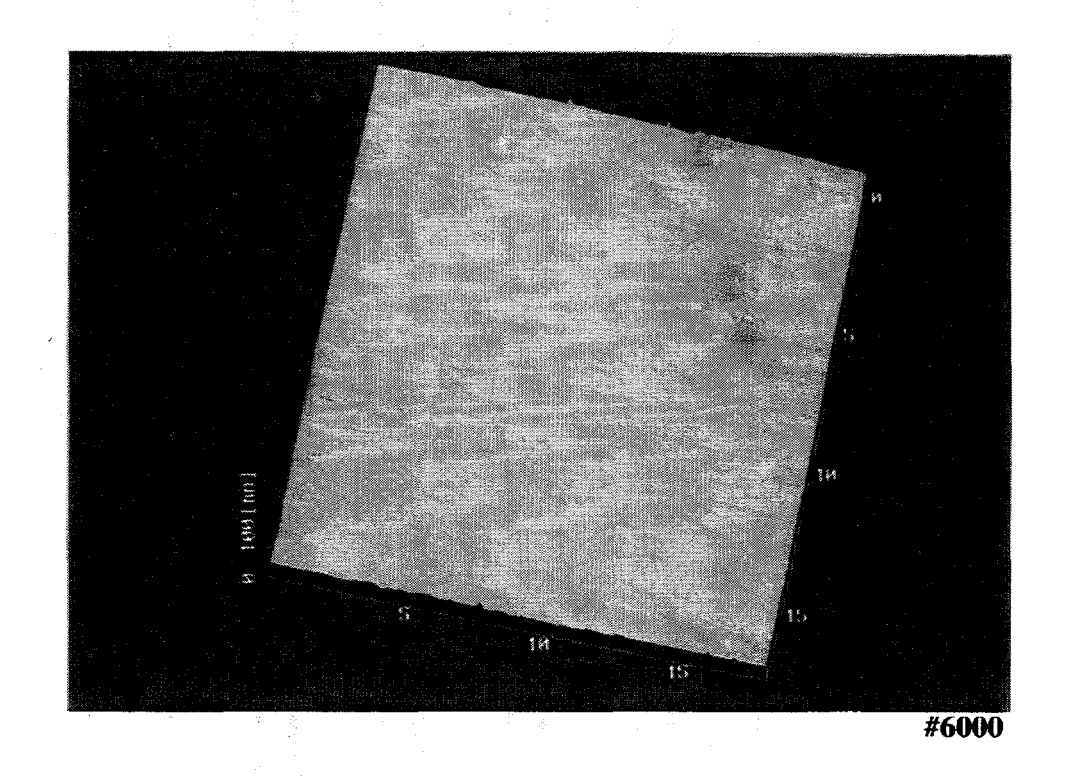
#2000



#4000

FIGURE 9: AFM MICROGRAPHS

57



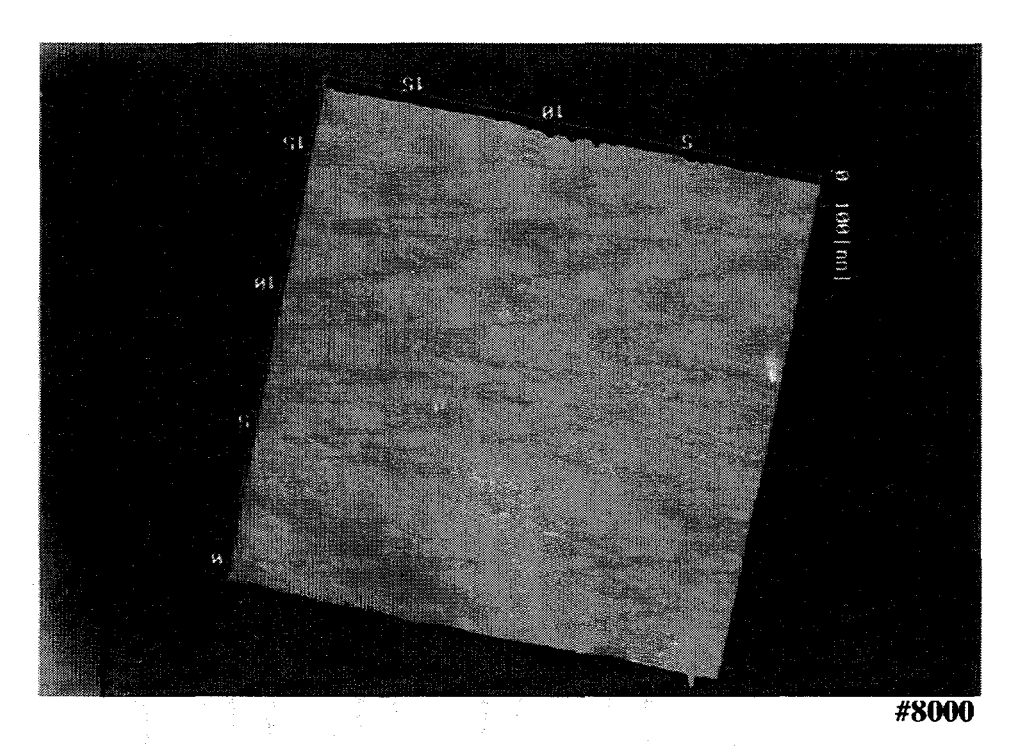


FIGURE 9: AFM MICROGRAPHS

58

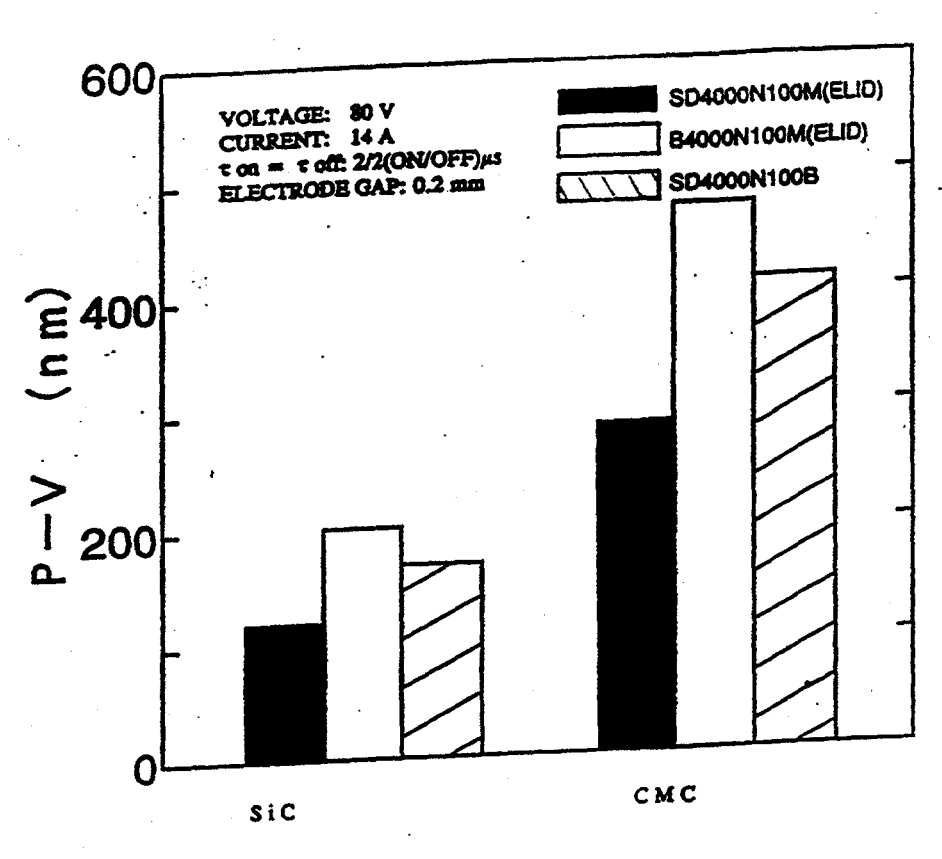


FIGURE 10. SURFACE ROUGHNESS AFTER FINISH GRINDING BY DIFFERENT WHEELS

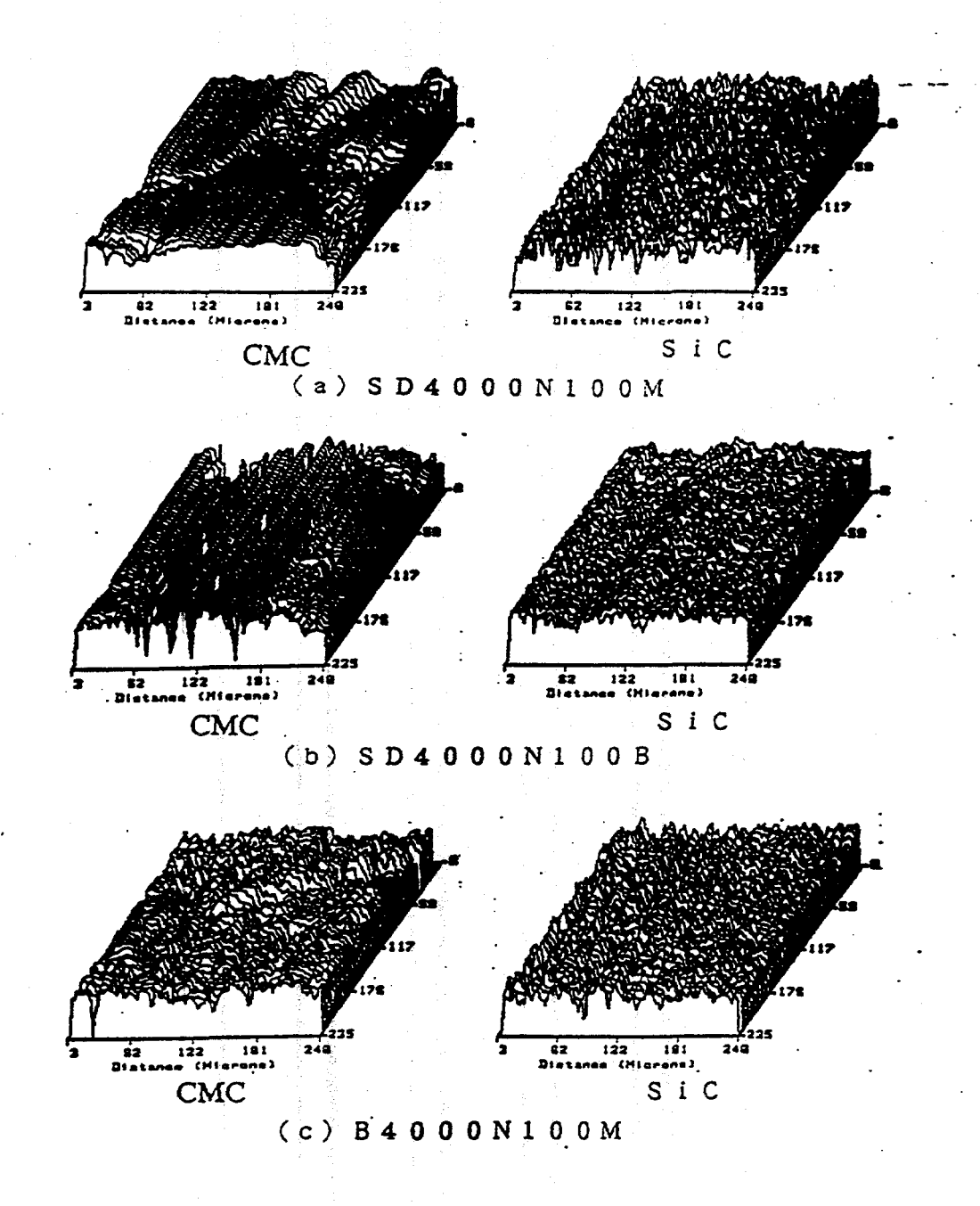


FIGURE 11. RESULTS OF 3-DIMENSIONAL SURFACE PROFILE MEASUREMENT

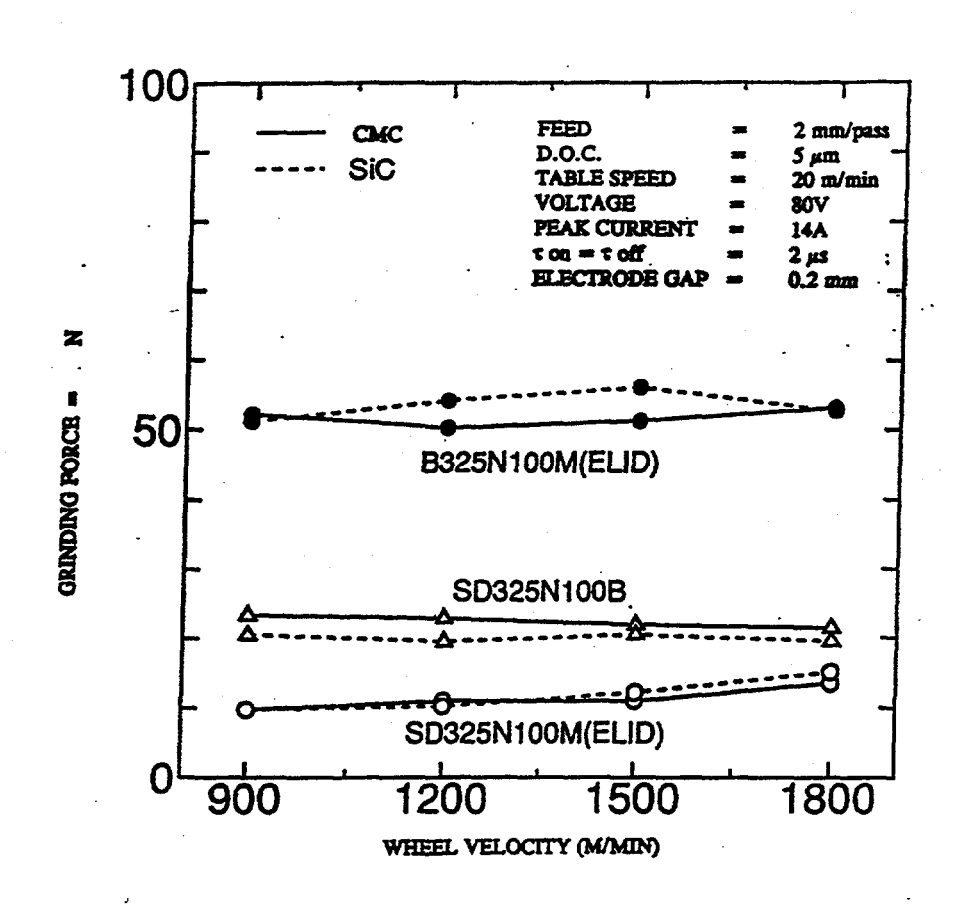


FIGURE 12. INFLUENCE OF WHEEL VELOCITY ON THE GRINDING FORCE DUE TO WHEEL TYPE

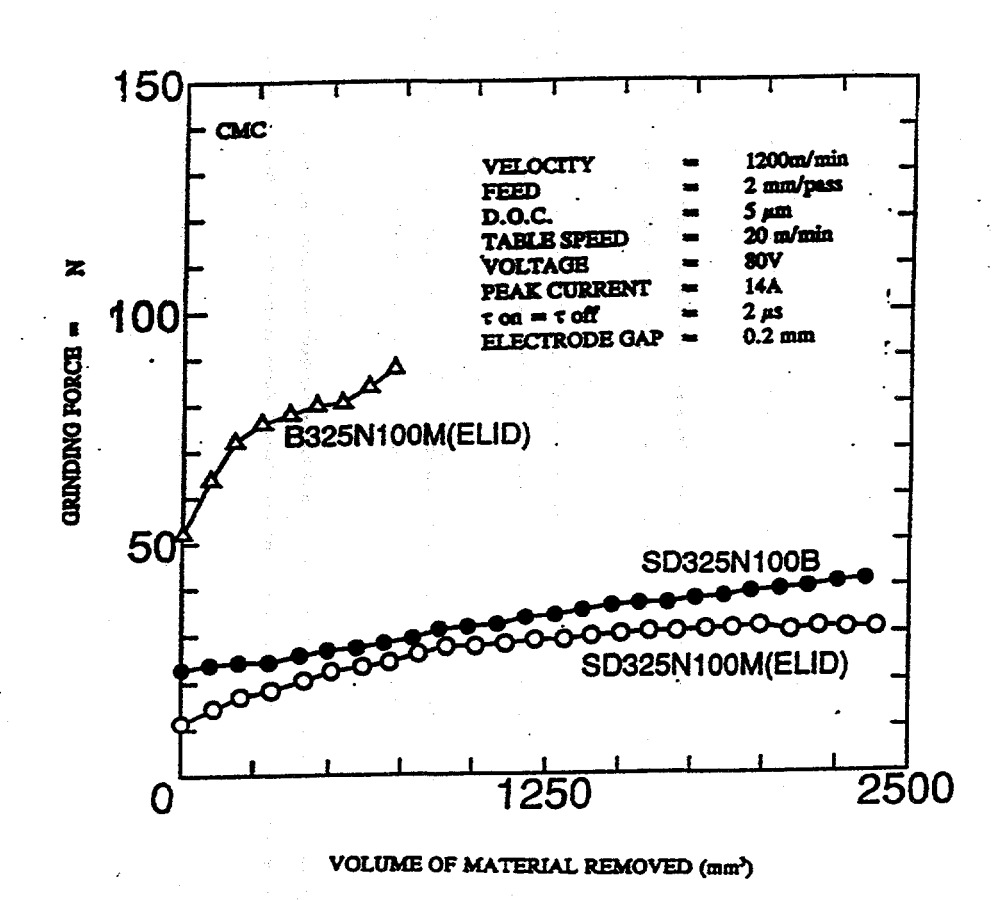


FIGURE 13. RELATIONSHIP BETWEEN THE GRINDING FORCE AND THE VOLUME OF MATERIAL REMOVED FOR COMPOSITE CERAMICS

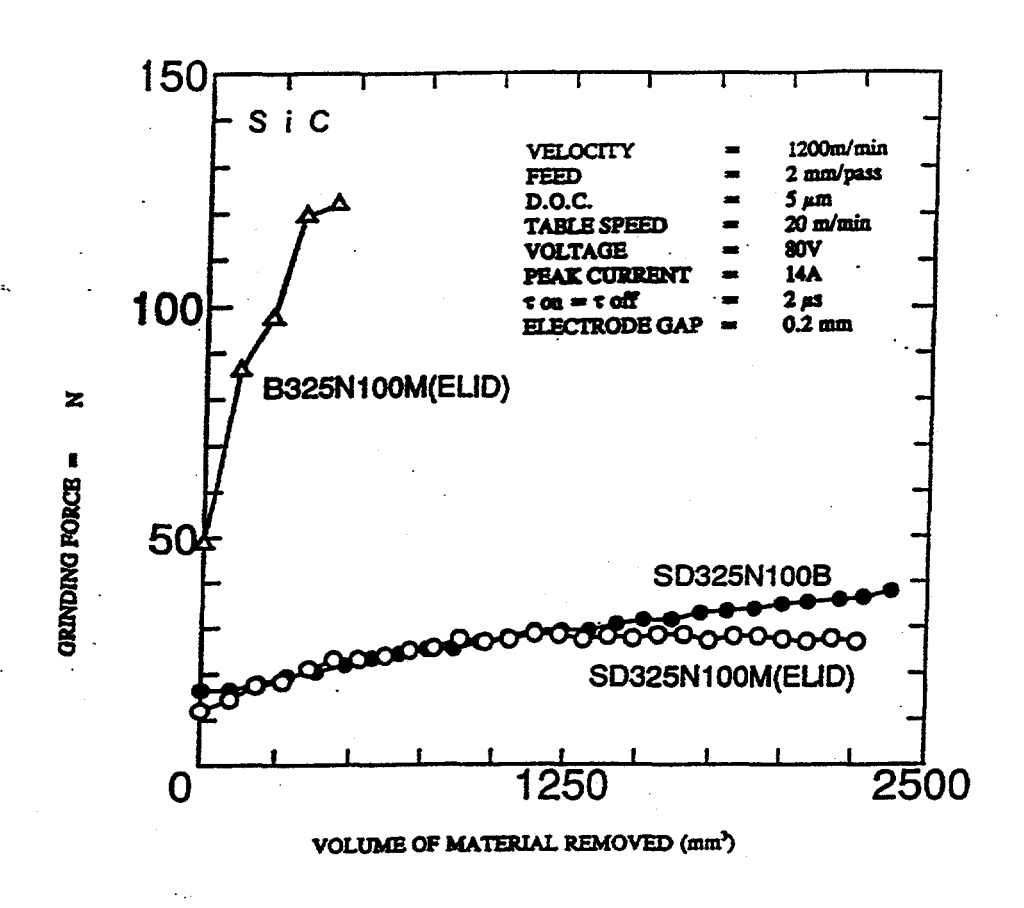
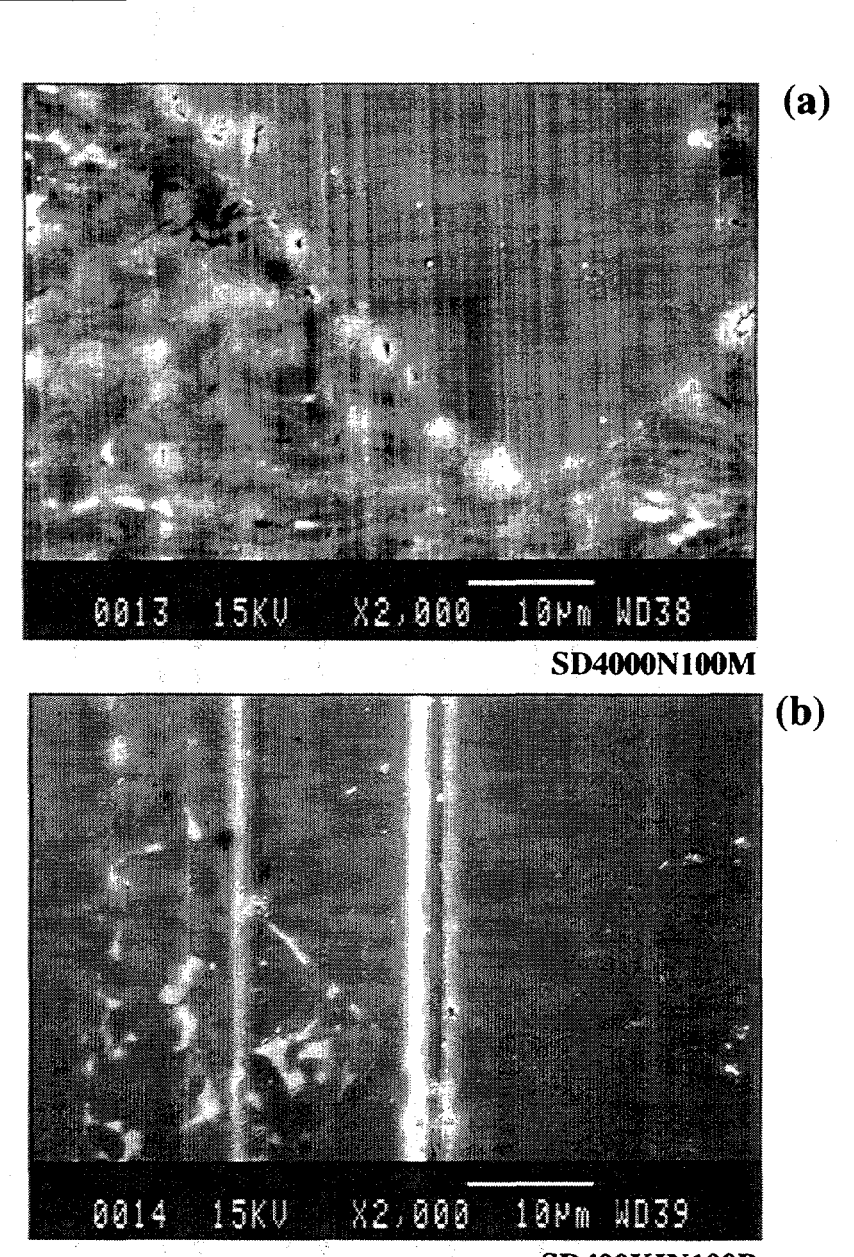


FIGURE 14. RELATIONSHIP BETWEEN THE GRINDING FORCE AND THE VOLUME OF MATERIAL REMOVED FOR SILICON CARBIDE



SD400KIN100B
(c)

0008 15KU X2,000 10Ph MD39

B4000N100M

FIGURE 15: SEM MICROGRAPHS OF CMC AFTER FINISH GRINDING

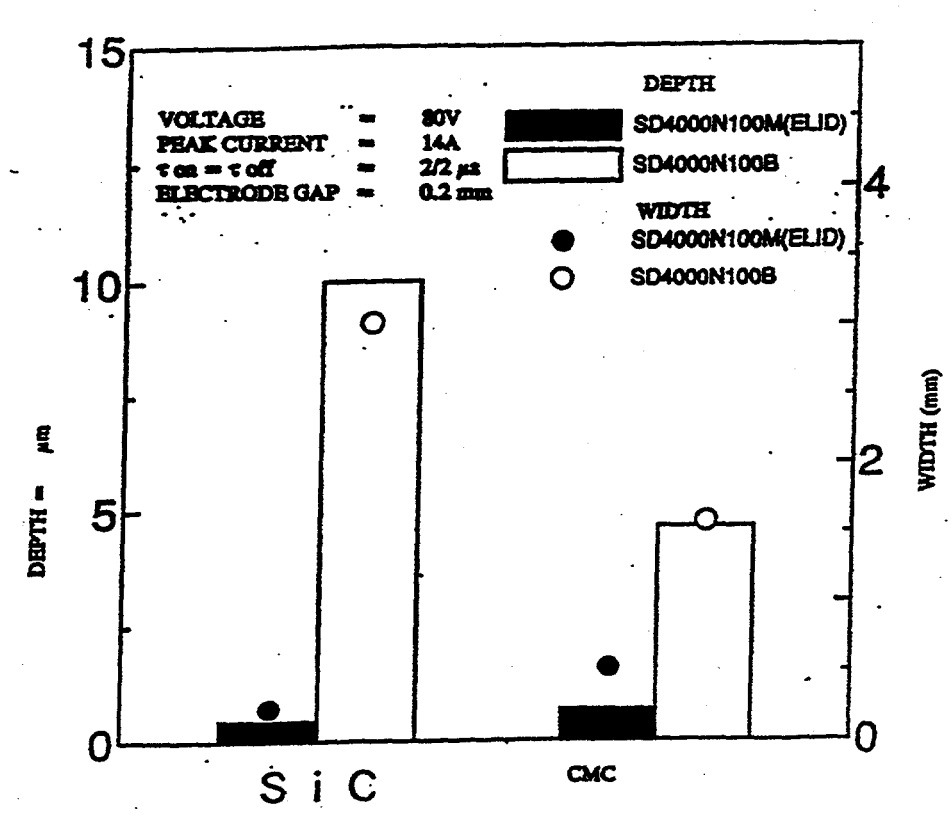


FIGURE 16. DEPTH AND WIDTH OF DULLED AREA AT EDGES IN GROUND DIRECTION

ORNL/SUB/96-SV716/1

INTERNAL DISTRIBUTION

1.	L. A. Abbatiello	32.	T. O. Morris
2-11.	P. J. Blau	33.	R. Ott
12.	R. A. Bradley	34.	A. E. Pasto
. 13.	K. Breder	35.	L. Riester
14.	D. F. Craig	36.	A. C. Schaffhauser
15.	M. K. Ferber	37.	D. P. Stinton
16.	C. L. Fitzpatrick	38.	S. G. Winslow
17-26.	D. R. Johnson	39.	J. M. Wyrick
27 .	F. W. Jones	40.	E. S. Zanoria
28.	W. K. Kahl	41.	R. E. Ziegler
29.	M. A. Karnitz	42.	Central Research Library
30.	R. L. Martin	43.	Document Reference Section
31.	S. B. McSpadden	44-46.	Laboratory Records
		47.	Laboratory Records-RC
		48.	ORNL Patent Section

EXTERNAL DISTRIBUTION

- Marc Abouaf, Saint Gobain/Norton Industrial Ceramics, Goddard Road, Northboro, MA 01532-1545
- Meryl D. W. Adler, Corning RD&E Div., SP PR 01 C21 PRC, Corning, NY 14831
- 51. Kenneth A. Anderson, Jr., WR Grace/Diamonite, 453 W. McConkey Street, Shreve, OH 44676
- 52. Patrick R. Annese, BMS, 334 Washington Street, Somerville, MA 02143
- 53. Bob Baker, Ceradyne, Inc., 3169 Redhill Avenue, Costa Mesa, CA 92626
- 54. Peter C. Balson, Diacraft Inc., 9033 General Drive, Plymouth, MI 48170
- 55. Richard Bandister, VERTEX Diamond Tool Company, 940 Cienega Ave., San Dimas, CA 91773
- 56-65. B. P. Bandyopadhyay, U. of North Dakota, Box 8359, Univ. Sta., Grand Forks, ND 58202-8359
 - Joe Basko, AlliedSignal, Inc., 401 N. Bendix Drive, P. O. Box 4001, South Bend, IN 46634
 - 67. Giles Becket, Cincinnati Milacron, Products Division, 4701 Marburg Avenue, Cincinnati, OH 45209
 - 68. Deepak Bhat, Valenite, Inc., 1711 Thunderbird Street, Troy, MI 48084
 - 69. Chander P. Bhateja, Contemporary Technologies, P. O. Box 5533, Oak Ridge, TN 37830-5533
 - James R. Blackmore, AlliedSignal Ceramic Components, P. O. Box 2960, Torrance, CA 90509-2960
 - 71. Ernst Borchert, S. E. Huffman Corporation, 1050 Huffman Way, Clover, SC 29710
 - 72. Joseph F. Braza, Torrington/Advanced Technology, 59 Field Street, Torrington, CT 06790
 - 73. Richard A. Brigham, Ferro Corporation, Diamonite Plant, 453 West McConkey Street, Shreve, OH 44676
 - John R. Bush, Abrasive Technology, Inc., 8400 Green Meadows Dr., Westerville, OH 43081
 - 75. Bernard J. Busovne, AlliedSignal Inc., 2525 W. 190th Street, Torrance, CA 90509-2960
 - Alan C. Carius, GE Superabrasives, 6325 Huntley Road, Worthington., OH 43085

- 77. Ronald H. Chand, Chand Kare Technical Ceramics, 2 Coppage Drive, Worcester, MA 01603-1252
- J. Mark Chenoweth, Coors Technical Ceramics, 1100 Commerce Park Drive, Oak Ridge, TN 37830
- 79. William J. Chmura, Torrington Company, 59 Field Street, Torrington, CT 06790
- 80. Tom Collins, Nissan Motor Manufacturing Corp. U.S.A., 983 Nissan Drive, Smyrna, TN 37167
- 81. Keith P. Costello, Chand Kare Technical Ceramics, 2 Coppage Drive, Worcester, MA 01603-1262
- 82. Tom L. Davidson, Diacraft, P.O. Box 1135, Dickson, TN 37055
- 83. Frank G. Davis, Allied-Signal Aerospace Company, 7550 Lucerne Drive, #203, Middleburg Heights, OH 44130
- 84. Barry S. Draskovich, AlliedSignal Ceramic Components, 2525 West 190th Street, TOR 1/S-1-2700, Torrance, CA 90504
- 85. Ernest J. Duwell, 212 Elm Street, Hudson, WI 54016
- 86. Chuck J. Dziedzic, Nucermet, P. O. Box 667, Hendersonville, NC 28793
- 87. David Edwards, Cincinnati Milacron, P.O. Box 9013, Cincinnati, OH 45209
- 88. Tommy Ellenburg, Greenville, Weavexx, 3384 Blue Springs Parkway, Greeneville, TN 37743
- William A. Ellingson, Argonne National Laboratory, 6700 S. Cass Avenue, ET Division, Bldg. 212, Argonne, IL 60439
- 90. David T. Ellis, Machined Ceramics, 629 N. Graham Street, Bowling Green, KY 42101
- 91. Bill English, GE Superabrasives, 6325 Huntley Road, P. O. Box 568, Worthington, OH 43085
- Christopher J. Evans, NIST, Bldg. 220, Room A117, Precision Engineering Division, Gaithersburg, MD 20899
- 93. John R. Evans, Ferro Corporation/Diamonite Plant, Specialty Ceramics Division, 453 West McConkey Street, Shreve, OH 44676
- 94. Robert W. Evans, Jr., Abrasive Technology, 7062 Landsdonne Street, Worthington, OH 43085
- Ron Felix, United Technologies Pratt & Whitney, 400 Main Street, MS:114-38, East Hartford, CT 06108
- 96. Michael E. Finn, I A M S, 111 Edison Drive, Cincinnati, OH 45069
- Paul M. Fleischer, Mattison Machine Works, 545 Blackhawk Park Ave., Rockford, IL 61104-5135
- 98. James D. Flinchbaugh, Weldon Machine Tool, Inc., 1800 W. King Street, York, PA 17404
- 99. Robert Frech, Eonic, Inc., 464 E. Hollywood, Detroit, MI 48203-2099
- 100. David Fried, Xerox, 800 Phillips Road, Bldg. 6 208-06E, Webster, NY 14580
- 101. Roger Gary, Cincinnati Milacron, P. O. Box 9013, Cincinnati, OH 45209
- 102. J. Randall Gilmore, ExtrudeHone, 8075 Pennsylvania Avenue, Irwin, PA 15642
- 103. Leigh C. Girard, Gallmeyer & Livingston, 336 Straight Avenue S.W., Grand Rapids, MI 49504
- 104. Ed Gizonski, Eonic, Inc., 464 E. Hollywood, Detroit, MI 48203-2099
- 105. Brian H. Gold, STC Corp., P.O. Box 1028, St. Albans, VT 05478
- 106. Allan E. Goldman, U.S. Graphite, Inc., 907 West Outer Drive, Oak Ridge, TN 37830
- 107. Frank Gorman, Astro-Met Inc., 9974 Springfield Pike, Cincinnati, OH 45215
- 108. Bill Grant, Cummins Engine Co., 1900 McKinley Avenue (50183), Columbus, IN 47202-3005
- 109. Lance Groseclose, Allison Engine Company, P. O. Box 420, MS W-05, Indianapolis, IN 46206
- 110. Changsheng Guo, Chand Kare Technical Ceramics, 2 Coppage Drive, Worcester, MA 01603
- 111. H. Gupta, U. of CT-Grind Res Ct. 191 Auditorium Road, Storrs, CT 06269-3237
- 112. Robert A. Haines, INSACO, Inc., P.O. Box 9006, Quakertown, PA 18951-9006
- 113. Nabil S. Hakim, Detroit Diesel Corporation, 13400 Outer Drive West, Detroit, MI 48239-4001
- 114. Keith Hale, Deco-Group, Inc., 4850 Coolidge Hwy., Royal Oak, MI 48073-1023
- 115. Sim Hall, Process Forming Systems, 4545 McIntyre St., Golden, CO 80403
- 116. Marcel R. Hanard II., Caterpillar Technical Center., P.O. Box 1875, Peoria, IL 61656-1875
- 117. Tom Hannon, Moore Tool Company, 800 Union Avenue, Bridgeport, CT 06607-0088
- Mark D. Hargis, Advanced Technology Projects, Williams International, 2280 West Maple Road,
 P. O. Box 200, Walled Lake, MI 48390-0200

- 119. Doug Harmon, Litton/Landis, 20 E. Sixth Street, Waynesboro, PA 17268-2050
- 120. Alan M. Hart, Dow Chemical Company, 1776 Building, Midland, MI 48674
- Michael H. Haselkorn, Caterpillar Technical Center, Bldg. E, P.O. Box 1875, Peoria, IL 61656-1875
- 122. Debbie Haught, Department of Energy, 1000 Independence Avenue, S.W., Code EE-32, Washington, DC 20585
- Norman L. Hecht, Univ. of Dayton Research Institute, 300 College Park, KL 165, Dayton, OH 45469-0172
- 124. Dave Herrala, Boride Products, Inc., 2879 Aero Park Drive, Traverse City, MI 49684
- 125. Patricia Hoffman, U.S. Department of Energy, EE-23 Forrestal Building, 1000 Independence Avenue, Washington, DC 20585
- 126. Gary A. Hollridge, EONIC, Inc., 464 E. Hollywood, Detroit, MI 48203-2099
- 127. Stephen M. Hsu, DOC/NIST, Bldg. 223, Room A256, Route 270 & Quince Orchard Road, Gaithersburg, MD 20899
- 128. Gary Huzinec, Cincinnati Milacron, P. O. Box 9013, Cincinnati, OH 45209
- Lewis K. Ives, NIST, Quince Orchard & Clopper Road, Building 223, Room A256, Gaithersburg, MD 20899
- 130. Said Jahanmir, NIST, Bldg. 220, Rm. A-215, Gaithersburg, MD 20899
- 131. Jinmyun Jo, CTC, 1450 Scalp Ave., Johnstown, PA 15904
- 132. Yury Kalish, Detroit Diesel Corporation, 13400 Outer Drive, West, Detroit, MI 48239-4001
- 133. Ray Keefe, Eaton Corporation, Manufacturing Technologies Center, 32500 Chardon Road, Willoughby Hills, OH 44094
- 134. Richard Kegg, Cincinnati Milacron, P. O. Box 9013, Cincinnati, OH 45209
- 135. Ralph Kelly, Cincinnati Milacron, P.O. Box 9013, Cincinnati, OH 45209
- 136. Kristi Keyser, Machined Ceramics, Inc., 629 North Graham Street, Bowling Green, KY 42101
- 137. Michael P. King, Carborundum Company, P.O. Box 337, Niagara Falls, NY 14302
- 138. Robert N. Kopp, Norton Company, 105 Greystone Drive, Franklin, TN 37069-4301
- 139. Joseph Kovach, Eaton Corporation, 32500 Chardon Road, Willoughby Hills, OH 44094
- 140. Edwin Kraft, Kyocera Industrial Ceramics, 5713 E. Fourth Plain Blvd., Vancouver, WA 98661
- 141. Kishor M. Kulkarni, AMP, 12227 Crestwood Dr., Carmel, IN 46033-4322
- 142. K. V. Kumar, GE Superabrasives, 6325 Huntley Road, Worthington, OH 43085
- 143. Peter Kuo, Norton Company, 1 New Bond Street, Worcester, MA 01615
- Vencel Lasic, Eaton Corporation, Engine Components Division, 824 Industrial Road, Marshall, MI 49068
- 145. Mike Laurich, Eaton Corporation, 32500 Chardon Road, Willoughby Hills, OH 44094
- Robert H. Licht, Norton Company, Northboro R&D Center, Goddard Road, Northboro, MA 01532-1545
- 147. Mel Liebers, Professional Instrumenta Company, 7800 Powell Road, Hopkins, MNs 55343
- 148. Edward Lilley, Norton Company, Northboro Research Center, Northboro, MA 01532
- 149. Santosh Limaye, LoTEC, Inc., 1840 West Parkway Blvd., West Valley City, UT 84119
- 150. Jack F. Lininger, DU-CO Ceramics Co., 155 S. Rebecca Street, Saxonburg, PA 16056
- 151. Stephen J. Lombardo, Saint \-Gobain Industrial Ceramics, Northboro Research and Development Center, Goddard Road, Northboro, MA 01532-1545
- 152. Paul T. Louks, The Dow Chemical Company, Building 1776, Midland, MI 48674
- 153. Jay Lunzer, Lunzer Inc., Applied Technology, 330 W. 42nd Street, New York, NY 10036
- 154. William A. Mack, Carborundum Company, P.O. Box 337, Niagara Falls, NY 14302
- 155. Larry Mains, Deco Group, 4850 Coolidge Highway, Royal Oak, MI 48073-1023
- Steven Malkin, U. of Massachusetts, Dept. of Mech. & Ind. Engineering, ELAB Building, Amherst, MA 01003-2210
- 157. John Mangels, Ceradyne, Inc., 3169 Redhill Avenue, Costa Mesa, CA 92626

- 158. Ken A. Marshall, Machined Ceramics, Inc., 629 North Graham Street, Bowling Green, KY 42101
- 159. Richard Marshall, Diacraft Inc., 9033 General Drive, Plymouth, MI 48170
- Iaon D. Marinescu, Abrasive Micromachining Center, Kansas State University, 244 Durland Hall,
 Manhattan, KS 66506-5112
- Newman Marsilius, Moore Tool Company, 800 Union Avenue, Bridgeport, CT 06607-0088
- 162. John E. Mayer, Jr., Texas A&M Univ., 117G Thompson Hall, College Station, TX 77843-3367
- 163. Martha McCrum, RayCham Corporation, 300 Constitution Drive, Menlo Park, CA 94025
- 164. Dale E. McCullum, Univ. of Dayton Research Institute, 300 College Park, KL 165, Dayton, OH 45469-0172
- 165. Brian McEntire, Norton Company, Goddard Road, Northboro, MA 01532-1545
- 166. John McGinnis, AlSiMag Technical Ceramics, Inc., Highway 14, Laurens, SC 29360
- Donny McInturff, Coors Technical Ceramics Company, 1100 Commerce Park Drive, Oak Ridge, TN 37830
- 168. Nanu Menon, AlliedSignal Engines, MS 301-227, P. O. Box 52181, Phoenix, AZ 85072-2181
- 169. David Merrion, Detroit Diesel Corporation, 13400 Outer Drive, West, Detroit, MI 48239-4001
- 170. Clifford Michaud, United Technologies Pratt & Whitney, 400 Main Street, MS:115-78, East Hartford, CT 06108
- 171. Biljana Mikijelj, Ceradyne, Inc., 3169 Red Hill Avenue, Costa Mesa, CA 92626
- 172. Bradley J. Miller, Pakco, 55 Hillview Avenue, Latrobe, PA 15650
- 173. Mitch O. Miller, S. E. Huffman Corp., 1050 Huffman Way, Clover, SC 29710
- 174. Robert A. Miller, Materials Development, TAFA, 146 Pembroke Road, Concord, NH 03301
- 175. Sanjay Mishra, Chand Kare Technical Ceramics, 2 Coppage Drive, Worcester, MA 01603
- 176. Bob Nath, Quatro Corporation, 6100 Jefferson Street, N.E., Albuquerque, NM 87109
- 177. Bruce E. Nelson, Norton Company, 749 Cabot Drive, Knoxville, TN 37922
- Devdas M. Pai, NC Agricultural & Technical State University, Dept. of Mech. Engr., Greensboro, NC 27411
- 179. Duane Parsons, Allison Engine Company, P. O. Box 420, MS 0-08, Indianapolis, IN 46206
- 180. Thomas E. Parsons, INSACO, Inc., 1365 Canary Road, P. O. Box 9006, Quakertown, PA 18951-9006
- 181. Thomas J. Parsons, Dow Chemical Company, 1616 Building, Midland, MI 48667
- 182. James W. Patten, Cummins Engine Company, Inc., Mail Code 50183, Box 3005, Columbus, IN 47203-3005
- 183. William W. Pflager, Litton Ind. Automat., 20 E. 6th Street, Waynesboro, PA 17268
- 184. Joseph Picone, Norton Company, 1 New Bond Street, Worcester, MA 01606
- 185. Ken Potter, Diesel Technology Company, P. O. Box 919, 2300 Burlingame Avenue, S.W., Wyoming, MI 49509-0919
- 186. Bob R. Powell, General Motors Corporation NAO, 30200 Mound Road, Warren, MI 48090-9055
- 187. Vimal K. Pujari, Norton Company, Goddard Road, Northboro, MA 01532-1545
- 188. Brad L. Rainey, Materials & Processes Engineering, Williams International, 2280 West Maple Road, P.O. Box 200, Walled Lake, MI 48390-0200
- 189. F. Rastegar, Cummins Engine Company, Inc., Piston Ring Division, 4500 Leeds AVenue, Suite 118, Charleston, SC 29405
- 190. Richard G. Rateick, Jr., Allied-Signal, 717 N. Bendix Drive, South Bend, IN 46620
- 191. Jerry Rearick, Electrofuel Industries, Inc., 2000 Ford Circle, Milford, OH 45150
- 192. Stephen G. Reder, Torrington Company, 59 Field Street, Torrington, CT 06790-4942
- 193. Patrick Redington, Norton Company, 1 New Bond Street, Bldg. 410, Worcester, MA 01606
- 194. Frank D. Reed, INSACO, Inc., P.O. Box 9006, Quakertown, PA 18951-9006
- 195. Jules Routbort, Argonne National Laboratory, ET Division, Bldg. 212, Argonne, IL 60439
- 196. Steven L. Sanner, Professional Instruments Co., 7800 Powell Road, Hopkins, MN 55343
- 197. Maryann V. Santos, Cal Poly Pomona, 220 S. Myrtlewood Street, West Covina, CA 91791

- 198. Maxine Savitz, AlliedSignal, Inc., 2525 West 190th Street, P. O. Box 1960, Torrance, CA 90509-2960
- 199. John Sayre, Manufacturing Program Development Department, Sandia National Laboratories, MS:0961, Albuquerque, NM 87185-5800
- 200. Ronald P. Scattergood, N.C. State University, Campus Box 7918, Raleigh, NC 27695-7918
- Christopher Schilling, Iowa State University, 110 Engineering Annex, Ames, IA 50011-2070
- 202. Julie M. Schoenung, California State Polytechnic University, Department of Chemistry and Materials Engineering, Pomona, CA 91768-4069
- 203. Robert B. Schulz, U.S. Department of Energy, EE-33 Forrestal Building, Washington, DC 20585
- 204. Steve Schwegler, Radiac Abrasives Inc., 742A Bates Road, Lebanon, TN 37087
- 205. Terence Sheehan, Alpex Wheel Company, Tenafly, NJ 07670
- 206. Charles Shelly, INSACO, Inc., P. O. Box 9006, Quakertown, PA 18951-9006
- 207. George Shier, Dow Chemical Company, 1801 Building, Midland, MI 48674-1801
- 208. Albert J. Shih, Cummins Engine Company, P. O. Box 3005, 1460 National Road, MC 41618, Columbus, IN 47201
- 209. P. C. Smith, WESGO, 477 Harbor Blvd., Belmont, CA 94002
- Russell G. Smith, Lanxide Corporation, 1300 Marrows Road, P. O. Box 6077, Newark, DE 19714-6077
- 211. Cors Smits, Cincinnati Milacron, P. O. Box 9013, Cincinnati, OH 45209
- 212. Anil Srivastava, IAMS, 1111 Edison Drive, Cincinnati, OH 45215-2265
- 213. Bill Stegmuller, Cincinnati Milacron, P. O. Box 9013, Cincinnati, OH 45209
- Chris R. Stephens, Alsimag Technical Ceramics, One Technology Place, Hwy. 14, Laurens, SC 29360-0089
- Robert Straub, Diesel Technology, 2300 Burlingame Avenue, S.W., Wyoming, MI 49509-0919
- 216. Dan Strong, Corning RD&E Div., SP PR 01 C34 PRC, Painted Post, NY 14870
- 217. Peter Strzepa, CarboMedics, 1300 East Anderson Lane, Austin, TX 78752
- 218. K. Subramanian, Norton Company, 1 New Bond Street, Worcester, MA 01615-0008
- Jiangang Sun, Argonne National Laboratory, 9700 South Cass Avenue, ET/212, Argonne, IL 60439
- 220. Victor J. Tennery, 113 Newell Lane, Oak Ridge, TN 37830
- Allen Thompson, Coors Technical Ceramics Co., 1100 Commerce Park Drive, Oak Ridge, TN 37830
- 222. Dennis M. Tracey, St. Gobain/Norton, Goddard Road, Northboro, MA 01532-1545
- 223. Clyde T. Treadwell, Sonic-Mill, 7500 Bluewater Road, Albuquerque, NM 87121
- 224. Marc Tricard, Norton Company, 1 New Bond Street, Box #15008, MS 413-201, Worcester, MA 01562-0008
- Daniel Uffer, Saint-Gobain Industrial Ceramics, Advanced Ceramics Division, SE\epr B.P.1, 84131 LE Pontet Cedex, France
- 226. Joseph B. Vincent, Norton Company, 4 Isham Lane, Savannah, GA 31411
- 227. Ron Walecki, AlliedSignal Inc., 2525 W. 190th Street, Torrance, CA 90509-2960
- 228. Stephen K. Weaver, INSACO, Inc., P. O. Box 9006, Quakertown, PA 18951-9006
- 229. John A. Webster, U. of Connecticut U-119, Storrs, CT 06269-5119
- William H. Werst, Jr., U.S. Advanced Ceramic Association, 1600 Wilson Blvd., Suite 901, Arlington, VA 22209
- 231. Perry P. Yaney, University of Dayton, Department of Physics, Dayton, OH 45469-2314
- 232. Charles Yang, Cincinnati Milacron, Products Division, 4701 Marburg Avenue, Cincinnati, OH 45209

- 233. Thomas M. Yonushonis, Cummins Engine Company, Inc., MC 50183, 1900 McKinley Avenue, Columbus, IN 47201
- 234. Bi Zhang, Univ. of Connecticut, PMC, U-119, Longley Bldg., Rt. 44, Storrs, CT 06269-5119
- 235. Zhenqi Zhu, Univ. of Connecticut, PMC, U-119, Longley Bldg., Rt. 44, Storrs, CT 06269-5119
- 236-237. Office of Scientific & Technical Information, P. O. Box 62, Oak Ridge, TN 37831